UNIVERSITY OF CALIFORNIA, SAN DIEGO

Function of Bearded family proteins in Notch signaling during mechanosensory organ development in *Drosophila melanogaster*

A dissertation submitted in partial satisfaction of the requirements for the degree Doctor of Philosophy

in

Biology

by

Joseph Rosario Fontana

Committee in charge:

Professor James W. Posakony, Chair
Professor Elizabeth A. Komives
Professor Gentry N. Patrick
Professor Sandra L. Schmid
Professor Steven A. Wasserman

2010

ProQuest LLC
789 East Eisenhower Parkway
P.O. Box 1346
Ann Arbor, MI 48106-1346

The Dissertation of Joseph Rosario Fontana is approved, and it is acceptable in quality and form for publication on microfilm and electronically:

_____

_____

_____

_____

_____

Chair

University of California, San Diego

2010

DEDICATION

To my parents, John and Adeline Fontana, who have supported me from Day 1...no matter how much trouble I've been.

And to my fiancée, Amber Dawn Davis, for her patience, understanding, and willingness to share her life with me.

EPIGRAPH

Knowledge is far superior to belief,
for belief is the way of the uninformed.

Scott Cunningham

TABLE OF CONTENTS

LIST OF FIGURES

LIST OF TABLES

ACKNOWLEDGEMENTS

None of this work would have been possible without the advice and guidance of many individuals. First and foremost, I would like to thank my research advisor, Jim Posakony. Jim allowed me a great degree of freedom to develop ideas and pursue lines of investigation. I feel this freedom was a great contributor to my individual growth as a scientific thinker. He also had a door that was almost always open for us to disturb him. Whether it was to go over data, recently published articles, or how to best achieve career goals, he gladly put aside his work to spend time in discussions. I am grateful for those occasions in which he has been able to cheerily encourage me to push on when all appeared bleak. And while my butchering of the English language may never evolve to his mastery of it, I'd like to think he has been able to partially impart upon me his enviable skill of critically analyzing and interpreting data in a meaningful way. It has been a great experience learning from him, and I look forward to being his colleague in the field of Developmental Biology.

I also need to acknowledge the guidance of Andrew Groover, whom I consider a friend more than a previous boss. Andrew took me under his wing years ago while he was a post-doc in the lab of Rob Martienssen at Cold Spring Harbor Laboratories. It was the summer of 1999, and I was still an undergrad that barely knew how to operate a pipette-man properly. For about 8 months he trained me in various techniques...and let me "play" with radiation. It was during this time that I

realized what I'd be doing for the rest of my life. When I finished up my undergraduate work, he allowed me to follow him across the country to Davis, California where he set up his first lab. In addition to teaching me as much as possible for my eventual entry into graduate school, we enjoyed many Friday evenings at the Cantina discussing life and drinking beers. I'd like to thank him for all he taught me, the references he's written for me, and the friendship we still share.

To my thesis committee members, Steve Wasserman, Gentry Patrick, Betsy Komives, Sandy Schmid, and Vivek Malhotra (who started on my committee, but has since moved away), I'd like to send my appreciation. They have all provided me with invaluable input and made sure I kept my research focused.

I would also like to thank all of the grad students and post-docs I have had the pleasure of interacting with over the years. I'm especially grateful to my current and previous lab-mates: Steve Miller, Feng Liu, Mariano Loza Coll, Nick Reeves, Mark "Orange-G" Rebeiz, Brian Castro, Sui Zhang and Tammie Stone. A motley crew to say the least! Even so, they have all contributed in one way or another to a productive and enjoyable research environment.

Last, but certainly not least, I would like to thank our Project Assistant, Jackie Vignes. For organizing travel plans, reimbursing expenses, taking care of paperwork, reserving classrooms and lecture halls, providing delicious food for seminars and meetings, contacting

various people around campus for me, having a constant supply of chocolate available for those late afternoon cravings, and a million other things, Jackie was someone who could always be counted on. Thank you for making everything run so smoothly.

Chapter 1, in full, is a reprint of the material as it appears in Developmental Biology 2009. Fontana, Joseph R.; Posakony, James W., Elsevier Inc., 2009. The dissertation author was the primary investigator and primary author of this paper. It has been reformatted to fit the required specifications for this Dissertation.

Chapter 2, in full, is currently being prepared for submission for publication of the material. Fontana, Joseph R.; Posakony, James W. The dissertation author was the primary investigator and author of this material. It has been reformatted to fit the required specifications for this Dissertation.

VITA

2000 Bachelor of Arts, Colgate University

2010 Doctor of Philosophy, University of California, San Diego

PUBLICATIONS

Fontana, J.R., Posakony, J.W., 2009. Both inhibition and activation of Notch signaling rely on a conserved Neuralized-binding motif in Bearded proteins and the Notch ligand Delta. Dev. Biol. 333, 373-385.

Groover, A.T., Mansfield, S.D., DiFazio, S.P., Dupper, G., Fontana, J.R., Millar, R., Wang, Y., 2006. The *Populus* homeobox gene *ARBORKNOX1* reveals overlapping mechanisms regulating the shoot apical meristem and the vascular cambium. Plant Mol. Biol. 61, 917-932.

Groover, A., Fontana, J.R., Dupper, G., Ma, C., Martienssen, R., Strauss, S., Meilan, R., 2004. Gene and enhancer trap tagging of vascular-expressed genes in poplar trees. Plant Physiol. 134, 1742-1751.

Brown, G.R., Bassoni, D.L., Gill, G.P., Fontana, J.R., Wheeler, N.C., Megraw, R.A., Davis, M.F., Sewell, M.M., Tuskan, G.A., Neale, D.B., 2003. Identification of quantitative trait loci influencing wood property traits in loblolly pine (*Pinus taeda* L.). III. QTL Verification and candidate gene mapping. Genetics 164, 1537-1546.

Byrne, M.E., Groover, A.T., Fontana, J.R., Martienssen, R.A., 2003. Phyllotactic pattern and stem cell fate are determined by the *Arabidopsis* homeobox gene *BELLRINGER*. Development 130, 3941-3950.

Groover, A.T., Fontana, J.R., Arroyo, J.M., Yordan, C., McCombie, W.R., Martienssen, R.A., 2003. Secretion trap tagging of secreted and membrane-spanning proteins using Arabidopsis gene traps. Plant Physiol. 132, 698-708.

ABSTRACT OF THE DISSERTATION

Function of Bearded family proteins in Notch signaling during mechanosensory organ development in *Drosophila melanogaster*

by

Joseph Rosario Fontana

Doctor of Philosophy

University of California, San Diego, 2010

Professor James W. Posakony, Chair

The Notch pathway is a cell-cell signaling pathway conserved in metazoans and utilized extensively during development to mediate cell fate decisions. Signaling is initiated by a functional interaction between the transmembrane Notch (N) receptor on the surface of one cell with a transmembrane ligand on a neighboring cell. Stimulation of the N receptor leads to transcriptional activation of N-target genes in signal-receiving

cells. Many N-dependent processes also rely on the activity of the E3 ubiquitin ligase, Neuralized (Neur), in the signal-sending cell. In the fruit fly, *Drosophila melanogaster*, Neur activates the signaling capability of the N ligands Delta (Dl) and Serrate (Ser) by directing their ubiquitination-mediated endocytosis.

The activity of Neur is inhibited by a family of N-target genes known as the *Bearded* (*Brd*) family. In Chapter 1, we demonstrate that Brd proteins and the N ligand Dl use a common protein motif, which we call the NXXN motif, to directly interact with Neur. We show that the NXXN motifs of Dl are required in vivo for its Neur-dependent endocytosis. In Brd proteins, we find that NXXN motifs are required to disrupt an in vitro Neur-Dl interaction and inhibit Neur activity in vivo. In Chapter 2, we find that the basic amphipathic α-helix, or B domain, of Brd proteins mediates an in vitro interaction with PI(3)P. The B domain is necessary for Brd proteins to colocalize with Neur in PI(3)P-positive endosomes in vivo. Using additional markers of endocytic compartments we observe that Brd protein/Neur endosomes also colocalize with the late endosomal and lysosomal proteins Rab7 and LAMP1, suggesting Brd proteins mediate the targeting of Neur to lysosomes for degradation. In Chapter 3, we describe several generated null alleles of *Brd* family genes. Cells mutant for *Brd* genes are found to be sensitized to levels of Neur activity. We show that *Brd* genes act redundantly to inhibit Neur activity in non-SOP cells of the proneural cluster during lateral inhibition.

Introduction

The development of multicellular animals, or metazoans, is a complex process in which cells must divide, migrate, form epithelial sheets, acquire specialized properties, terminally differentiate, or, in some cases, undergo programmed death. The coordination of these various events relies heavily on the abilities of individual cells to detect the properties of their extracellular environments and to communicate with one another. Without this, a cell would have no way of determining where it resides in the body of a developing animal, nor what fate it should adopt. Communication between cells may be achieved via the activity of a relatively few number of evolutionarily conserved cell-cell signaling pathways. These cell-cell signaling pathways are iteratively used during development for many processes and provide both long and short distance communication. One of these pathways, the Notch (N) cell-cell signaling pathway is a short-range communication pathway whereby the transmembrane Notch receptor is activated by a transmembrane ligand on neighboring cells. In this system, a cell that has the potential to follow two distinct developmental pathways will adopt one fate, the “Notch-independent” fate, in the absence of signaling, and the alternative, “Notch-dependent”, fate when signaling is active in that cell.

The role of N signaling in these binary cell-fate decisions has been documented in an extraordinary number of developmental processes. In vertebrates, some of these processes include somitogenesis (Dunwoodie, 2009), intestinal stem cell maintenance and cell fate decisions of progeny

cells (Casali and Batlle, 2009), vascular patterning (Jakobsson et al., 2009), lymphocyte development (de La Coste and Freitas, 2006), myogenesis (Vasyutina et al., 2007), and cardiac development (Niessen and Karsan, 2008). In addition to many of the processes listed for vertebrates, N signaling in the fruit fly, *Drosophila melanogaster*, has also been well characterized in oogenesis (Roth, 2001), hematopoiesis (Radtke et al., 2005), and nervous system development (Cau and Blader, 2009). With a role in so many processes, it is easy to see how failures of the signaling pathway may lead to developmental defects and disease states. Indeed, Notch signaling has been implicated in a number of human cancers (Strizzi et al., 2009).

Sensory Organ Development

The development of the peripheral nervous system (PNS) in *Drosophila* has been a useful system in which to study the details of the Notch signaling pathway. The bodies of adult *Drosophila* contain a large array of cuticular bristle structures that are positioned in a highly stereotypical pattern. The larger bristles are known as macrochaetes and the smaller known as microchaetes. Each of these bristles is part of a complete mechanosensory organ composed of four cells: a neuron, a sheath cell (thecogen), a shaft cell (trichogen) that produces the cuticular bristle structure, and a socket cell (tormogen) that produces a cuticular socket structure to support the bristle (Posakony, 1994) (Figure I.1A).

During development, all cells of each mechanosensory organ are derived from a single parent cell called the sensory organ precursor (SOP) cell (Hartenstein and Posakony, 1989). The SOP cell undergoes a series of asymmetric cell divisions during which N signaling from one daughter cell to its sibling is required for the cells to acquire their different fates (Posakony, 1994; Rhyu et al., 1994; Frise et al., 1996; Guo et al., 1996) (Figure I.1B). After the first division, signaling from the pIIB to the pIIA confers different fate potentials upon these cells. The pIIA will divide 1 additional time and asymmetric N signaling allows the specification of the shaft cell (Notch-independent fate) and the socket cell (Notch-dependent fate). On the pIIB side of the SOP lineage, 2 additional rounds of cell division occur. The first gives rise to the pIIIB cell and a glial cell, which undergoes apoptosis (Gho et al., 1999). The pIIIB cell then divides, and asymmetric N signaling between the daughter cells results in a neuron (Notch-independent fate) and a sheath cell (Notch-dependent fate). Hyperactivity or failure of N signaling at any step during this process leads to predictable and easily identifiable phenotypes. For example, failure of N signaling throughout this entire process causes the presumptive pIIA cell to adopt a pIIB fate (the Notch-independent fate). The two pIIB cells will divide, producing two pIIIB cells. The two pIIIB cells divide and the presumptive sheath cells will adopt neuronal fates (Notch-independent fate). Thus, four neurons will be produced at the expense of the shaft, socket, and sheath cells. This results in a balding phenotype on the adult

fly, since no bristles or sockets are formed. Hyperactivity of the N pathway in both sibling cells throughout this process results in a different phenotype. In this case, the presumptive pIIB cell will adopt a pIIA cell fate (Notch-dependent fate). The two pIIA cells will then divide and the presumptive shaft cells will adopt socket cell fates (Notch-dependent fate). This leads to the appearance of four sockets produced on the adult fly, with no bristles. Close examination would also reveal the neuron and sheath are not present.

N signaling is also required during the specification of the SOP in a process called “lateral inhibition” (Muskavitch, 1994; Chitnis, 1995). The SOP cell is specified from among a group of equipotent cells termed the proneural cluster (PNC), identifiable by the expression of the proneural bHLH transcriptional activators Achaete or Scute (Cubas et al., 1991; Skeath and Carroll, 1991). A N signal sent from a single cell of the PNC is received by the surrounding cells of the PNC. The cell that sends out this N signal becomes the SOP. The cells that receive the N signal are inhibited from becoming SOPs, ensuring only a single SOP is specified. Like in the SOP lineage, disruption or hyperactivity of N signaling during lateral inhibition produces easily identifiable phenotypes. Hyperactivating the N signal in all cells of the PNC would result in a balding phenotype on the adult fly. This occurs because the N signal inhibits the SOP cell fate in all cells of the PNC. Without an SOP, no mechanosensory organ will develop. Conversely, the loss of N signaling would result in dense

patches of bristles in positions where only one bristle would normally be present. Without a N signal, many cells of the PNC adopt an SOP fate. These supernumerary SOP cells then go on to produce full mechanosensory organs.

The Notch Receptor

Disruptions of the *Notch* locus were first recorded in *Drosophila* almost one hundred years ago, before the molecular nature of genes were even known (Dexter, 1914; Mohr, 1919). The first inheritable dominant mutation obtained was named “Perfect Notched” due to the characteristic notching seen in the wings of the adult fly (Figure I.2A). Decades later, the cloning of the *Notch* locus would reveal a large gene, spanning 40 kb. This gene produces a transcript approximately 10.5 kb long, encoding a protein product of 2,703 amino acids (Artavanis-Tsakonas et al., 1983; Kidd et al., 1983; Wharton et al., 1985; Kidd et al., 1986). The characterization of the Notch (N) receptor in *Drosophila* led to the identification of N orthologs in many other organisms. *Caenorhabditis elegans* contains two N orthologs, LIN-12 and GLP-1, involved in various cell fate decisions during development (Yochem et al., 1988; Austin et al., 1989; Yochem and Greenwald, 1989). The first vertebrate N ortholog was discovered in *Xenopus laevis*, and was soon followed by the identification of N proteins in rat, mouse, and human (Coffman et al., 1990; Ellisen et al., 1991; Weinmaster et al., 1991; Reaume et al., 1992). Suggesting a

very ancient evolutionary history, a N receptor has also been characterized in the cnidarian *Hydra vulgaris* (Käsbauer et al., 2007).

Many properties of the N receptor have been constrained throughout evolution. N proteins contain an N-terminal extracellular domain, a single transmembrane domain, and a C-terminal intracellular domain (Figure I.2B). A majority of the N molecules in a cell are proteolytically cleaved N-terminal to the transmembrane domain by a furin-like convertase in the trans-Golgi (Logeat et al., 1998). The two fragments are then linked through dimerization domains near the site of cleavage and the receptor is presented at the plasma membrane as a heterodimer (Blaumueller et al., 1997). The extracellular domain of the receptor consists of a tandem array of 36 EGF-like repeats in *Drosophila* (Wharton et al., 1985; Kidd et al., 1986). The number of EGF-like repeats in other organisms is variable, with 29-36 repeats in mammalian N receptors, 10 in GLP-1, 13 in LIN-12, and 6 in *Hydra* Notch (Yochem et al., 1988; Yochem and Greenwald, 1989; Käsbauer et al., 2007; Kopan and Ilagan, 2009). Following the EGF-like repeats are 3 cysteine-rich repeats called LIN-12/Notch Repeats, or LNRs (Wharton et al., 1985; Kidd et al., 1986). The intracellular domain of N receptors also contains several conserved features. The first is a RAM domain (RBP-Jκ Association Motif) that is involved in binding to CSL (CBF1/RBP-Jκ or RBP-L in mammals, Suppressor of Hairless [Su(H)] in *Drosophila*, LAG-1 in *C. elegans*) transcription factors (Tamura et al., 1995). Following the RAM

domain are 6 ankyrin repeats, which mediate protein-protein interactions, and a C-terminal PEST sequence, implicated in degradation (Breeden and Nasmyth, 1987; Rechsteiner, 1988; Lux et al., 1990).

Notch ligands and their activation in signal-sending cells

Activation of the N receptor in both mammals and flies occurs after an interaction with one of two types of N ligands present on the surface of a neighboring cell. One class of ligand includes Delta (Dl) in insects and 3 Delta-like (Dll) proteins in mammals, Dll1, Dll3, and Dll4 (Vässin et al., 1987; Kopczynski et al., 1988; Bettenhausen et al., 1995; Dunwoodie et al., 1997; Shutter et al., 2000). The second class includes Serrate (Ser) in insects and Jagged1 and Jagged2 in mammals (Fleming et al., 1990; Rebay et al., 1991; Lindsell et al., 1995; Shawber et al., 1996). Both Dl and Ser ligands are single-pass transmembrane proteins with an extracellular N-terminus and an intracellular C-terminus (Figure I.2B). At the N-terminus of both ligand classes is a DSL domain [Dl, Ser, LAG-2 (C. elegans)] required for the interaction with the N receptor (Tax et al., 1994; Shimizu et al., 1999; Cordle et al., 2008). Both Dl and Ser ligands also possess a variable number of EGF-like repeats in their extracellular domains. The presence of an extracellular cysteine-rich repeat near the transmembrane domain of Ser ligands is what distinguishes them from the Dl ligands (Thomas et al., 1991).

Before Dl and Ser can stimulate the N receptor on neighboring cells, accumulating evidence has indicated that the ligands must be

targeted for Epsin-dependent endocytosis (Overstreet et al., 2004; Wang and Struhl, 2004). Epsin is a clathrin-adapter protein that can bind mono-ubiquitinated target proteins and direct their entry into the endocytic pathway (Wendland, 2002). In the absence of Epsin, DSL ligands may still undergo endocytosis, however these events do not stimulate N signaling on neighboring cells (Wang and Struhl, 2004). The Epsin-dependent activation of DSL ligands requires the activity of an E3 ubiquitin ligase, either Mind Bomb (Mib) or Neuralized (Neur) (Wang and Struhl, 2005). In *Drosophila*, these two E3 ligases are required for distinct subsets of N-dependent processes, although mutation in one can be rescued by expression of the other (Lai et al., 2005a; Le Borgne et al., 2005b; Wang and Struhl, 2005). During lateral inhibition and sensory organ development in the notum, Neur has the primary role of activating the N-ligand Dl (Boulianne et al., 1991; Yeh et al., 2000).

The ubiquitin ligase activity of Neur is conferred upon it by a C-terminal RING domain. This domain is required for the ubiquitination of Dl in vitro and for Neur-dependent endocytosis of Dl in vivo (Lai et al., 2001; Yeh et al., 2001). In addition to its RING domain, Neur contains two NHR (Neur Homology Repeat) domains of about 150 amino acids each, and a short poly-basic region N-terminal to NHR1. The NHR1 domain has been shown to be both necessary and sufficient for an interaction with the intracellular domain of Dl, while the poly-basic region has been implicated in phosphoinositide binding (Commisso and Boulianne, 2007; Skwarek et

al., 2007). Both are required for Neur-dependent endocytosis of Dl and activation of N signaling.

Activation of the N receptor and expression of target genes

The role of ubiquitin-mediated endocytosis of N-ligands in activating N signaling remains unclear. Several proposed models are explained in a review by Le Borgne et al. (2005a). Regardless of the exact mechanism of Neur-dependent ligand activation, a successful ligand-receptor interaction stimulates two cleavages of the N receptor. The first cleavage (S2 cleavage) occurs in the extracellular portion of the transmembrane fragment of the N heterodimer. This cleavage is carried out by the ADAM/TACE metalloprotease, Kuzbanian (Pan and Rubin, 1997; Sotillos et al., 1997). The next cleavage (S3 cleavage) is carried out by the gamma-secretase complex and releases the cytoplasmic intracellular domain of the N receptor (NICD) (De Strooper et al., 1999). A nuclear localization signal in NICD then mediates its translocation into the nucleus (Struhl and Adachi, 1998).

In the nucleus of cells in which there is no active N signal, the sequence-specific DNA binding transcription factor Su(H) is bound by a transcriptional repressor complex consisting of the proteins Hairless, CtBP and Groucho (Barolo et al., 2002). This Su(H)-Hairless-repressor complex keeps expression of N-target genes off (Bang et al., 1995; Castro et al., 2005). When N signaling is active in a cell, NICD in the nucleus displaces the Hairless-repressor complex by associating with Su(H) via its RAM

domain (Bailey and Posakony, 1995; Tamura et al., 1995; Barolo et al., 2002). A Su(H)-NICD complex associates with the transcriptional activator Mastermind to then turn on the transcription of N-target genes (Fortini and Artavanis-Tsakonas, 1994; Petcherski and Kimble, 2000).

During lateral inhibition, the combination of an NICD activation complex with the proneural bHLH activator proteins, Achaete or Scute, promotes the expression of two major classes of N-target genes in non-SOP cells of the PNC (Bailey and Posakony, 1995; Lecourtois and Schweisguth, 1995; Wurmbach et al., 1999). The first class is made up of the bHLH repressor genes of the *Enhancer of split* [*E*(*spl*)]-Complex: *mγ*, *mδ*, *mβ*, *m3*, *m5*, *m7* and *m8*. The protein products of these genes are involved in transcriptional repression and are necessary for the inhibition of the SOP fate in these cells (Delidakis and Artavanis-Tsakonas, 1992; Knust et al., 1992). The second class is made up of the *Bearded* (*Brd*) family of genes which includes the *E*(*spl*)-Complex genes *mα*, *m2*, *m4*, and *m6* and the *Brd*-Complex genes *Brd*, *Brother of Bearded* (*Bob*), *Twin of m4* (*Tom*) and *Ocho* (Leviten et al., 1997; Lai et al., 2000a; Lai et al., 2000b). The role of Brd proteins in N signaling is the main topic of this Dissertation and is discussed in more detail below and in the chapters that follow.

Transcriptional and post-transcriptional control of the Brd *genes*

As mentioned above, the *Brd* genes are regulated by a combination of N signaling and proneural protein expression. As would be expected

from this regulatory code, most *Brd* family members (BFMs), are expressed in the PNCs of the developing notum (Leviten et al., 1997; Lai et al., 2000a; Lai et al., 2000b). The combination of Su(H) and proneural protein binding sites has been shown to be required for *E(spl)mα* expression in the non-SOP cells of the PNC, where N-signaling is active (Castro et al., 2005). In the SOP, which does not receive a N signal, the Su(H) sites are occupied by the Su(H)-Hairless-repressor complex, keeping expression of the gene turned off (Bang et al., 1995; Castro et al., 2005). While the BFMs *Bob* and *Tom* are expressed in other regions of active N-signaling, they do not show expression in the PNCs of the developing notum (Lai, 1999; Lai et al., 2000a). This suggests there are additional regulatory inputs controlling the expression of BFMs. Indeed, a Twist consensus-binding site upstream of the *E(spl)m6* gene controls expression of this BFM in the muscle precursors in the wing imaginal disc (Lai et al., 2000b; Bodner, 2002).

Once transcribed, a number of conserved 3' UTR sequence motifs provide post-transcriptional control of BFMs. These motifs [the Brd box (AGCTTTA), the GY box (GTCTTCC), and the K box (TGTGAT)] have varying numbers of occurrences in the 3' UTRs of both BFM and *E*(*spl*) bHLH repressor transcripts (Leviten et al., 1997; Lai and Posakony, 1997; Lai et al., 1998; Lai et al., 2000a; Lai et al., 2000b). By linking the 3' UTRs of *Brd* and *E*(*spl*)*m8* to a reporter transgene it was shown that these 3' UTRs negatively effect protein expression. These effects have been

directly attributed to the various motifs due to the observations that mutations in these motifs relieve the negative regulatory effects (Lai and Posakony, 1997; Lai et al., 1998). Evidence has indicated that this post-transcriptional regulation is mediated by several microRNAs whose 5' UTR seed motifs are complementary to the corresponding 3' UTR motifs of the BFMs (Lai et al., 2004; Lai et al., 2005b).

Brd *gain-of-function phenotype*

The first characterized allele of a BFM was a gain-of-function allele of *Brd* caused by the loss of the negative regulation conferred upon it by its 3' UTR (Leviten and Posakony, 1996; Leviten et al., 1997). The *Brd* gain-of-function phenotype results in defects of mechanosensory organ development reminiscent of *N* loss-of-function phenotypes (Leviten and Posakony, 1996). In weak alleles there is a failure of lateral inhibition in the PNC that results in the production of extra SOPs. This results in the development of extra mechanosensory organs in positions where only one should reside (Figure I.3A-B). Stronger gain-of-function alleles produce a balding phenotype on the adult notum. This is cause by cell-fate transformations in the SOP lineage resulting in the specification of multiple neurons at the expense of the other cells of the organ. This, too, is reminiscent of a *N* loss-of-function phenotype. These *Brd* gain-of-function phenotypes can be recreated by misexpression of the *Brd* gene, or any BFM with the exception of *E*(*spl*)*m2*, in PNCs using the UAS/GAL4 system

(Leviten et al., 1997; Apidianakis et al., 1999; Lai et al., 2000a; Lai et al., 2000b; Zaffran and Frasch, 2000).

Brd proteins and conserved motifs

The *Brd* genes encode small proteins ranging from 70 to 218 amino acids in *D. melanogaster* (Figure I.3D). Since first being characterized, the universally recognized feature has been the presence of a predicted, highly basic amphipathic α-helix near the N-terminus termed the B domain (for Basic) (Leviten et al., 1997; Lai et al., 2000a; Lai et al., 2000b; Zaffran and Frasch, 2000). While the residues of individual B domains have not been considered to be constrained, a helical wheel plot of the region clearly shows that the basic residues Arg and Lys are clustered on one side of the predicted helix, with hydrophobic residues on the other (Figure I.3C). In *Drosophila*, the canonical BFMs E(spl)mα, E(spl)m4, Tom, and Ocho contain three additional conserved motifs (Figure I.3D) (Apidianakis et al., 1999; Lai et al., 2000a; Lai et al., 2000b; Zaffran and Frasch, 2000). The first was named the “N motif” due to the characteristic pattern of Asn residues in the published NXANE(K/R)(L/M) consensus. In recently published work (presented here as “Chapter 1”) we redefine this consensus as (D/E/Q)NXXN and rename the motif the “NXXN motif” (Fontana and Posakony, 2009). The next conserved motif has the consensus VPVHFARTXXGTFFWT and is termed the G motif. The last is found at the C-terminal end of the canonical BFMs and is termed the D motif for the consensus DRW(A/V)QA. Brd and Bob contain an NXXN

motif, but are missing a G and D motif. E(spl)m6 contains an NXXN and G motif. E(spl)m2 contains a G motif, and is the only BFM not containing an NXXN motif (Figure I.3D).

Function of Brd proteins in N signaling

A *Drosophila* protein yeast two-hybrid screen revealed an interaction between Neur and the canonical Brd protein Tom (Giot et al., 2003). Work from the Schweisguth lab extended this by showing all BFMs, except E(spl)m2, interact with Neur in a two-hybrid assay (Bardin and Schweisguth, 2006). They pursued a line of investigation that went on to show that BFMs could inhibit Neur-mediated endocytosis of Dl. Similar work from another lab showed Tom expression inhibits Neur-dependent endocytosis of Dl in the embryo (De Renzis et al., 2006). The following chapters of this Dissertation are dedicated to furthering our understanding of the role of BFMs during N signaling.

In Chapter 1, we show that BFMs directly interact with Neur via their NXXN motifs and we report the existence of multiple functional NXXN motifs in E(spl)mα, E(spl)m4 and Tom. We find that the intracellular domain of Dl contains a conserved NXXN motif that is responsible for its in vitro interaction with Neur and required for its Neur-dependent endocytosis in vivo. BFMs can directly compete with Dl for binding to Neur in an NXXN motif-dependent manner, suggesting this competition as the mechanism through which BFMs inhibit N signaling.

In Chapter 2, we examine the role of the B domain in Brd protein function. We show that the B domain mediates a specific in vitro interaction with the phosphoinositide PI(3)P. In vivo, we find the B domain is required for the ability of BFMs to colocalize with Neur in PI(3)P-positive endosomes. Furthermore, Neur/E(spl)mα endosomes are also positive for the late endosomal and lysosomal markers Rab7 and LAMP1. These results suggest that BFMs target Neur for degradation in the lysosome.

Chapter 3 is a description of several BFM loss-of-function alleles that were generated. Deletions of *Tom* and *Brd* were created through the imprecise excision of P-transposable elements. Homologous recombination was used to generate null alleles of *E(spl)mα* and *E(spl)m4*. Our data indicate that endogenously coexpressed BFMs function redundantly during lateral inhibition and loss of BFM function sensitizes cells of the PNC to levels of Neur activity.

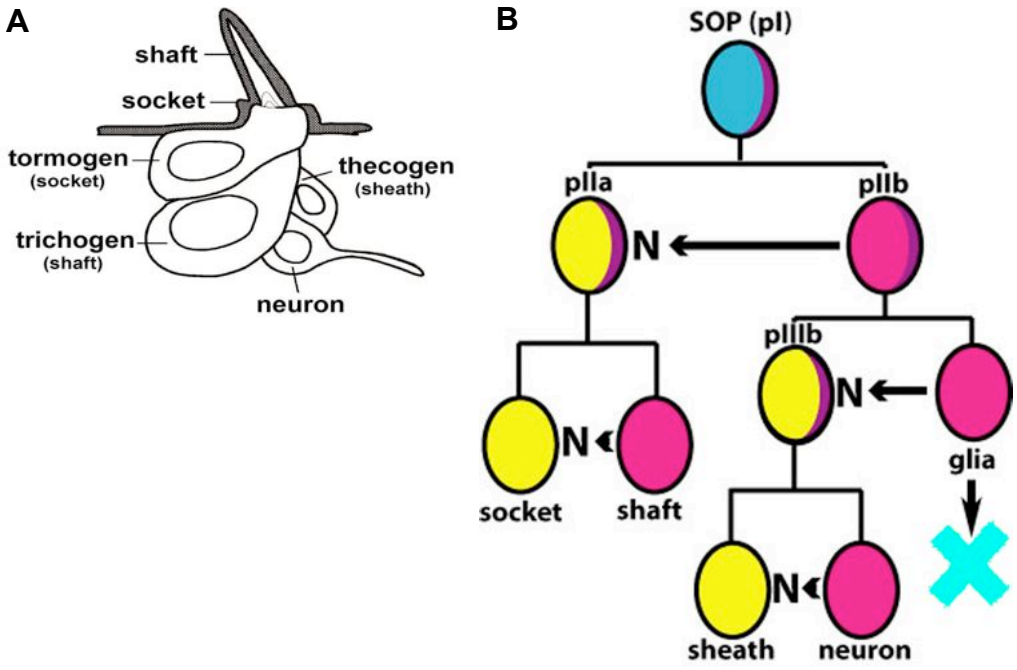

Figure I.1: Structure and cell lineage map of the Drosophila mechano-sensory organ. (A) Cartoon illustrating the organization of cells that make up the mechanosensory organ. Taken from Posakony (1994). Anterior is to the right. (B) The SOP cell lineage. A series of asymmetric cell divisions followed by Notch signaling from one daughter cell to its sibling leads to the specification of the four distinct cell types of the mature mechanosensory organ.

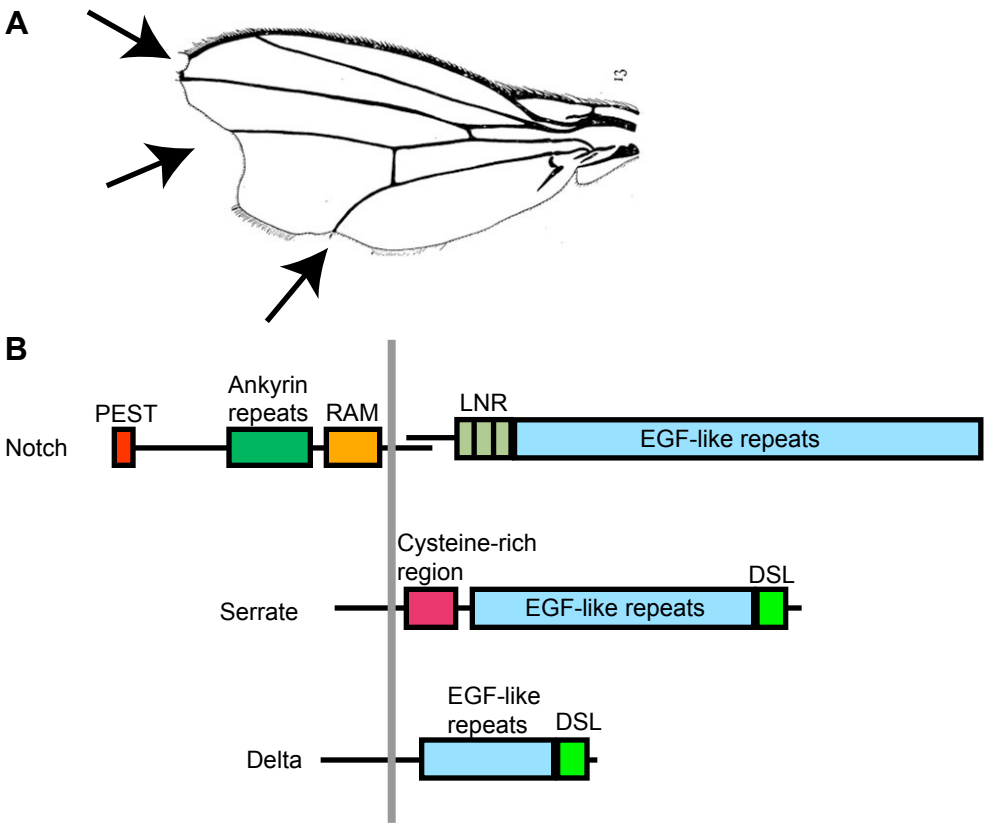

Figure I.2: The Notch phenotype and components of the signaling pathway. (A) Drawing of the wing phenotype from the Perfect Notched mutant. Image from Dexter (1914). Arrows added to show regions of wing "notching." (B) Illustration of the Notch receptor and the ligands Delta and Serrate. Protein motifs are shown in colored boxes. The vertical gray bar represents the plasma membrane. Intracellular is to the left, extracellular is to the right. RAM = RBP-Jκ Association Motif; LNR = LIN-12/Notch Repeat; DSL = Delta/Serrate/LAG-2

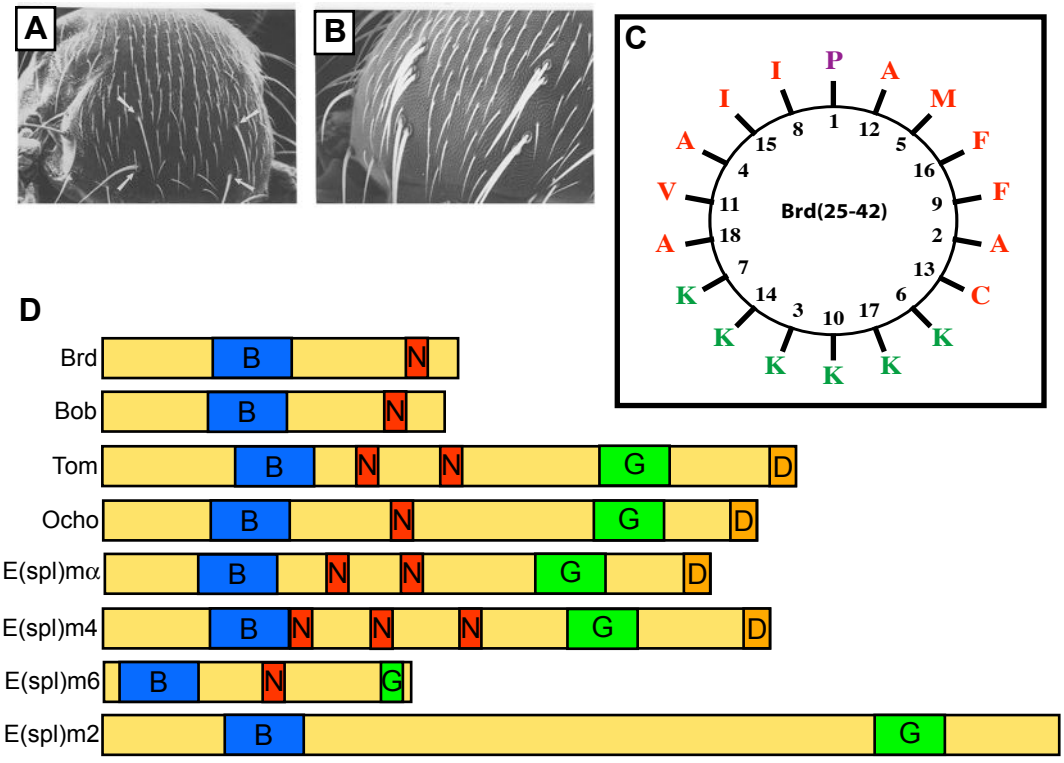

Figure I.3: The Brd phenotype and structure of the Brd proteins. (A-B) Images of a wild-type (A) and *Brd* ^{1} (B) notum taken from Leviten and Posakony (1996). Arrows in the wild-type image (A) mark the positions of four dorsocentral machrochaete bristles. In the *Brd* ^{1} homozygous mutant (B), extra bristles are seen at each of the dorsocentral positions. (C) Helical wheel plot illustrating the amphipathicity of the B domain of Brd. Amino acids 25-42 are shown. Hydrophobic residues are depicted in red and basic residues are depicted in green. (D) Cartoon representations of the *Drosophila* Brd proteins. Blue box = B domain. Red box = NXXN motif (Marked with "N"). Green box = G motif. Orange box = D motif.

References

Apidianakis, Y., Nagel, A.C., Chalkiadaki, A., Preiss, A., Delidakis, C., 1999. Overexpression of the *m4* and *mα* genes of the *E(spl)-Complex* antagonizes Notch mediated lateral inhibition. Mech. Dev. 86, 39–50.

Artavanis-Tsakonas, S., Muskavitch, M.A.T., Yedvobnick, B., 1983. Molecular cloning of *Notch*, a locus affecting neurogenesis in *Drosophila melanogaster*. Proc. Natl. Acad. Sci. USA 80, 1977-1981.

Austin, J., Maine, E.M., Kimble, J., 1989. Genetics of intercellular signalling in *C. elegans*. Development 107 Suppl, 53-57.

Bailey, A.M., Posakony, J.W., 1995. Suppressor of Hairless directly activates transcription of Enhancer of split Complex genes in response to Notch receptor activity. Genes Dev. 9, 2609-2622.

Bang, A.G., Bailey, A.M., Posakony, J.W., 1995. *Hairless* promotes stable commitment to the sensory organ precursor cell fate by negatively regulating the activity of the *Notch* signaling pathway. Dev. Biol. 172, 479-494.

Bardin, A., Schweisguth, F., 2006. Bearded family members inhibit Neuralized-mediated endocytosis and signaling activity of Delta in *Drosophila*. Dev. Cell 10, 245-255.

Barolo, S., Stone, T., Bang, A.G., Posakony, J.W., 2002. Default repression and Notch signaling: Hairless acts as an adaptor to recruit the corepressors Groucho and dCtBP to Suppressor of Hairless. Genes Dev. 16, 1964-1976.

Bettenhausen, B., de Angelis, M.H., Simon, D., Guénet, J.-L., Gossler, A., 1995. Transient and restricted expression during mouse embryogenesis of *Dll1*, a murine gene closely related to *Drosophila Delta*. Development 121, 2407-2418.

Blaumueller, C.M., Qi, H., Zagouras, P., Artavanis-Tsakonas, S., 1997. Intracellular cleavage of Notch leads to a heterodimeric receptor on the plasma membrane. Cell 90, 281-291.

Bodner, R.A., 2002. Transcriptional regulation and function of the *Drosophila* Bearded family of Notch pathway genes. PhD Dissertation, Department of Biology, University of California San Diego.

Boulianne, G.L., de la Concha, A., Campos-Ortega, J.A., Jan, L.Y., Jan, Y.N., 1991. The *Drosophila* neurogenic gene *neuralized* encodes a novel protein and is expressed in precursors of larval and adult neurons. EMBO J. 10, 2975-2983.

Breeden, L., Nasmyth, K., 1987. Similarity between cell-cycle genes of budding yeast and fission yeast and the *Notch* gene of *Drosophila*. Nature 329, 651-654.

Casali, A., Batlle, E., 2009. Intestinal stem cells in mammals and *Drosophila*. Cell Stem Cell 4, 124-127.

Castro, B., Barolo, S., Bailey, A.M., Posakony, J.W., 2005. Lateral inhibition in proneural clusters: cis-regulatory logic and default repression by Suppressor of Hairless. Development 132, 3333-3344.

Cau, E., Blader, P., 2009. Notch activity in the nervous system: to switch or not to switch? Neural Dev. 4, 36.

Chitnis, A.B., 1995. The role of Notch in lateral inhibition and cell fate specification. Mol. Cell. Neurosci. 6, 311-321.

Coffman, C., Harris, W., Kintner, C., 1990. *Xotch*, the *Xenopus* homolog of *Drosophila Notch*. Science 249, 1438-1441

Commisso, C., Boulianne, G.L., 2007. The NHR1 domain of Neuralized binds Delta and mediates Delta trafficking and Notch signaling. Mol. Biol. Cell 18, 1-13.

Cordle, J., Johnson, S., Tay, J.Z.Y., Roversi, P., Wilkin, M.B., de Madrid, B.H., Shimizu, H., Jensen, S., Whiteman, P., Jin, B., Redfield, C., Baron, M., Lea, S.M., Handford, P.A., 2008. A conserved face of the Jagged/Serrate DSL domain is involved in Notch *trans*-activation and *cis*-inhibition. Nat. Struct. Mol. Biol. 15, 849-857.

Cubas, P., de Celis, J.-F., Campuzano, S., Modolell, J., 1991. Proneural clusters of *achaete-scute* expression and the generation of sensory organs in the *Drosophila* imaginal wing disc. Genes Dev. 5, 996-1008.

de La Coste, A., Freitas, A.A., 2006. Notch signaling: Distinct ligands induce specific signals during lymphocyte development and maturation. Immunol. Lett. 102, 1-9.

De Renzis, S., Yu, J., Zinzen, R., Wieschaus, E., 2006. Dorsal-ventral pattern of Delta trafficking is established by a Snail-Tom-Neuralized pathway. Dev. Cell 10, 257-264.

De Strooper, B., Annaert, W., Cupers, P., Craessaerts, K., Mumm, J.S., Schroeter, E.H., Schrijvers, V., Wolfe, M.S., Ray, W.J., Goate, A., Kopan, R., 1999. A presenilin-1-dependent gamma-secretase-like protease mediates release of Notch intracellular domain. Nature 398, 518-522.

Delidakis, C., Artavanis-Tsakonas, S., 1992. The Enhancer of split [*E*(*spl*)] locus of *Drosophila* encodes seven independent helix-loop-helix proteins. Proc. Natl. Acad. Sci. USA 89, 8731-8735.

Dexter, J.S., 1914. The analysis of a case of continuous variation in Drosophila by a study of its linkage relations. The American Naturalist 48, 712-758.

Dunwoodie, S.L., 2009. The role of Notch in patterning the human vertebral column. Curr. Opin. Genet. Dev. 19, 329-337.

Dunwoodie, S.L., Henrique, D., Harrison, S.M., Beddington, R.S.P., 1997. Mouse *Dll3*: a novel divergent *Delta* gene which may complement the function of other *Delta* homologues during early pattern formation in the mouse embryo. Development 124, 3065-3076.

Ellisen, L.W., Bird, J., West, D.C., Soreng, A.L., Reynolds, T.C., Smith, S.D., Sklar, J., 1991. *TAN-1*, the human homolog of the Drosophila *Notch* gene, is broken by chromosomal translocations in T lymphoblastic neoplasms. Cell 66, 649-661.

Fleming, R.J., Scottgale, T.N., Diederich, R.J., Artavanis-Tsakonas, S., 1990. The gene *Serrate* encodes a putative EGF-like transmembrane protein essential for proper ectodermal development in *Drosophila melanogaster*. Genes Dev. 4, 2188-2201.

Fontana, J.R., Posakony, J.W., 2009. Both inhibition and activation of Notch signaling rely on a conserved Neuralized-binding motif in Bearded proteins and the Notch ligand Delta. Dev. Biol. 333, 373-385.

Fortini, M.E., Artavanis-Tsakonas, S., 1994. The Suppressor of Hairless protein participates in Notch receptor signaling. Cell 79, 273-282.

Frise, E., Knoblich, J.A., Younger-Shepherd, S., Jan, L.Y., Jan, Y.N., 1996. The *Drosophila* Numb protein inhibits signaling of the Notch receptor during cell-cell interaction in sensory organ lineage. Proc. Natl. Acad. Sci. USA 93, 11925-11932.

Gho, M., Bellaïche, Y., Schweisguth, F., 1999. Revisiting the *Drosophila* microchaete lineage: a novel intrinsically asymmetric cell division generates a glial cell. Development 126, 3573-3584.

Giot, L., Bader, J.S., Brouwer, C., Chaudhuri, A., Kuang, B., Li, Y., Hao, Y.L., Ooi, C.E., Godwin, B., Vitols, E., Vijayadamodar, G., Pochart, P., Machineni, H., Welsh, M., Kong, Y., Zerhusen, B., Malcolm, R., Varrone, Z., Collis, A., Minto, M., Burgess, S., Mcdaniel, L., Stimpson, E., Spriggs, F., Williams, J., Neurath, K., Ioime, N., Agee, M., Voss, E., Furtak, K., Renzulli, R., Aanensen, N., Carrolla, S., Bickelhaupt, E., Lazovatsky, Y., Dasilva, A., Zhong, J., Stanyon, C.A., Finley Jr., R.L., White, K.P., Braverman, M., Jarvie, T., Gold, S., Leach, M., Knight, J., Shimkets, R.A., Mckenna, M.P., Chant, J., Rothberg, J.M., 2003. A protein interaction map of *Drosophila melanogaster*. Science 302, 1727-1736.

Guo, M., Jan, L.Y., Jan, Y.N., 1996. Control of daughter cell fates during asymmetric division: Interaction of Numb and Notch. Neuron 17, 27-41.

Hartenstein, V., Posakony, J.W., 1989. Development of adult sensilla on the wing and notum of *Drosophila melanogaster*. Development 107, 389-405.

Jakobsson, L., Bentley, K., Gerhardt, H., 2009. VEGFRs and Notch: a dynamic collaboration in vascular patterning. Biochem. Soc. Trans. 37, 1233-1236.

Käsbauer, T., Towb, P., Alexandrova, O., David, C.N., Dall'Armi, E., Staudigl, A., Stiening, B., Böttger, A., 2007. The Notch signaling pathway in the cnidarian *Hydra*. Dev. Biol. 303, 376-390.

Kidd, S., Lockett, T.J., Young, M.W., 1983. The *Notch* locus of Drosophila melanogaster. Cell 34, 421-433.

Kidd, S., Kelley, M.R., Young, M.W., 1986. Sequence of the Notch locus of *Drosophila melanogaster*: Relationship of the encoded protein to mammalian clotting and growth factors. Mol. Cell. Biol. 6, 3094-3108.

Knust, E., Schrons, H., Grawe, F., Campos-Ortega, J.A., 1992. Seven genes of the *Enhancer of split* Complex of *Drosophila melanogaster* encode helix-loop-helix proteins. Genetics 132, 505-518.

Kopan, R., Ilagan, M.X.G., 2009. The canonical Notch signaling pathway: unfolding the activation mechanism. Cell 137, 216-233.

Kopczynski, C.C., Alton, A.K., Fechtel, K., Kooh, P.J., Muskavitch, M.A.T., 1988. *Delta*, a *Drosophila* neurogenic gene, is transcriptionally complex and encodes a protein related to blood coagulation factors and epidermal growth factor of vertebrates. Genes Dev. 2, 1723-1735.

Lai, E.C., 1999. Regulation of pattern formation during development of the *Drosophila* peripheral nervous system. PhD Dissertation, Department of Biology, University of California San Diego.

Lai, E.C., Posakony, J.W., 1997. The Bearded box, a novel 3′ UTR sequence motif, mediates negative post-transcriptional regulation of *Bearded* and *Enhancer of split* Complex gene expression. Development 124, 4847-4856.

Lai, E.C., Burks, C., Posakony, J.W., 1998. The K box, a conserved 3′ UTR sequence motif, negatively regulates accumulation of *Enhancer of split* Complex transcripts. Development 125, 4077-4088.

Lai, E.C., Bodner, R., Kavaler, J., Freschi, G., Posakony, J.W., 2000a. Antagonism of Notch signaling activity by members of a novel protein family encoded by the Bearded and Enhancer of split gene complexes. Development 127, 291-306.

Lai, E.C., Bodner, R., Posakony, J.W., 2000b. The Enhancer of split Complex of *Drosophila* includes four Notch-regulated members of the Bearded gene family. Development 127, 3441-3455.

Lai, E.C., Deblandre, G.A., Kintner, C., Rubin, G.M., 2001. *Drosophila* Neuralized is a ubiquitin ligase that promotes the internalization and degradation of Delta. Dev. Cell 1, 783-794.

Lai, E.C., Wiel., C., Rubin, G.M., 2004. Complementary miRNA pairs suggest a regulatory role for miRNA:miRNA duplexes. RNA 10, 171-175.

Lai, E.C., Roegiers, F., Qin, X., Jan, Y.N., Rubin, G.M., 2005a. The ubiquitin ligase *Drosophila* Mind bomb promotes Notch signaling by regulating the localization and activity of Serrate and Delta. Development 132, 2319-2332.

Lai, E., Tam, B., Rubin, G., 2005b. Pervasive regulation of *Drosophila* Notch target genes by GY-box-, Brd-box-, and K-box-class microRNAs. Genes Dev. 19, 1067-1080.

Le Bornge, R., Bardin, A., Schweisguth, F., 2005a. The roles of receptor and ligand endocytosis in regulating Notch signaling. Development 132, 1751-1762.

Le Borgne, R., Remaud, S., Hamel, S., Schweisguth, F., 2005b. Two distinct E3 ubiquitin ligases have complementary functions in the regulation of Delta and Serrate signaling in *Drosophila*. PLoS Biol. 3, e96.

Lecourtois, M., Schweisguth, F., 1995. The neurogenic Suppressor of Hairless DNA-binding protein mediates the transcriptional activation of the *Enhancer of split* Complex genes triggered by Notch signaling. Genes Dev. 9, 2598-2608.

Leviten, M.W., Posakony, J.W., 1996. Gain-of-function alleles of *Bearded* interfere with alternative cell fate decisions in *Drosophila* adult sensory organ development. Dev. Biol. 176, 264-283.

Leviten, M.W., Lai, E.C., Posakony, J.W., 1997. The *Drosophila* gene *Bearded* encodes a novel small protein and shares 3′ UTR sequence motifs with multiple *Enhancer of split* Complex genes. Development 124, 4039–4051.

Lindsell, C.E., Shawber, C.J., Boulter, J., Weinmaster, G., 1995. Jagged: A mammalian ligand that activates Notch1. Cell 80, 909-917.

Logeat, F., Bessia, C., Brou, C., LeBail, O., Jarriault, S., Seidah, N.G., Israël, A., 1998. The Notch1 receptor is cleaved constitutively by a furin-like convertase. Proc. Natl. Acad. Sci. USA 95, 8108-8112.

Lux, S.E., John, K.M., Bennett, V., 1990. Analysis of cDNA for human erythrocyte ankyrin indicates a repeated structure with homology to tissue-differentiation and cell-cycle control proteins. Nature 344, 36-42.

Mohr, O.L., 1919. Character changes caused by mutation of an entire region of a chromosome in Drosophila. Genetics 4, 275-282.

Muskavitch, M.A.T., 1994. Delta-Notch signaling and *Drosophila* cell fate choice. Dev. Biol. 166, 415-430.

Niessen, K., Karsan, A., 2008. Notch signaling in cardiac development. Circ. Res. 102, 1169-1181.

Overstreet, E., Fitch, E., Fischer, J.A., 2004. Fat facets and Liquid facets promote Delta endocytosis and Delta signaling in the signaling cells. Development 131, 5355-5366.

Pan, D., Rubin, G.M., 1997. Kuzbanian controls proteolytic processing of Notch and mediates lateral inhibition during Drosophila and vertebrate neurogenesis. Cell 90, 271-280.

Petcherski, A.G., Kimble, J., 2000. Mastermind is a putative activator for Notch. Curr. Biol. 10, R471-R473.

Posakony, J.W., 1994. Nature versus nurture: asymmetric cell divisions in Drosophila bristle development. Cell 76, 415-418.

Radtke, F., Wilson, A., MacDonald, H.R., 2005. Notch signaling in hematopoiesis and lymphopoiesis: lessons from *Drosophila*. Bioessays 27, 1117-1128.

Reaume, A.G., Conlon, R.A., Zirngibl, R., Yamaguchi, T.P., Rossant, J., 1992. Expression analysis of a *Notch* homologue in the mouse embryo. Dev. Biol. 154, 377-387.

Rebay, I., Fleming, R.J., Fehon, R.G., Cherbas, L., Cherbas, P., Artavanis-Tsakonas, S., 1991. Specific EGF repeats of Notch mediate interactions with Delta and Serrate: Implications for Notch as a multifunctional receptor. Cell 67, 687-699.

Rechsteiner, M., 1988. Regulation of enzyme levels by proteolysis: the role of PEST regions. Adv. Enzyme Regul. 27, 135-151.

Rhyu, M.S., Jan, L.Y., Jan, Y.N., 1994. Asymmetric distribution of numb protein during division of the sensory organ precursor cell confers distinct fates to daughter cells. Cell 76, 477-491.

Roth, S., 2001. *Drosophila* oogenesis: Coordinating germ line and soma. Curr. Biol. 11, R779-R781

Shawber, C., Boulter, J., Lindsell, C.E., Weinmaster, G., 1996. *Jagged2*: A Serrate-like gene expressed during rat embryogenesis. Dev. Biol. 180, 370-376.

Shimizu, K., Chiba, S., Kumano, K., Hosoya, N., Takahashi, T., Kanda, Y., Hamada, Y., Yazaki, Y., Hirai, H., 1999. Mouse Jagged1 physically interacts with Notch2 and other Notch receptors. J. Biol. Chem. 274, 32961-32969.

Shutter, J.R., Scully, S., Fan, W., Richards, W.G., Kitajewski, J., Deblandre, G.A., Kintner, C.R., Stark, K.L., 2000. *Dll4*, a Notch ligand expressed in arterial endothelium. Genes Dev. 14, 1313-1318.

Skeath, J.B., Carroll, S.B., 1991. Regulation of *achaete-scute* gene expression and sensory organ pattern formation in the *Drosophila* wing. Genes Dev. 5, 984-995.

Skwarek, L., Garroni, M.K., Commisso, C., Boulianne, G.L., 2007. Neuralized contains a phosphoinositide-binding motif required downstream of ubiquitination for Delta endocytosis and Notch signaling. Dev. Cell 13, 783-795.

Sotillos, S., Roch, F., Campuzano, S., 1997. The metalloprotease-disintegrin Kuzbanian participates in Notch activation during growth and patterning of *Drosophila* imaginal discs. Development 124, 4769-4779.

Strizzi, L., Hardy, K.M., Seftor, E.A., Costa, F.F., Kirschmann, D.A., Seftor, R.E.B., Postovit, L.-M., Hendrix, M.J.C., 2009. Development and cancer: At the crossroads of Nodal and Notch signaling. Cancer Res. 69, 7131-7134.

Struhl, G., Adachi, A., 1998. Nuclear access and action of Notch in vivo. Cell 93, 649-660.

Tamura, K., Taniguchi, Y., Minoguchi, S., Sakai, T., Tun, T., Furukawa, T., Honjo, T., 1995. Physical interaction between a novel domain of the receptor Notch and the transcription factor RBP-Jκ/Su(H). Curr. Biol. 5, 1416-1423.

Tax, F.E., Yeargers, J.J., Thomas, J.H., 1994. Sequence of *C. elegans lag-2* reveals a cell-signalling domain shared with *Delta* and *Serrate* of *Drosophila*. Nature 368, 150-154.

Thomas, U., Speicher, S.A., Knust, E., 1991. The *Drosophila* gene *Serrate* encodes an EGF-like transmembrane protein with a complex expression pattern in embryos and wing discs. Development 111, 749-761.

Vässin, H., Bremer, K.A., Knust, E., Campos-Ortega, J.A., 1987. The neurogenic gene Delta of *Drosophila melanogaster* is expressed in neurogenic territories and encodes a putative transmembrane protein with EGF-like repeats. EMBO J. 6, 3431-3440.

Vasyutina, E., Lehhard, D.C., Birchmeier, C., 2007. Notch function in myogenesis. Cell Cycle 6, 1451-1454.

Wang, W., Struhl, G., 2004. *Drosophila* Epsin mediates a select endocytic pathway that DSL ligands must enter to activate Notch. Development 131, 5367-5380.

Wang, W., Struhl, G., 2005. Distinct roles for Mind bomb, Neuralized and Epsin in mediating DSL endocytosis and signaling in *Drosophila*. Development 132, 2883-2894.

Weinmaster, G., Roberts, V.J., Lemke, G., 1991. A homolog of *Drosophila Notch* expressed during mammalian development. Development 113, 199-205.

Wendland, B., 2002. Epsins: adaptors in endocytosis? Nat. Rev. Mol. Cell Biol. 3, 971-977.

Wharton, K.A., Johansen, K.M., Xu, T., Artavanis-Tsakonas, S., 1985. Nucleotide sequence from the neurogenic locus Notch implies a gene product that shares homology with proteins containing EGF-like repeats. Cell 43, 567-581.

Wurmbach, E., Wech, I., Preiss, A., 1999. The *Enhancer of Split* complex of *Drosophila melanogaster* harbors three classes of Notch responsive genes. Mech. Dev. 80, 171-180.

Yeh, E., Zhou, L., Rudzik, N., Boulianne, G.L., 2000. Neuralized functions cell autonomously to regulate *Drosophila* sense organ development. EMBO J. 19, 4827-4837.

Yeh, E., Dermer, M., Commisso, C., Zhou., L., McGlade, C.J., Boulianne, G.L., 2001. Neuralized functions as an E3 ubiquitin ligase during *Drosophila* development. Curr. Biol. 11, 1675-1679.

Yochem, J., Weston, K., Greenwald, I., 1988. The *Caenorhabditis elegans lin-12* gene encodes a transmembrane protein with overall similarity to *Drosophila Notch*. Nature 335, 547-550.

Yochem, J., Greenwald, I., 1989. *glp-1* and *lin-12*, genes implicated in distinct cell-cell interactions in C. elegans, encode similar transmembrane proteins. Cell 58, 553-563.

Zaffran, S., Frasch, M., 2000. *Barbu*: an *E(spl) m4/m*α-related gene that antagonizes Notch signaling and is required for the establishment of ommatidial polarity. Development 127, 1115-1130.

Chapter 1

Both inhibition and activation of Notch signaling rely on a conserved Neuralized-binding motif in Bearded proteins and the Notch ligand Delta

Abstract

Lateral inhibition is one of the key functions of Notch signaling during animal development. In the proneural clusters that give rise to *Drosophila* mechanosensory bristles, Delta (Dl) ligand in the sensory organ precursor (SOP) cell is targeted for ubiquitination by the E3 ligase Neuralized (Neur), resulting in activation of Dl's capacity to signal to the Notch receptor on neighboring cells. The cells that receive this signal activate a genetic program that suppresses their SOP fate potential, insuring that only a single SOP develops within each cluster. Using multiple lines of investigation, we provide evidence that members of the Bearded family of proteins (BFMs) inhibit Dl activation in non-SOP cells by binding to Neur and preventing it from interacting with Dl. We show that this activity of BFMs is dependent on the conserved NXXN motif, and report the unexpected finding that several BFMs include multiple functional copies of this motif. We find that a conserved NXXN motif in the intracellular domain of Dl is responsible for its interaction with Neur, indicating direct competition between Dl and BFMs for binding to Neur, and we show that Neur-dependent endocytosis of Dl requires the integrity of its NXXN motif. Our results illuminate the mechanism of an important regulatory event in Notch signaling that appears to be conserved between insects and crustaceans.

Introduction

The evolutionarily conserved Notch cell-cell signaling pathway is utilized extensively for cell fate specification in developing metazoans. During peripheral nervous system (PNS) development in *Drosophila*, Notch-mediated lateral inhibition results in the specification of a single sensory organ precursor (SOP) cell from a field of cells, known as a proneural cluster (PNC), that all express proneural transcriptional activator proteins and hence have SOP cell fate potential. In the SOP, the Notch ligand Delta (Dl) is targeted by the E3 ubiquitin ligase Neuralized (Neur), which leads to Dl's ubiquitination and endocytosis (Deblandre et al., 2001; Lai et al., 2001; Pavlopoulos et al., 2001), processes necessary to make the SOP an effective Notch pathway signaling cell (Pavlopoulos et al., 2001; Li and Baker, 2004; Wang and Struhl, 2004). In response to this signal from the SOP, the surrounding cells in the PNC activate a genetic program that suppresses their potential to become SOPs and commits them instead to an epidermal fate. Among the direct transcriptional targets of the Notch pathway in responding cells are the basic helix-loop-helix (bHLH) repressor genes of the *Enhancer of split* Complex [E(spl)-C] and members of the *Bearded* (*Brd*) family of genes, which reside in the E(spl)-C and in the *Brd* Complex (Brd-C) (Bailey and Posakony, 1995; Furukawa et al., 1995; Lecourtois and Schweisguth, 1995; Nellesen et al., 1999; Lai et al., 2000a; Lai et al., 2000b).

The *Brd* gene family was discovered through genetic and molecular analysis of a gain-of-function mutation of the *Brd* gene that confers mutant phenotypes in the adult PNS suggestive of a loss of Notch signaling capacity, including a bristle “tufting” effect resulting from the failure of lateral inhibition (Leviten and Posakony, 1996; Leviten et al., 1997). Indeed, it was subsequently shown that nearly all *Brd* family genes, including the E(spl)-C genes *mα*, *m4*, and *m6*, and the Brd-C genes *Brd*, *Brother of Bearded* (*Bob*), *Twin of m4* (*Tom*), and *Ocho*, produce a similar Notch pathway loss-of-function phenotype when over- or misexpressed in PNCs (Apidianakis et al., 1999; Lai et al., 2000a; Lai et al., 2000b; Zaffran and Frasch, 2000). In contrast, the E(spl)-C *Brd* family gene *m2* produces an oppositely directed phenotype (SOP loss) when misexpressed, reminiscent of Notch pathway hyperactivity (Lai et al., 2000b).

Brd family genes, which have thus far been found only in insects (Lai et al., 2000b; Lai et al., 2005; Schlatter and Maier, 2005), encode small proteins (70–218 a.a. in *Drosophila*) that are characterized by a predicted highly basic amphipathic alpha-helix located near the N terminus, termed the B domain (Leviten et al., 1997; Lai et al., 2000a; Lai et al., 2000b). The canonical members of the family in *Drosophila*, E(spl)mα, E(spl)m4, Tom, and Ocho, also share three additional conserved motifs (Lai et al., 2000a; Lai et al., 2000b): the N motif [NxANE(K/R)L], the G motif (VPVHFARTXXGTFFWT), and the D motif [DRW(A/V)QA]. The non-canonical family members [Brd, Bob, E(spl)m2,

and E(spl)m6] contain one or two of these additional motifs, with E(spl)m2 being the only family member that does not bear an N motif (Leviten et al., 1997; Lai et al., 2000a; Lai et al., 2000b).

An interaction between Brd family proteins and Neur was first revealed in a comprehensive yeast two-hybrid screen, which detected Tom as a partner for Neur (Giot et al., 2003). Subsequent studies showed that, during the Notch-mediated specification of the mesoderm-ectoderm boundary in the *Drosophila* embryo, Tom acts as a Neur antagonist, capable of preventing the Neur-dependent endocytosis of Dl (Bardin and Schweisguth, 2006; De Renzis et al., 2006). It was also found that Tom can interfere with the co-immunoprecipitation of Dl and Neur in a cell culture assay, suggesting that Tom inhibits Dl-Neur binding (Bardin and Schweisguth, 2006). The N motif of Tom was shown to be important for its interaction with Neur, in that deletion or mutation of the motif weakened the interaction in both the yeast two-hybrid and co-immunoprecipitation assays. While these studies illuminated the interaction between Brd family proteins and Neur, the interaction between Neur and the Notch ligands Dl and Serrate (Ser) remains poorly understood. Furthermore, a requirement for the N motif in the inhibitory activities of Brd family proteins has not been demonstrated.

In this study, we have investigated the function of Brd proteins during lateral inhibition. We report the unexpected finding that the canonical Brd proteins E(spl)mα and E(spl)m4 contain multiple N motifs,

and we show that these sequences are responsible for mediating the interaction with Neur. Integrity of these N motifs is also required for the capacity of E(spl)mα and E(spl)m4 to disrupt Neur-Dl binding in vitro and to interfere with lateral inhibition in vivo. Our definition of a more comprehensive consensus for the N motif permitted us to identify it as a conserved feature of the intracellular domains of arthropod Dl and Ser proteins. We show that, as for Brd proteins, Dl's N motif is required for its binding to Neur in vitro, and we present in vivo evidence that the motif is also required for Neur-dependent endocytosis of Dl. We therefore propose that Brd family proteins antagonize Notch signaling by competing directly with Dl for N motif-mediated binding to Neur. Finally, we report the existence of a gene encoding a Brd family protein in the crustacean *Daphnia pulex*, pushing the known origin of this family back to more than 400 Mya. We show that this protein interacts specifically with *Drosophila* Neur in vitro, indicating the long-term evolutionary conservation of this key BFM activity.

Materials and Methods

GAL4/UAS driver and responder lines

The following GAL4 driver lines were used for mis- or overexpression of *UAS* responder transgenes: *yw*; *sca-GAL4* (Hinz et al., 1994; Nakao and Campos-Ortega, 1996); w^{1118} *E(spl)mα-GAL4* (Castro et al., 2005); *yw;* $neur^{P72}$*-GAL4 UAS-PonGFP/TM6C* (Bellaiche et al., 2001); and w^{1118}*; dpp-GAL4/CyO* (kindly provided by Ethan Bier). *UAS-neur* and *UAS-GFP* (*UAS-Stinger*) have been described previously (Barolo et al., 2000; Lai and Rubin, 2001).

Generation of pUAST-V5-HIS

To create a UAS vector capable of C-terminally tagging expressed proteins with a V5 epitope and polyhistidine sequence, the multiple cloning site (MCS) and epitope region of the vector pAc5.1-V5-HIS-A (Invitrogen) were amplified using the forward primer GGCAATTGGGTACCTACTAGTCCAGT and the reverse primer GGGCTAGCCCTTAGAAGGCACAGTCGA, which introduce a 5′ MfeI site and 3′ NheI site. This amplicon was cloned into the pUAST vector (Brand and Perrimon, 1993) cut with EcoRI and XbaI, replacing the entire MCS of pUAST with this new sequence.

Misexpression constructs

FLAG-m4 constructs were generated by introducing the codons for a 1x FLAG tag (DYKDDDDK) after the starting M codon of *E(spl)m4*; 20 bp of the gene's 3′ UTR sequence were also included in the construct.

E(spl)mα constructs included 7 bp of 5′ UTR sequence along with the coding sequence. *Dl* and Dl^{N} constructs were generated using the full *Dl* coding sequence, isolated from w^{1118} embryo cDNA. Dl^{N} was mutated so as to encode the NEQNAV→AAAAAA substitution illustrated in Figure 1.6C. These transgenes were cloned into the pUAST vector or the pUAST-V5-HIS vector and transformed into *Drosophila* using a standard P transposable element injection protocol (Rubin and Spradling, 1982).

By in situ hybridization to late third-instar wing discs, we verified that transcripts from the various *E(spl)m4* and *E(spl)mα UAS* transgenes accumulate to comparable levels when driven by *sca-GAL4* (see Figure 1.S1).

In vitro constructs

Plasmid constructs encoding GST-tagged and His-tagged proteins were generated by cloning into pGEX-5X (Amersham Biosciences) and pRSET (Invitrogen) vectors, respectively. *His-mα*, *His-m4*, $His\text{-}Dl^{intra}$, and *His-DpBFM* constructs all contained 7 bp of 5′ UTR from *E(spl)mα* along with their respective coding sequences. *His-mα-N* encodes a peptide that includes amino acids 63-80 of *E(spl)mα*, centered on the N motif (AEID**ENAANEKL**AQLAHS). *His-mα-N mutant* substitutes the two asparagine residues of the core NXXN motif with alanines (AEIDEAAAAEKLAQLAHS). $His\text{-}Hairless^{148\text{-}311}$ ($His\text{-}H^{148\text{-}311}$) encodes amino acids 148-311 of the Hairless protein, and was kindly provided by Feng Liu.

Bristle count assays

For *Brd* family gain-of-function phenotypes, 25 females per independent insertion line, from 2-4 representative lines per construct, were scored for the number of extra bristles present at 18 notum positions (notopleurals, presuturals, supra-alars, post-alars, dorsocentrals) and eight head positions (post-verticals, inner verticals, outer verticals, occellars), for a total of 26 bristle positions. The GAL4 drivers *sca-GAL4*, *E(spl)mα-GAL4*, and *neur-GAL4* were used to direct expression in PNCs, non-SOPs of the cluster, and SOPs, respectively.

In vitro pulldown assays: preparation of tagged proteins

Tagged proteins were expressed in *E. coli* strain BL21(DE3) using an IPTG-inducible T7 promoter. Bacterial cultures were grown at 37°C to OD_{600}=0.6-0.7, induced with 0.8 mM IPTG, and incubated for 3 h at 30°C. Bacteria were spun down at 6000 x g for 15 min and pellets were frozen at −80°C.

Bacterial pellets for His-tagged proteins were resuspended in Cell Lysis Buffer (20 mM Tris-HCl pH 8.0; 200 mM NaCl; 0.5% Nonidet P-40; 2 µg/mL Aprotenin; 2 µg/mL Leupeptin; 0.2 mM PMSF; 1 µg/mL Pepstatin A) (2.5 mL per 40 mL culture) and lysed with 100 µg/mL lysozyme for 30 min on ice. 5 mM DTT was added, and the lysate was sonicated and centrifuged at 4°C for 25 min at 10,000 x g. Supernatant containing the His-tagged protein was saved and used directly for the pulldown assays.

His-Neur lysate was not subjected to the last centrifugation step, and was instead run through a 25-gauge needle five times.

Bacterial pellets for GST-tagged proteins were resuspended in STE buffer [10 mM Tris-HCl pH 8.0; 150 mM NaCl; 1 mM EDTA; 2 µg/mL Aprotenin; 2 µg/mL Leupeptin; 0.2 mM PMSF; 1 µg/mL Pepstatin A; (Mercado-Pimentel et al., 2002)] (6 mL per 100 mL culture) and lysed with 100 µg/mL lysozyme for 30 min on ice. 1% Sarcosyl and 5 mM DTT were added, and the lysate was sonicated and centrifuged at 4°C for 25 min at 10,000 x g. The cleared lysate was incubated with Glutathione Sepharose 4B beads (GE Healthcare Life Sciences) for 3-4 h at 4°C with rocking to bind the GST-tagged proteins. Beads were washed 4x with Cell Lysis Buffer and this purified sample was used for the pulldown assay.

In vitro pulldown assays: assay conditions

For GST-Neur pulldowns, 25 µL of packed Glutathione Sepharose beads with bound GST-tagged protein was incubated with His-tagged protein lysate in Cell Lysis Buffer in a total volume of 400 µL for 2-4 h at 4°C with rocking. Beads were spun down at 300 x g for 1.5 min and washed 3x, 1 mL each, with Cell Lysis Buffer minus protease inhibitors. Washed resin was resuspended in SDS-loading dye with 10 mM DTT, boiled for 6 min and Western blotted using standard procedures. Mouse anti-HisG antibody (Invitrogen) was used at a 1:5000 dilution and goat anti-mouse-HRP (Jackson Laboratories) was used at 1:10,000. Western

Lightning Chemiluminescence Reagent Plus (NEL105, Perkin-Elmer) was used for detection.

For GST-Dl^{intra} pulldowns, 25 µL of packed Glutathione Sepharose beads with bound GST-tagged protein was incubated with His-Neur in Cell Lysis Buffer in a total volume of 400 µL for 2 h at 4°C with rocking. Resin was spun down at 300 x g for 1.5 min, and the supernatant was removed. His-tagged competitors in Cell Lysis Buffer were added to a total volume of 400 µL and incubated at 4°C for 2 h with rocking. Resin was spun, washed, resuspended, and blotted as above.

For all assays, we verified by Coomassie staining that the amount of control GST protein bound to the beads was at least equal to, and in most cases greatly exceeded, the amount of experimental GST-X protein.

Immunohistochemistry

Late third-instar larvae were dissected in phosphate-buffered saline (PBS) + 0.1% Triton X-100, fixed for 25 min with 4% paraformaldehyde in PBS + 0.3% Triton X-100, and washed 5 x 10 min with PBS + 0.1% Triton X-100. Misexpressed mα-V5-HIS variants were visualized with mouse monoclonal anti-V5 (Invitrogen) diluted 1:400 and Alexa Fluor 488 donkey anti-mouse IgG (Molecular Probes) diluted 1:500. Misexpressed Dl and Dl^{N} were visualized with mouse monoclonal anti-Dl (C594-9B; Developmental Studies Hybridoma Bank) diluted 1:100 and Alexa Fluor 488 donkey anti-mouse IgG diluted 1:500. Images were acquired on a Leica TCS SP2 confocal microscope.

Identification and cloning of a Daphnia Brd family gene (Dp BFM)

Using a TBLASTN search with *Drosophila* bHLH repressor (bHLH-R) sequences on the *Daphnia pulex* genome (http://wfleabase.org/), we identified three bHLH-R genes on scaffold 170. Loading the scaffold sequence into GenePalette (Rebeiz and Posakony, 2004), we searched for conserved regulatory sequence motifs associated with *Brd* family genes in insects, including proneural protein (RCAGSTG) and Su(H) (YGTGDGAA) binding sites, as well as three 3′ UTR "seed" motifs that mediate miRNA recognition, the GY box (GTCTTCC), K box (TGTGAT), and Brd box (AGCTTTA). Scanning the scaffold for clusters of these motifs, we identified several regions with the potential to contain a *Brd* family gene; we then inspected the conceptual translations of these regions for the presence of conserved protein motifs typically found in Brd family proteins. The identified BFM was cloned from the Log50 strain of *D. pulex*, obtained from Dr. Matthias Westphal at the Center for Genomics and Bioinformatics, Indiana University, Bloomington.

Results

Cell-type origin of the Brd *family gain-of-function phenotype*

We have reported previously that over- or misexpression of seven of the eight *Brd* family genes in *Drosophila* [*E(spl)m2* being the exception] causes developmental defects consistent with a loss of Notch signaling activity; i.e., failure of lateral inhibition in PNCs and cell fate transformations in the sensory organ lineage (Lai et al., 2000a; Lai et al., 2000b). These studies made use of the *scabrous* (*sca*)-*GAL4* driver, which is active in both of the distinct cell populations within PNCs, the SOP and the surrounding non-SOP cells. The observed phenotypes could arguably be caused by overexpression - abnormally high levels of BFMs in their normal domain of expression (non-SOP cells), possibly producing a dominant-negative effect by sequestering some important factor(s) necessary for Notch signal transduction. Alternatively, these effects could be due to misexpression - BFMs mimicking their normal function in a cell type in which they are not normally expressed at any significant level (SOP cells). To distinguish between these possibilities, we made use of available GAL4 drivers with distinct expression specificities. When activated throughout the PNC using *sca-GAL4*, two independent insertions of a *UAS* construct expressing N-terminally FLAG-tagged E(spl)m4 (*UAS-FLAG-m4*) produce 27 and 34 extra bristles per fly, respectively, scored at 26 bristle positions on the notum and dorsal head of the fly (Figure 1.1A,B). Driving high levels of *FLAG-m4* expression

specifically in non-SOP cells using *E(spl)mα-GAL4* fails to produce any significant mutant phenotype, with 0.16 and 0.40 extra bristles per fly for the two insertions, respectively. By contrast, when *FLAG-m4* is misexpressed solely in SOPs using a *neur-GAL4* driver, a substantial disruption of lateral inhibition is observed (9.2 and 20 extra bristles per fly for the two *UAS* responder insertions, respectively), suggesting that misexpression of a BFM in the SOP disrupts the sending of the Dl signal from that cell, perhaps mimicking the normal function of BFMs in non-SOPs.

The basic amphipathic character of the B domain of E(spl)m4 is required for the gain-of-function phenotype

To gain a better understanding of the mechanism of Brd family protein activity during lateral inhibition, we sought to identify the properties of these proteins that are required to produce the characteristic gain-of-function phenotype (see Introduction and previous section). We had observed earlier that disrupting the helical nature of the B domain of Brd, via four proline substitutions on the hydrophobic helical face, has no significant effect on the protein's ability to produce a neurogenic phenotype when misexpressed (Lai, 1999). By contrast, substituting neutral alanine residues for the basic lysine residues of the B domain in either Brd or Bob was found to eliminate the gain-of-function phenotype. In the present study, we extended these findings on non-canonical BFMs by testing several variants of the canonical BFM E(spl)m4 (Figure 1.1C).

When misexpressed using the *sca-GAL4* driver, FLAG-m4 produces an average of 28.9 extra bristles per fly (Figure 1.1B,E). The FLAG-m4$^{4K/A}$ variant eliminates the four basic lysine residues of the B domain, substituting them with alanines, which should not disrupt the helical nature of this region (Figure 1.1C,D). This mutation nearly abolishes the protein's ability to produce extra bristles when misexpressed (2.46 extra bristles per fly; Figure 1.1E), phenocopying the results obtained with the corresponding mutants of Brd and Bob (Lai, 1999). To test whether the lysine residues of the B domain per se are required to produce the misexpression phenotype, the FLAG-m4$^{4K/R}$ variant was created, replacing the lysine residues with arginines while retaining both the helical nature and the strong basic amphipathicity of the domain (Figure 1.1C,D). Misexpression of FLAG-m4$^{4K/R}$ produces 23 extra bristles per fly, indicating a retained capacity to disrupt lateral inhibition (Figure 1.1E). These data indicate that the basic amphipathic nature of E(spl)m4's B domain is required to disrupt lateral inhibition when misexpressed, while the lysine residues themselves are dispensable.

The N motif of E(spl)m4 contributes to its misexpression phenotype

Outside of the four conserved domains/motifs found in canonical Brd family proteins, overall sequence similarity between the various family members is low (Lai et al., 2000a; Lai et al., 2000b). To assess the importance of the other conserved motifs in producing a misexpression phenotype, additional variants of FLAG-m4 were created that disrupt the

N, G, and D motifs (Figure 1.1C). The FLAG-m4^{N1} variant mutates the core of the N motif to alanines (NEANERL to NEAAAAL; Figure 1.1B). When misexpressed, this variant produces an average of 10.5 additional macrochaete bristles per fly, compared with the wild-type FLAG-m4 phenotype of 28.9 extra bristles (Figure 1.1E). This weakening of the misexpression phenotype was consistently observed with four independent insertions of the construct, and points to a role for the N motif in disrupting lateral inhibition, though it seems not to be strictly required.

Two different G-motif variants were constructed, FLAG-m4^{G1} mutating all 16 amino acids of the extended G motif (VPVHFVRTAHGTFFWT) to alanines, and FLAG-m4^{G2} mutating only the more highly conserved region (FWT) to alanines (Figure 1.1C). Both FLAG-m4^{G1} and FLAG-m4^{G2} produce strong misexpression phenotypes, an average of 36 and 39 extra macrochaetes per fly, respectively (Figure 1.1E). We conclude that the G motif of E(spl)m4 is not required for the misexpression phenotype.

The D motif consists of six amino acids found at the C terminus of the protein (DRWVQA); its disruption was accomplished with a stop-codon truncation of the protein just N-terminal to this motif (Figure 1.1C). We find that the FLAG-m4^{D} variant produces a misexpression phenotype of 29 extra bristles per fly (Figure 1.1E), very similar to that of wild-type FLAG-m4, indicating that the D motif is likewise not required for the disruption of lateral inhibition in this assay.

The recognized conserved motifs of E(spl)mα are not required for interaction with Neur in vitro

It has been reported that the interaction of the Brd protein Tom with the E3 ubiquitin ligase Neur is mediated by the N motif, and it was suggested that this interaction is the basis of Notch signaling inhibition in vivo (Bardin and Schweisguth, 2006). However, the fact that mutating the N motif of E(spl)m4 only reduced, but did not eliminate, the protein's ability to disrupt lateral inhibition when misexpressed in the SOP led us to believe that another, unidentified, motif may participate in this function.

To assess the role of each of its conserved domains/motifs in direct protein-protein interaction with Neur, His-tagged variants of E(spl)mα were generated, similar to those described above for E(spl)m4 (Figure 1.2A, upper image). Bacterial cell lysates containing these His-tagged proteins were used in a pulldown assay with bacterially expressed and purified GST-Neur, or GST, bound to Glutathione Sepharose beads. The His-tagged negative control, His-Hairless$^{148–311}$ (His-H$^{148-311}$) was chosen because it is of comparable size to His-mα and is not expected to have affinity for GST-Neur. Indeed, His-H$^{148-311}$ does not bind to GST-Neur in this assay, whereas His-mα shows a strong interaction (Figure 1.2B). The E(spl)mα variants His-mα$^{4K/R}$, His-mα^{N}, His-mα^{G2}, and His-mα^{D} also show efficient binding to GST-Neur, whereas His-mα$^{4K/A}$ shows a substantial decrease in binding (Figure 1.2B). These data indicate that none of the three identified motifs in E(spl)mα (N, G, or D) is required for strong in

vitro interaction with Neur, while loss of the basic amphipathic character of the B domain impairs, but does not eliminate, binding to Neur.

We note that while all His-mα variants display more than one band when electrophoresed on SDS-polyacrylamide gels, all but His-mα$^{4K/A}$ exhibit an upper band containing the great majority of the protein, with a minor lower band of variable intensity depending on the preparation. His-mα$^{4K/A}$ instead consistently displays a gel pattern with the majority of the protein in the lower band. While this major lower band of His-mα$^{4K/A}$ binds poorly to GST-Neur, the minor upper band binds relatively more strongly (Figure 1.2B). We suggest that this exceptional behavior of His-mα$^{4K/A}$ may be due to abnormal folding of at least a majority of the protein. In any case, we reasoned that the residual Neur interaction observed with His-mα$^{4K/A}$ might be mediated by a second motif that cooperates with the B domain. Based on our misexpression data (above) and a previous report (Bardin and Schweisguth, 2006), it seemed likely that the N motif fills this role.

To test our hypothesis that multiple elements of E(spl)mα are important for its interaction with Neur, additional variants of the protein were generated, each containing mutations in two or more domains/motifs. We find that the double mutants His-mα$^{4K/A, N}$ and His-mα$^{4K/A, G2}$ behave like His-mα$^{4K/A}$, in that they both display a major-lower-band gel pattern and interact poorly, though clearly detectably, with GST-

Neur (Figure 1.2C). By contrast, we were surprised to observe that elimination of the D motif in the double mutant His-m$\alpha^{4K/A, D}$ restores both the protein's wild-type gel migration pattern and its ability to bind efficiently to GST-Neur. Moreover, both the triple mutant His-m$\alpha^{N, G2, D}$ and the quadruple mutant His-m$\alpha^{4K/A, N, G2, D}$ likewise migrate quite normally and interact strongly with GST-Neur (Figure 1.2C). From these data we conclude that none of the recognized conserved domains/motifs of E(spl)mα is required for a strong interaction with Neur. The implication is that E(spl)mα contains one or more uncharacterized motifs capable of interacting with Neur.

The aberrant migration displayed by the His-m$\alpha^{4K/A}$ variant seems to result from disrupting the amphipathicity of the B domain [Figure 1.2B; recall that m$\alpha^{4K/R}$ displays a normal migration pattern (Figure 1.2B)]. We find that mutating the lysines of the B domain to uncharged, polar glutamines (m$\alpha^{4K/Q}$) produces this same effect, as does mutating only the five nonpolar residues of E(spl)mα's B domain to glutamine (m$\alpha^{5np/Q}$; data not shown; see Figure 1.2B). In all cases, deletion of the D motif in combination with the B domain mutation restores a wild-type gel migration pattern, as well as strong binding of the protein to Neur (data not shown).

E(spl)mα and E(spl)m4 each contain multiple N motifs capable of mediating interaction with Neur

Because we have observed that a truncated version of E(spl)mα, extending from the N terminus to a point just N-terminal to the N motif, is capable of binding to Neur (data not shown), we focused on this region in our search for a possible uncharacterized motif capable of interacting with Neur. Using the triple mutant His-mα$^{N, G2, D}$ as a backbone, we substituted large stretches of amino acids in the N-terminal portion of the protein with glutamine residues. The variant mα$^{X, N, G2, D}$ contains a poly-Q stretch covering amino acids 5–20, mα$^{B, N, G2, D}$ a.a. 21–38 (the entire B domain), mα$^{Y, N, G2, D}$ a.a. 39–53, and mα$^{Z, N, G2, D}$ a.a. 54–67 (just N-terminal to the N motif; Figure 1.2A, lower image).

Region X and the B domain are not required for interaction with Neur, as mutations in these blocks of amino acids did not affect the apparent affinity of the corresponding His-mα variants for GST-Neur (Figure 1.2D). However, binding to GST-Neur is completely eliminated for both His-mα$^{Y, N, G2, D}$ and His-mα$^{Z, N, G2, D}$ (Figure 1.2D), indicating that there exists at least one functional element in the section of E(spl)mα between the B domain and the N motif, possibly near the junction of the Y and Z regions (Figure 1.2A, lower image). Repeating the pulldown assay using E(spl)mα variants bearing fewer substituted amino acids in these two regions led to the discovery of an N-like motif [NLRNAQV, termed N′ (“N-prime”)] that spans the junction between Y and Z and is required for interaction with Neur in an mα$^{N, G2, D}$ background (data not shown). To

test the possibility that E(spl)mα contains two N motifs that are independently capable of mediating interaction with Neur, the single-motif mutant His-mα$^{N'}$ and the double mutant His-mα$^{N', N}$ were generated (Figure 1.2A). His-mα$^{N'}$ behaves like His-mα^{N} and interacts strongly with Neur, while the His-mα$^{N', N}$ variant lacks affinity for GST-Neur (Figure 1.2E). From these data we conclude that E(spl)mα contains two N motifs that are each individually capable of mediating a robust interaction with Neur.

The finding of a second N motif in E(spl)mα raised the possibility that other Brd family proteins may also contain additional N motifs. The previously recognized consensus sequence for the N motif was NXANE(K/R)L (Lai et al., 2000b). The N′ element in E(spl)mα shares only the core NXXN with this consensus. Using this simplified motif definition (with X≠N), we find that among the canonical Brd family proteins, E(spl)m4 contains three potential N motifs, while Tom and Ocho include two and one potential N motifs, respectively (Figure 1.3A). [We suggest that the existence of a second (N′) motif in Tom is likely to account for the failure of mutations affecting its original N motif to fully eliminate Tom-Neur co-immunoprecipitation (Bardin and Schweisguth, 2006).] The non-canonical family members Brd, Bob, and E(spl)m6 appear to contain only the single previously identified N motif, while E(spl)m2 has no N motifs, even with this looser definition. Aligning all of these N motifs yields the new consensus (D/E/Q)NXXNXX(L/M/V) (Figure 1.3A).

We sought to determine whether all three potential N motifs in E(spl)m4 are capable of mediating interaction with Neur by assaying the single-motif mutants His-m4^{N2}, His-m4$^{N'}$, and His-m4$^{N''}$, as well as the triple N-motif mutant and every combination of double N-motif mutant (Figure 1.3B,C). Consistent with the results obtained with E(spl)mα, E(spl)m4 is capable of interacting strongly with Neur as long as it contains any of the three N motifs. Binding to Neur is severely reduced only when all three N motifs are mutant (Figure 1.3C). Finally, in contrast to a previous finding concerning the N motif of Tom (Bardin and Schweisguth, 2006), we observe that a short peptide containing the N motif of E(spl)mα is sufficient to mediate a weak interaction with Neur in the pulldown assay, in a manner dependent on the two asparagine residues of the NXXN core (Figure 1.3D).

The N motifs of E(spl)mα and E(spl)m4 are required to disrupt the Neur-Dl interaction

We have seen that misexpression of BFMs in the SOP of a PNC prevents the SOP from sending an effective inhibitory signal to the Notch receptor on non-SOPs, thus disrupting lateral inhibition. Given their interaction with Neur (Giot et al., 2003; Bardin and Schweisguth, 2006), BFMs might do this either by interfering with the E3 ligase activity of Neur, thus preventing the conversion of Dl into an active ligand for Notch, or by interfering with the binding of Neur to its substrate Dl. To test this latter possibility, we employed an in vitro binding inhibition assay (Figure 1.4A).

Bacterially expressed, purified, GST-tagged Dl intracellular domain (GST-Dl^{intra}), bound to Glutathione Sepharose beads, was incubated with bacterial cell lysate containing His-tagged Neur (His-Neur) to permit binding between the two proteins to occur. Following incubation, a His-tagged competitor, either His-$H^{148-311}$ (negative control) or a His-mα variant, was added. After a second incubation period, the amount of His-Neur still bound to GST-Dl^{intra} was assayed (Figure 1.4A).

His-Neur binds efficiently to GST-Dl^{intra}, an interaction that is not significantly affected by the addition of the control competitor His-$H^{148-311}$ (Figure 1.4B). The addition of wild-type His-mα as a competitor severely reduces the amount of His-Neur that is pulled down with GST-Dl^{intra}, consistent with the interpretation that the binding of Neur to E(spl)mα is able to disrupt and prevent the binding of Neur to Dl^{intra}. Additionally, we find that this competition is dose-dependent: a 5x concentration of His-mα is more effective than a 1x concentration at disrupting the Neur-Dl^{intra} interaction. The E(spl)mα variants His-$mα^{4K/A}$, His-$mα^{4K/Q}$, His-$mα^{4K/R}$, His-$mα^{G2}$, and His-$mα^{D}$ are all equally capable of disrupting the Neur-Dl^{intra} interaction, excluding a requirement for the B domain and the G and D motifs for this activity. The variant His-$mα^{N}$ also retains some ability to disrupt the Neur-Dl^{intra} interaction; however, its efficiency is reduced compared to that of wild-type mα (Figure 1.4B).

The intact N′ motif seemed the most likely source of the residual activity of His-mα^{N} in this assay. We tested this inference by comparing the activities of His-mα^{N}, His-m$\alpha^{N'}$, and His-m$\alpha^{N', N}$. While His-mα^{N} and His-m$\alpha^{N'}$ both show a weakened ability to disrupt the Neur-Dl^{intra} interaction when compared with His-mα, the double mutant His-m$\alpha^{N', N}$ has lost this ability completely (Figure 1.4C). These data indicate that the N and N′ motifs of E(spl)mα each contribute independently to the protein's capacity to disrupt binding between Neur and Dl^{intra}.

Since E(spl)m4 contains three functional N motifs that mediate binding to Neur (see Figure 1.3B,C), we asked if all three likewise contribute to the protein's ability to disrupt the Neur-Dl interaction. The single-motif mutants His-m4^{N2}, His-m4$^{N'}$, and His-m4$^{N''}$ are each able to compete for binding to Neur nearly as efficiently as wild-type His-m4, suggesting that the presence of two intact N motifs in these variants is sufficient to disrupt Neur-Dl^{intra} binding (Figure 1.4D). The double-motif mutants His-m4$^{N, N2}$ and His-m4$^{N'', N'}$ are also very effective at disrupting the Neur-Dl^{intra} interaction, indicating that the presence of either the N or N′ motif is largely sufficient to confer this capacity. The variant His-m4$^{N, N2}$ shows a significant decrease in competitive ability, suggesting that the N″ motif is functionally weaker than the N and N′ motifs. Finally, as expected, the triple-motif mutant His-m4$^{N'', N', N2}$ is completely impaired in its ability to disrupt the Neur-Dl^{intra} interaction, consistent with its near lack of binding affinity for Neur (see Figure 1.3C).

The N motifs of E(spl)mα and E(spl)m4 are required to confer a misexpression phenotype

Knowing that E(spl)mα and E(spl)m4 contain multiple functional N motifs, we hypothesized that the remaining intact N motifs (N′ and N″) are responsible for the substantial residual ability of FLAG-m4^{N1} to disrupt lateral inhibition and generate an extra-bristle phenotype (see Figure 1.1E). To test this proposition, we generated and misexpressed a transgene construct encoding the triple mutant FLAG-m4$^{N″, N′, N2}$. As predicted, FLAG-m4$^{N″, N′, N2}$ fails to confer the misexpression phenotype (0.03 extra bristles per fly; Figure 1.5A).

Misexpressing E(spl)mα variants in this same manner produces results comparable to those for E(spl)m4. Wild-type mα misexpression produces a mean of 9.6 extra bristles per fly while mα$^{N′, N}$ lacks a significant capacity to disrupt lateral inhibition, producing only 0.85 extra bristles per fly (Figure 1.5B). Interestingly, mα^{N} is only slightly less efficient than wild-type mα in conferring the misexpression phenotype (6.7 extra bristles per fly), while mα$^{N′}$ is severely impaired in this ability (0.97 extra bristles per fly). This may suggest that the in vivo affinity of Neur for specific N motifs may vary by more than what is observed using in vitro binding assays (see Figure 1.2E). Also comparable to the E(spl)m4 results, mα$^{4K/R}$ is capable of strongly disrupting lateral inhibition, generating 8.1 extra bristles per fly, while mα$^{4K/A}$ nearly lacks this ability,

yielding 0.11 extra bristles per fly (Figure 1.5B). Finally, mα^{D} produces 6.5 extra bristles per fly, indicating that, like FLAG-m4^{D}, this variant retains the capacity to disrupt lateral inhibition (Figure 1.5B; see Figure 1.1E).

The differing phenotypic effects of the various E(spl)mα variants in the gain-of-function assay could potentially be attributable to differences in protein accumulation in vivo. However, visualization of misexpressed V5-tagged versions of these variants by immunofluorescence shows comparable levels of accumulation (see Figure 1.S2A–E).

Dl^{intra} contains an N motif that is required for binding to Neur

Our findings that N motifs are required both for the binding of Brd family proteins to Neur, and for their ability to compete with Dl^{intra} for binding to Neur, raised the possibility that Dl^{intra} and Brd family proteins compete in vivo for the same binding site(s) on Neur. This model would suggest that Dl^{intra} contains a motif similar to the N motif of Brd family proteins. Indeed, a survey of the amino acid sequence of the intracellular domain of Dl (a.a. 619–833) uncovered a motif near the transmembrane domain that strongly resembles an N motif (QNEQNAVA) and shows a high level of conservation in other arthropods (Figure 1.6A). The presence of this conserved N motif in Dl is consistent with a similar mode of interaction for Dl and Brd family proteins with Neur. We have also found a putative N motif in the intracellular domain of the other *Drosophila* Notch ligand, Ser (Figure 1.6B), and we note that the region containing it has previously been found to be important for the activation of Notch

signaling and for Ser-Neur co-immunoprecipitation (Glittenberg et al., 2006). The conserved N motif [QNEEN(L/F)RR] we have identified in arthropod Ser proteins contrasts very significantly in its proposed critical residues with the (E/D)(E/D)X_{2-3}NNX_5NX_{3-5}NP(L/I) motif suggested by Glittenberg et al. (2006) to be shared between insect Ser and vertebrate Jagged proteins; for example, the first asparagine residue of the N motif's critical NXXN core is unconstrained ("X") in the latter consensus.

To investigate the possible requirement for its putative N motif in Dl's interaction with Neur, we created versions of His-tagged Dl^{intra} with and without an N-motif mutation (His-$Dl^{intra-N}$ and His-Dl^{intra}; Figure 1.6C). Using a pulldown assay with GST-Neur or GST, we find that His-Dl^{intra} interacts strongly with GST-Neur, while the mutant His-$Dl^{intra-N}$ fails to interact (Figure 1.6D). This tells us that Dl and Brd family proteins interact with Neur via similar motifs, and are most likely competing for the same binding site(s) in Neur.

The N motif of Delta is required for its Neur-dependent endocytosis

Coexpression of Neur and Dl in vivo leads to the endocytosis of Dl at the cell surface into intracellular vesicles (Lai et al., 2001; Pavlopoulos et al., 2001). Having identified an N motif in the intracellular domain of Dl that is required to mediate its interaction with Neur in vitro, we proceeded to test whether a form of Dl mutant for this motif (Dl^N) would be impaired in its ability to undergo Neur-dependent endocytosis. When expressed alone under the control of either the *mα-GAL4* or the *dpp-GAL4* driver,

both Dl and Dl^N are found associated with the plasma membrane in the apical region of the cell and in intracellular vesicles basally (Figure 1.6E,F; data not shown; see Figure 1.S2F,G). This indicates that Dl^N, like wild-type Dl, can localize properly to the cell cortex and is capable of being trafficked into vesicles. When coexpressed with Neur, wild-type Dl is depleted from the apical cell surface and appears primarily in intracellular vesicles that are more numerous and larger in size than when Neur is not present (Figure 1.6E,E′). However, when Neur and Dl^N are coexpressed, the intracellular localization of Dl^N is left unchanged (Figure 1.6F,F′). This result supports the conclusion that the N motif in its intracellular domain is required in vivo for endocytosis of Dl in a Neur-dependent manner.

Identification of a Brd *family gene in the crustacean* D. pulex

The recent availability of a genome sequence assembly for the waterflea, *D. pulex*, presented us with the opportunity to search for *Brd* family genes in a crustacean. Unsurprisingly, standard BLAST searches yield no significant matches to any known BFMs. Using the knowledge that *Brd* family genes in insects are typically found in the vicinity of conserved bHLH-R genes of the *Hairy/Enhancer of split* (*Hes*) class, we first identified scaffolds containing *Hes* genes, and then looked nearby for possible BFMs. Using this approach, we successfully identified a *Daphnia* BFM approximately 6 kb upstream of the bHLH-R gene that encodes the Hes protein Dp15 (Simionato et al., 2007) (Figure 1.7A). This crustacean BFM appears to be regulated in a manner consistent with BFM regulation

in *Drosophila* (Singson et al., 1994; Bailey and Posakony, 1995; Nellesen et al., 1999), as its immediate upstream region contains a proneural protein binding site, a “lone” binding site for Su(H), and a Su(H) paired site (SPS) (Bailey and Posakony, 1995) within 200 bp of the TATA element. Moreover, two K boxes and a single GY box are found in the predicted 3′ UTR of the gene, indicating that the transcript is likely subject to the same miRNA-mediated negative regulation as *Drosophila* BFMs (Lai and Posakony, 1997; Leviten et al., 1997; Lai et al., 1998; Lai, 2002; Stark et al., 2003; Lai et al., 2005) (Figure 1.7A). The *Daphnia* BFM gene is predicted to encode a 162-aa protein (Figure 1.7B), containing a basic amphipathic alpha-helix (Figure 1.7C) as well as an N motif (ENALNEAL) and a variation of the G motif (GTFWT vs. GTFFWT typically found in *Drosophila* BFMs). It does not include the C-terminal D motif (Figure 1.7B).

To test whether the *D. pulex* Brd family protein retains the property of binding to Neur, we generated a His-tagged version and performed a pulldown assay with *D. melanogaster* GST-Neur. *Drosophila* Neur is indeed able to interact with the *Daphnia* BFM in this assay, suggesting a conserved function of Brd family proteins in insects and crustaceans (Figure 1.7D).

Discussion

Multiple Neur-binding motifs in Brd family proteins

We have presented evidence here that the two canonical Brd family proteins encoded in the *Drosophila* E(spl)-C, E(spl)mα and E(spl)m4, contain previously unidentified sequence motifs that are structurally and functionally similar to the recognized N motif common to nearly all BFMs (Lai et al., 2000b). It appears that each of these motifs is independently capable of mediating binding to the E3 ubiquitin ligase Neur, and we show that the presence of at least one such motif is necessary for this interaction. Henceforth, we will refer to all of these sequence elements as NXXN motifs, both because of their characteristic pattern of asparagine residues and to avoid confusion with the "N" symbol for Notch.

The availability of whole-genome and EST sequence data for a broad range of insects has permitted the identification of BFMs in 12 *Drosophila* species and in other Dipterans (*Anopheles gambiae*, *Aedes aegypti*, *Culex pipiens*, *Ceratitis capitata*, and *Haematobia irritans*), several Lepidopterans (*Bombyx mori*, *Manduca sexta*, *Heliconius erato*, *Antheraea assama*, *Samia cynthia ricini*, and Plodia *interpunctella*), a Hymenopteran (*Apis mellifera*), a Coleopteran (*Tribolium castaneum*), a Hemipteran (*Acyrthosiphon pisum*), and a Phthirapteran (*Pediculus humanus corporis*); we also report here the recognition of BFMs in three more distantly related arthropods, the Crustaceans *D. pulex*, *Artemia franciscana*, and *Callinectes sapidus* (Figure 1.7; see Figure 1.S3; J. R.

Fontana and J. W. Posakony, unpublished). This in turn affords us the opportunity to refine our definition of the NXXN motif consensus [(D/E/Q)NXXNXX(I/L/M/V); see Figure 1.S3].

The overall picture that emerges from our examination of arthropod BFM NXXN motifs is that both the appearance of secondary (generally non-canonical) Brd family genes in the genome, and the appearance of additional NXXN motifs within a given Brd family protein, permit much greater variability in NXXN motif sequence to arise. It is tempting to interpret this as a form of subfunctionalization (Lynch and Force, 2000), even at the level of individual duplicated motifs within one protein. It is also reasonable to suggest that multiple NXXN motifs arise within even canonical BFMs such as *Drosophila* E(spl)mα, E(spl)m4, and Tom because this has the effect of lowering the dissociation constant between these proteins and Neur, making them more efficient inhibitors of Notch signaling. Indeed, we see that mutation of just one of the NXXN motifs in E(spl)mα or E(spl)m4 is sufficient to decrease the efficacy of these proteins in disrupting lateral inhibition (see Figure 1.5).

Lastly, we note that the short, relatively loose, consensus for the NXXN motif defined here is not unprecedented for target sequences bound by E3 ubiquitin ligases. For instance, the WW domain of Nedd4 proteins, a family of HECT-domain E3 ubiquitin ligases, binds the small PY motif consensus (L/P)PXY found in targets such as the sodium channel ENaC (Kasanov et al., 2001).

Conserved NXXN motifs in the intracellular domains of Notch ligands

The definition of a looser consensus for the Neur interaction motifs in Brd family proteins permitted the immediate recognition of potential NXXN motifs in the intracellular domains of the Notch ligands Dl and Ser (Figure 1.6A,B). The high level of conservation of these motifs in otherwise divergent sequence strongly suggests their functional importance. Indeed, we find NXXN motifs at comparable positions in the intracellular domains of Dl and Ser ligands from nonarthropod protostomes as well, including the nematode *Xiphinema index*, the polychaete annelid *Capitella sp. I*, the cephalopod mollusc *Euprymna scolopes*, and the gastropod mollusc *Lottia gigantea* (see Figure 1.S4A). Equally striking is the presence of similar conserved NXXN motifs in both the Delta-like1 (Figure 1.S4B) and Jagged1 (Figure 1.S4C) proteins of vertebrates, which suggests strongly that in these species, too, the NXXN motif mediates the interaction between Notch ligands and Neur orthologs. Moreover, the finding that both BFMs and Notch ligands make use of a similar conserved motif to bind to Neur suggests the feasibility of identifying other Neur substrates computationally.

NXXN motif-dependent regulation of Notch signaling

We have demonstrated here for the first time that Brd family NXXN motifs are required for the inhibitory activities of these proteins in two assays, in vitro inhibition of Neur-Dl interaction, and antagonism of Notch signaling activity in vivo. Likewise, we have shown that the NXXN motif of

Dl is required both for its interaction with Neur in vitro, and for the Neur-dependent endocytosis of Dl in vivo.

Our results support a specific model for how Brd family proteins function as antagonists of Notch pathway signaling activity; namely, that BFMs and the intracellular domains of Notch ligands compete directly, via their respective NXXN motifs, for binding to Neur. Thus, NXXN motifs are essential mediators both of the activation of the Notch pathway by the ligands Dl and Ser [which require Neur-dependent ubiquitination to be fully functional (Pavlopoulos et al., 2001; Wang and Struhl, 2004)], and of its inhibition by Brd family proteins (which act to prevent this modification as competitive antagonists of the Neur-substrate interaction).

Role of Brd family proteins during lateral inhibition

Taken together, the results presented here and in previous reports (Pavlopoulos et al., 2001; Li and Baker, 2004; Wang and Struhl, 2004; Bardin and Schweisguth, 2006; De Renzis et al., 2006) support the following relatively simple model for BFM function during lateral inhibition. In response to Notch signaling, *Brd* family genes are transcriptionally activated specifically in the non-SOP cells of the PNC (Nellesen et al., 1999; Castro et al., 2005). There the encoded BFM proteins act to inhibit Neur-dependent ubiquitination of Dl, by the mechanism of directly competing with Dl for binding to Neur via their respective NXXN motifs. Inhibiting the endocytosis-dependent activation of the Dl ligand in non-SOPs would in turn have the effect of preventing these cells from

becoming “strong signalers” that otherwise might laterally inhibit the SOP itself, or might themselves be resistant to signaling.

A critical question prompted by the simple model described above for Brd family protein function during lateral inhibition is, why is inhibition of Neur activity by BFMs in non-SOPs necessary if Neur is highly expressed only in SOPs? Work currently in progress in our laboratory (S.W. Miller and J.W. Posakony, unpublished observations) has established that *neur* is indeed actively transcribed in multiple cells early in the development of the PNC, potentially necessitating the deployment of BFMs as Neur inhibitors, in order to eliminate any threat to correct cell fate specification this may pose.

Evolutionary history of the Brd protein family

Our identification of a *Brd* family gene in the Crustacean *D. pulex* pushes back the origin of this family to perhaps the Silurian era, more than 400 Mya. The presence of a B domain and both N and G motifs in the predicted protein product (see Figure 1.7B,C) suggests that the ancestral BFM must have contained at least these three elements. The D motif may either have been lost in the crustaceans, or have appeared sometime later in the hexapod lineage. It also seems clear that both transcriptional and post-transcriptional modes of *Brd* family gene regulation have been conserved from a deep ancestor. The presence of high-affinity binding sites for proneural proteins and Su(H) in the immediate upstream region of the *Daphnia* BFM strongly suggests that it uses the “S+P” transcriptional

regulatory code first uncovered in studies of *Drosophila Brd* family and bHLH repressor genes (Singson et al., 1994; Bailey and Posakony, 1995; Nellesen et al., 1999; Castro et al., 2005). Likewise, the presence of K and GY boxes in the gene's 3′ UTR makes it equally likely that it is subject to the same miRNA-mediated negative regulation that applies to most *Drosophila* BFMs (Lai and Posakony,1997; Lai et al.,1998; Stark et al., 2003; Lai et al., 2005). Our demonstration that the *Daphnia* Brd family protein binds efficiently to *Drosophila* Neur in vitro (see Figure 1.7D) indicates that this functionality, too, is an ancient property of the family. Finally, the close genomic association of the *Daphnia* BFM with a Hes-type bHLH repressor gene, just as in insect E(spl)-C's (Schlatter and Maier, 2005), suggests both that this proximity dates from the common ancestor, and that the association is maintained by selection, for an as yet unknown reason. It is striking that so many features of the structure, function, and regulation of the *Brd* gene family have survived for such an extraordinarily long time.

Acknowledgements

We would like to thank Brian Castro, Feng Liu, Mariano Loza Coll, Steven Miller, Mark Rebeiz, Nick Reeves, and Sui Zhang for both material and mental support, and Gentry Patrick and Jeff Keil for helpful discussions. We also thank Tammie Stone for generating various in vitro reagents and for help with formulating pulldown assay conditions. We are grateful to Dr. Matthias Westphal at the Center for Genomics and Bioinformatics, Indiana University, Bloomington, for *Daphnia pulex* (Log50 strain) and protocol suggestions. F. Liu, M. Loza Coll, and S. Miller provided very useful critical comments during the preparation of the manuscript. J.R.F. was supported by a National Institutes of Health (NIH) pre-doctoral training grant in Developmental Biology. This work was supported by NIH grant GM075270 to J.W.P.

Figure 1.1: Integrity of the B domain and N motif of E(spl)m4 are important for the gain-of-function phenotype. (A) The *Brd* family gain-of-function phenotype results from misexpression in SOP cells. Expression of FLAG-m4 throughout PNCs (*sca-GAL4*; yellow bars) or specifically in SOPs (*neur-GAL4*; purple bars) results in the production of extra bristles on the notum and head. Overexpression in non-SOP cells of the PNC fails to produce a mutant phenotype (*mα-GAL4*; red bars). (B) Wild-type notum (left) shows the stereotypical pattern of macrochaete mechanosensory bristles, while flies expressing FLAG-tagged E(spl)m4 protein (FLAG-m4) under the control of the *sca-GAL4* driver (right) show extra macrochaetes at multiple positions (arrows). (C) Domain/motif variants of E(spl)m4. The B domain (basic amphipathic alpha-helix) and the N, G, and D motifs (Lai et al., 2000b) are indicated. Substituted residues are depicted in red. (D) Helical wheel plot of E(spl)m4's B domain predicts the clustering of non-polar residues on one face of the helix and of basic residues on the opposite face. (E) Extra-bristle phenotypes resulting from misexpression of FLAG-m4 variants using the *sca-GAL4* driver. Error bars indicate standard errors; asterisks denote statistical significance of differences from the wild-type (FLAG-m4) results ($P<0.04$; Mann-Whitney *U* test).

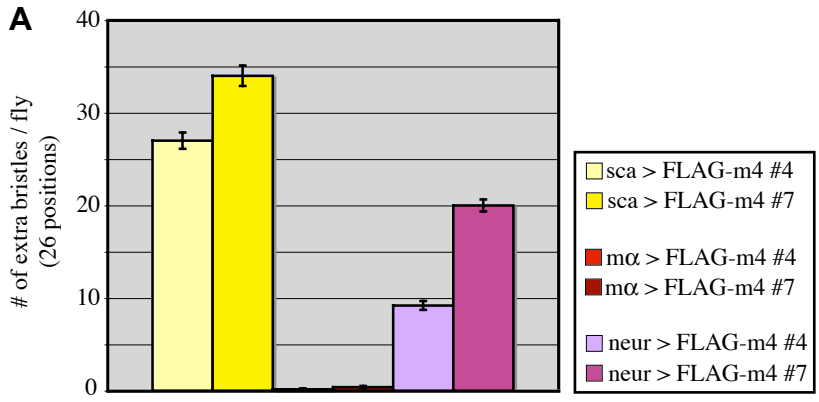
A
40
30
20
10
0
# of extra bristles / fly
(26 positions)
sca > FLAG-m4 #4
sca > FLAG-m4 #7
mα > FLAG-m4 #4
mα > FLAG-m4 #7
neur > FLAG-m4 #4
neur > FLAG-m4 #7

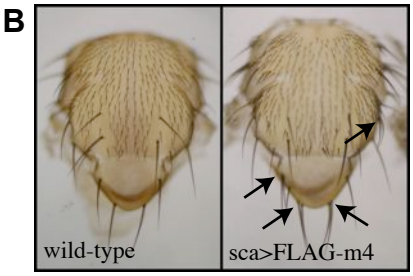
B
wild-type
sca>FLAG-m4

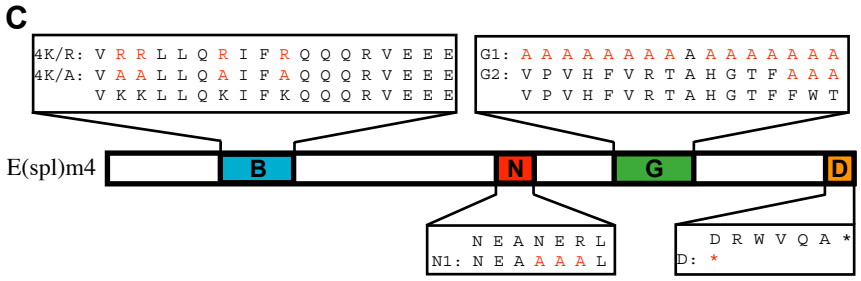
C
4K/R: V R R L L Q R I F R Q Q Q R V E E E
4K/A: V A A L L Q A I F A Q Q Q R V E E E
V K K L L Q K I F K Q Q Q R V E E E
G1: A A A A A A A A A A A A A A A A
G2: V P V H F V R T A H G T F A A A
V P V H F V R T A H G T F F W T
E(spl)m4
B
N
G
D
N E A N E R L
N1: N E A A A A L
D R W V Q A *
D: *

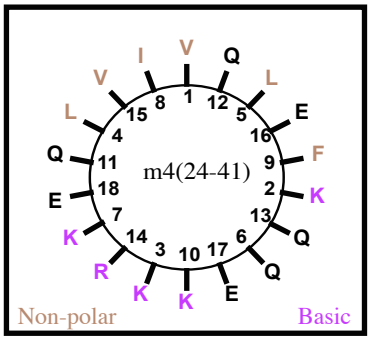
D
m4(24-41)
Non-polar
Basic

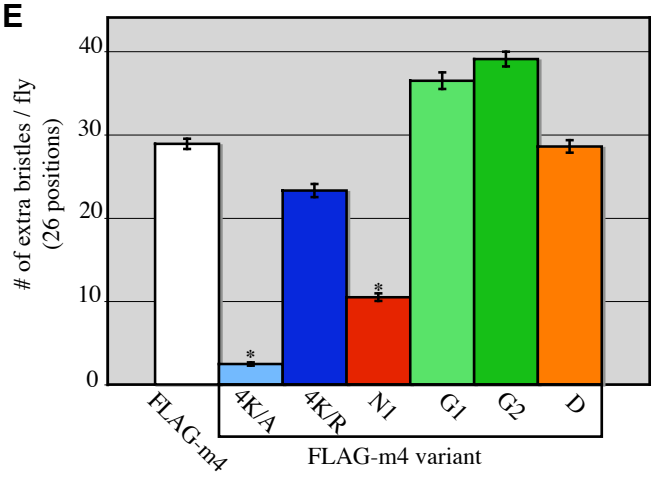
E
40
30
20
10
0
# of extra bristles / fly
(26 positions)
FLAG-m4
4K/A
4K/R
N1
G1
G2
D
FLAG-m4 variant

Figure 1.2: E(spl)mα contains two N motifs capable of interacting with Neur. (A) Variants of E(spl)mα. The B domain and the N, G, and D motifs are indicated. Substituted residues are depicted in red. (B–E) Western blots of pulldown assays of the interaction between Neur and E(spl)mα. Also shown are Coomassie-stained blots depicting amounts of bead-bound GST (control) and GST-Neur proteins in each assay. (B) The variant $m\alpha^{4K/A}$ is the only single mutant that weakens E(spl)mα's interaction with Neur; this variant also shows an atypical gel migration pattern. (C) Normal gel migration and strong interaction with Neur are both restored in the $m\alpha^{4K/A, D}$ double mutant, and mutation of all four conserved domains/motifs ($m\alpha^{4K/A, N, G2, D}$) does not abolish the E(spl)mα-Neur interaction. (D) In an $m\alpha^{N, G2, D}$ background, mutation of regions X and B have no affect on E(spl)mα's binding to Neur, while mutation of either region Y or region Z eliminates the interaction completely. (E) The N′ motif is found in the zone of overlap between regions Yand Z (see A). While the $m\alpha^{N}$ and $m\alpha^{N'}$ variants interact normally with Neur, the $m\alpha^{N', N}$ variant has lost this capacity.

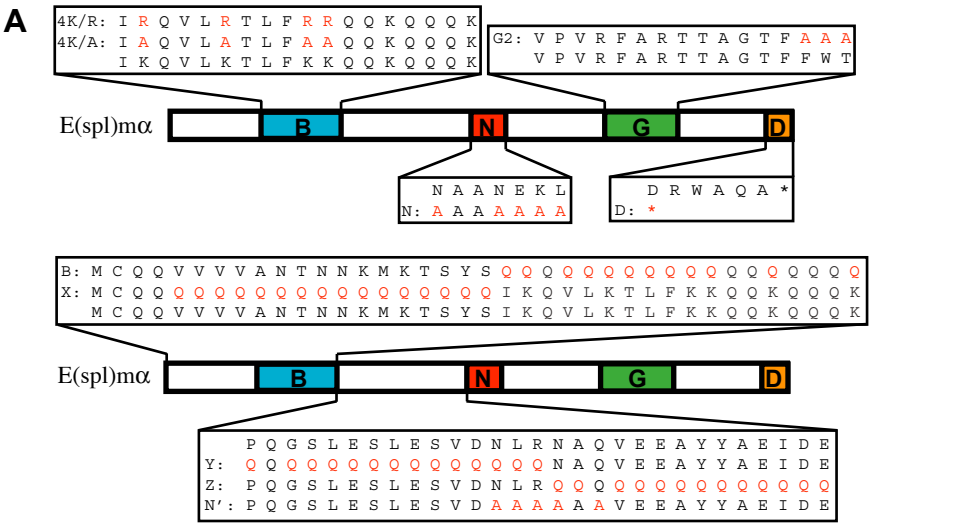
A
4K/R: I R Q V L R T L F R R Q Q K Q Q Q K
4K/A: I A Q V L A T L F A A Q Q K Q Q Q K
I K Q V L K T L F K K Q Q K Q Q Q K
G2: V P V R F A R T T A G T F A A A
V P V R F A R T T A G T F F W T
E(spl)mα
B
N
G
D
N A A N E K L
N: A A A A A A A
D R W A Q A *
D: *
B: M C Q Q V V V V A N T N N K M K T S Y S Q Q Q Q Q Q Q Q Q Q Q Q Q Q Q Q Q
X: M C Q Q Q Q Q Q Q Q Q Q Q Q Q Q Q Q I K Q V L K T L F K K Q Q K Q Q Q K
M C Q Q V V V V A N T N N K M K T S Y S I K Q V L K T L F K K Q Q K Q Q Q K
E(spl)mα
B
N
G
D
P Q G S L E S L E S V D N L R N A Q V E E A Y Y A E I D E
Y: Q Q Q Q Q Q Q Q Q Q Q Q Q Q N A Q V E E A Y Y A E I D E
Z: P Q G S L E S L E S V D N L R Q Q Q Q Q Q Q Q Q Q Q Q Q
N′: P Q G S L E S L E S V D A A A A A A A V E E A Y Y A E I D E

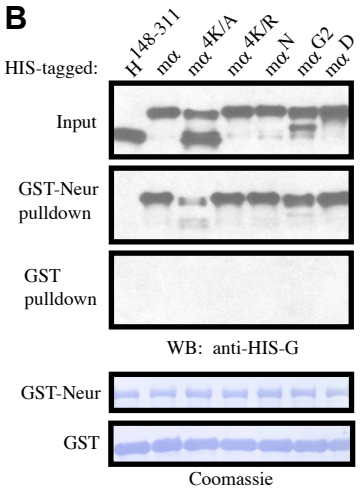
B
H 148-311
mα
mα 4K/A
mα 4K/R
mα N
mα G2
mα D
HIS-tagged:
Input
GST-Neur pulldown
GST pulldown
WB: anti-HIS-G
GST-Neur
GST
Coomassie

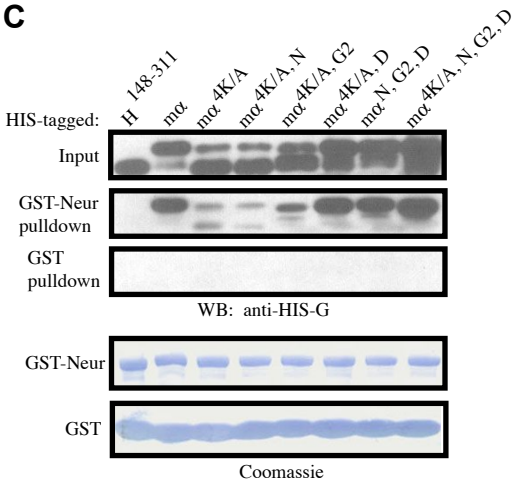
C
H 148-311
mα
mα 4K/A
mα 4K/A, N
mα 4K/A, G2
mα 4K/A, D
mα N, G2, D
mα 4K/A, N, G2, D
HIS-tagged:
Input
GST-Neur pulldown
GST pulldown
WB: anti-HIS-G
GST-Neur
GST
Coomassie

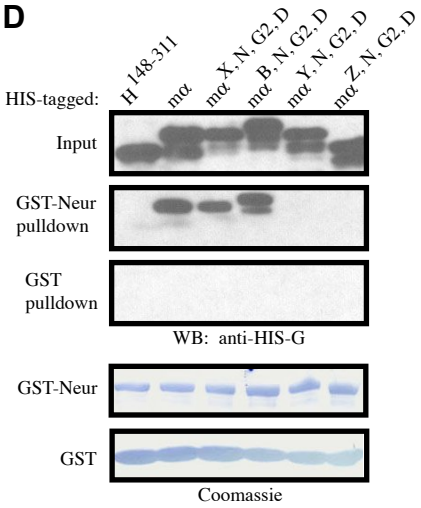
D
H 148-311
mα
mα X, N, G2, D
mα B, N, G2, D
mα Y, N, G2, D
mα Z, N, G2, D
HIS-tagged:
Input
GST-Neur pulldown
GST pulldown
WB: anti-HIS-G
GST-Neur
GST
Coomassie

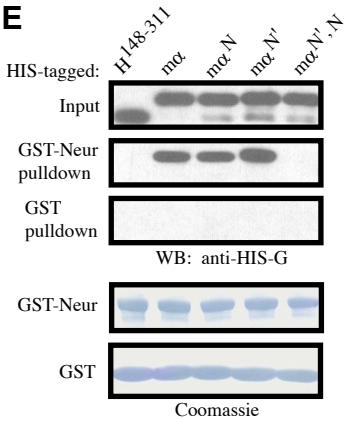
E
H 148-311
mα
mα N
mα N′
mα N′, N
HIS-tagged:
Input
GST-Neur pulldown
GST pulldown
WB: anti-HIS-G
GST-Neur
GST
Coomassie

Figure 1.3: A refined consensus identifies multiple N motifs in Brd family proteins, each sufficient to mediate binding to Neur. (A) Canonical BFMs E(spl)mα, E(spl)m4, and Tom contain two or more N motifs defined by the new consensus (D/E/Q)NXXNXX(non-polar). Conserved residues within each N motif are shown in bold; note that the N″ motif of E(spl)m4 violates the consensus at the non-polar residue position. (B) N-motif variants of E(spl)m4. The B domain and the N, G, and D motifs are indicated. Substituted residues are depicted in red. (C, D) Western blots of pulldown assays. Also shown are Coomassie-stained blots depicting amounts of bead-bound GST (control) and GST-Neur proteins in each assay. (C) The integrity of any of the three N motifs in E(spl)m4 is sufficient for interaction with Neur. Only mutation of all three of these motifs ($m4^{N'', N', N2}$) results in the disruption of the E(spl)m4–Neur interaction. (D) An 18-a.a. segment containing the E(spl)mα N motif (AEID**E<u>N</u>AA<u>N</u>EKL**AQLAHS) is sufficient to mediate a weak interaction with Neur. This interaction is dependent on the two asparagine residues of the core NXXN sequence, as a mutant peptide (AEID**E<u>A</u>AA<u>A</u>EKL**AQLAHS) fails to bind Neur.

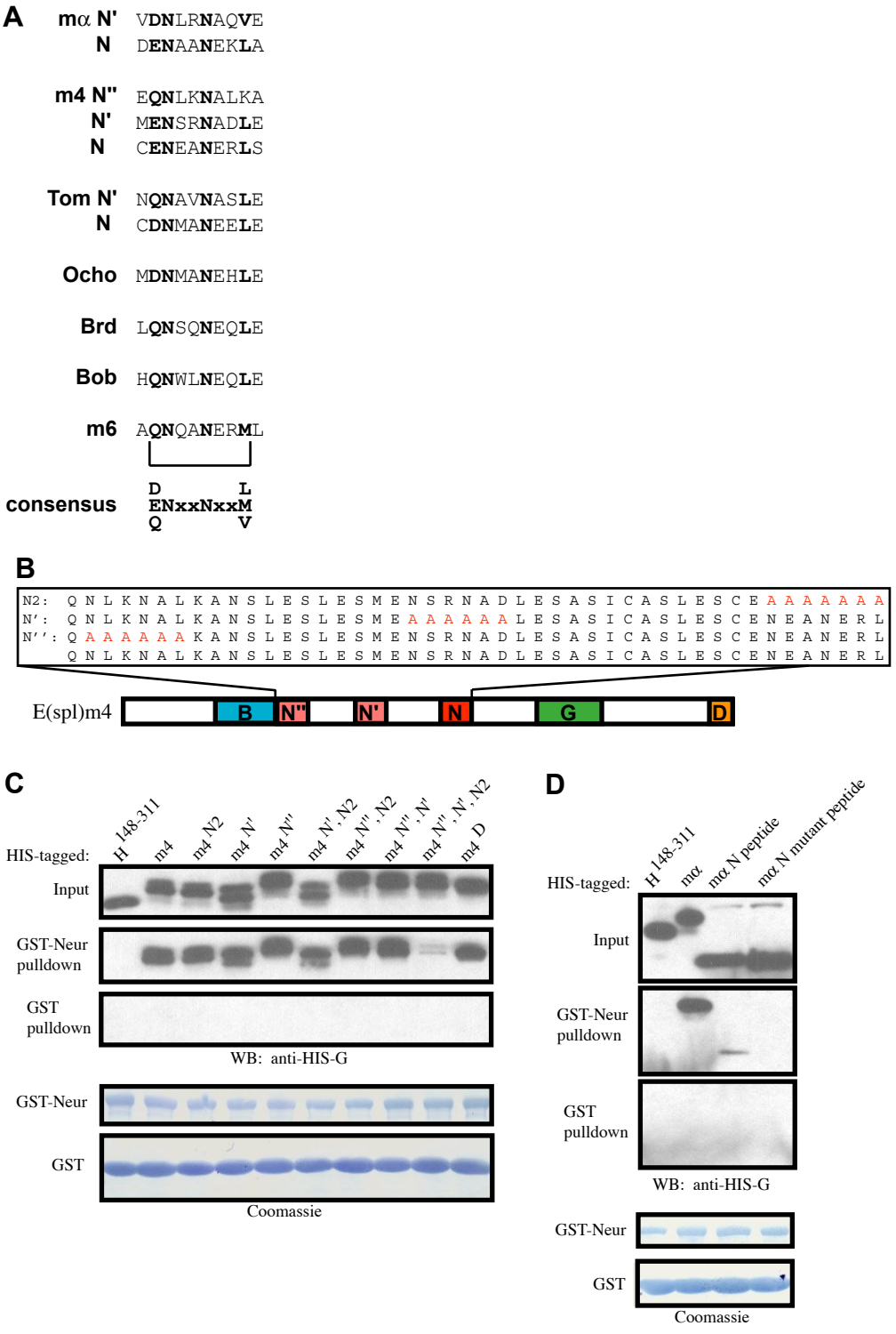
A
mα N' VDNLRNAQVE
N DENAANEKLA
m4 N'' EQNLKNALKA
N' MENSRNADLE
N CENEANERLS
Tom N' NQNAVNASLE
N CDNMANEELE
Ocho MDNMANEHLE
Brd LQNSQNEQLE
Bob HQNWLNEQLE
m6 AQNQANERML
consensus D L
ENxxNxxM
Q V
B
N2: Q N L K N A L K A N S L E S L E S M E N S R N A D L E S A S I C A S L E S C E A A A A A A A
N': Q N L K N A L K A N S L E S L E S M E A A A A A A A L E S A S I C A S L E S C E N E A N E R L
N'': Q A A A A A A A K A N S L E S L E S M E N S R N A D L E S A S I C A S L E S C E N E A N E R L
Q N L K N A L K A N S L E S L E S M E N S R N A D L E S A S I C A S L E S C E N E A N E R L
E(spl)m4
B
N"
N'
N
G
D
C
HIS-tagged:
H 148-311
m4
m4 N2
m4 N'
m4 N''
m4 N', N2
m4 N'', N2
m4 N'', N'
m4 N'', N', N2
m4 D
Input
GST-Neur pulldown
GST pulldown
WB: anti-HIS-G
GST-Neur
GST
Coomassie
D
HIS-tagged:
H 148-311
mα
mα N peptide
mα N mutant peptide
Input
GST-Neur pulldown
GST pulldown
WB: anti-HIS-G
GST-Neur
GST
Coomassie

Figure 1.4: Brd family proteins compete with Dl for binding to Neur. (A) Schematic of the competition pulldown assay. (B–D) Western blots of competition pulldown assays. Also shown are Coomassie-stained blots depicting amounts of bead-bound GST (control) and GST-Dl^{intra} proteins in each assay. Neur is efficiently pulled down by GST-Dl^{intra}, and this interaction is not strongly affected by the presence of the control competitor H$^{148-311}$. (B) Addition of wild-type mα, or any variant except mα^{N}, disrupts the Neur-Dl^{intra} interaction in a dose-dependent manner. (B, C) Mutation of either the N or N′ motif weakens E(spl)mα's ability to disrupt this interaction, while the double mutant m$\alpha^{N', N}$ lacks this ability (C). (D) Similarly, addition of E(spl)m4 also disrupts the Neur-Dl^{intra} interaction, and the triple mutant m4$^{N'', N', N2}$ loses this ability. The N″ motif of E(spl)m4 is weaker than the N or N′ motifs at disrupting the Neur-Dl^{intra} interaction, as seen with variant m4$^{N', N2}$.

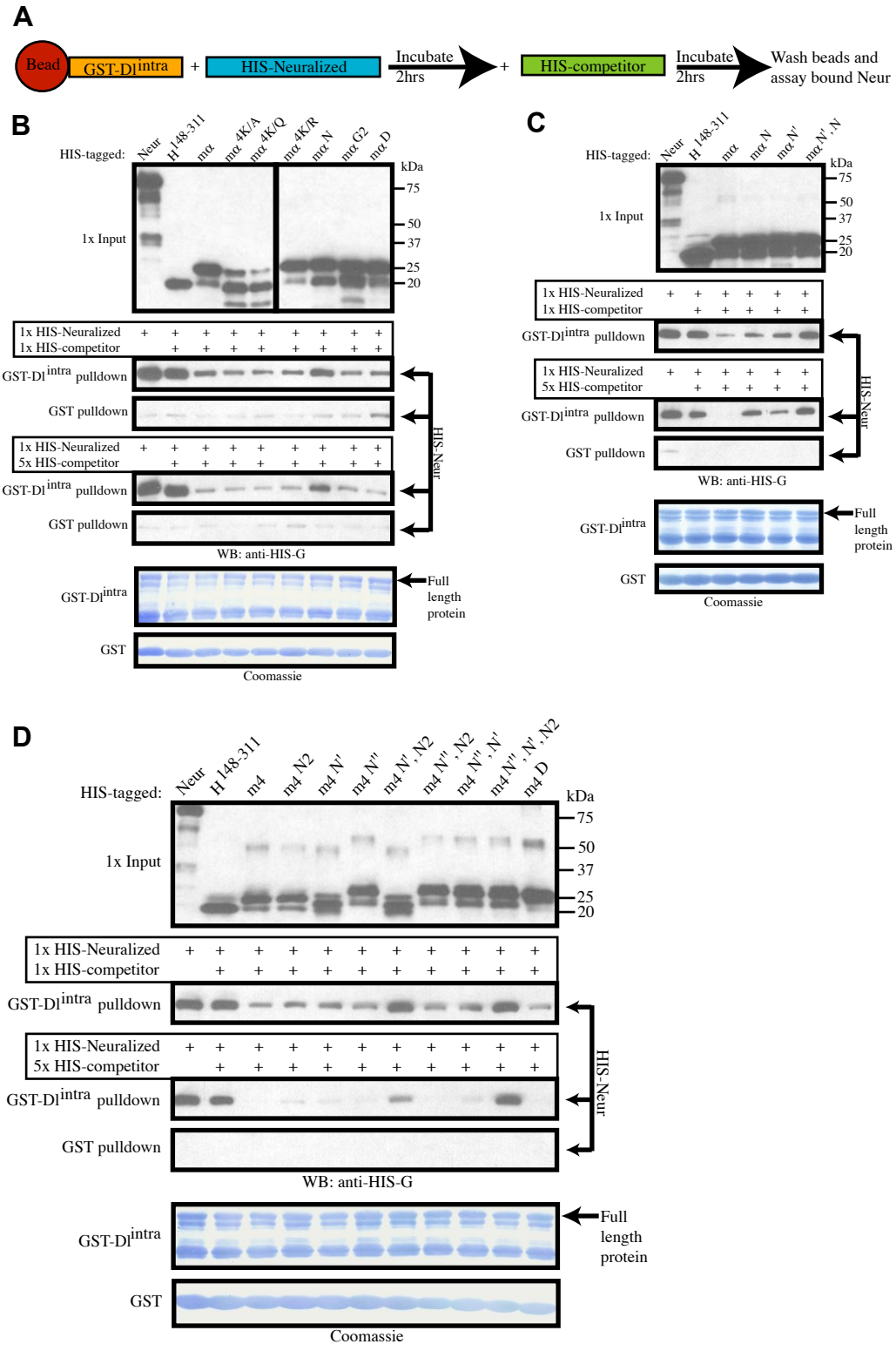
A
Bead
GST-Dl^intra
+
HIS-Neuralized
Incubate 2hrs
+
HIS-competitor
Incubate 2hrs
Wash beads and assay bound Neur
B
HIS-tagged:
Neur
H148-311
mα
mα 4K/A
mα 4K/Q
mα 4K/R
mα N
mα G2
mα D
kDa
75
50
37
25
20
1x Input
1x HIS-Neuralized
1x HIS-competitor
GST-Dl^intra pulldown
GST pulldown
5x HIS-competitor
HIS-Neur
WB: anti-HIS-G
GST-Dl^intra
Full length protein
GST
Coomassie
C
HIS-tagged:
Neur
H148-311
mα
mα N
mα N'
mα N', N
1x Input
GST-Dl^intra pulldown
GST pulldown
WB: anti-HIS-G
GST-Dl^intra
Full length protein
GST
Coomassie
D
HIS-tagged:
Neur
H148-311
m4
m4 N2
m4 N'
m4 N''
m4 N', N2
m4 N'', N2
m4 N'', N'
m4 N'', N', N2
m4 D
1x Input
GST-Dl^intra pulldown
GST pulldown
WB: anti-HIS-G
GST-Dl^intra
Full length protein
GST
Coomassie

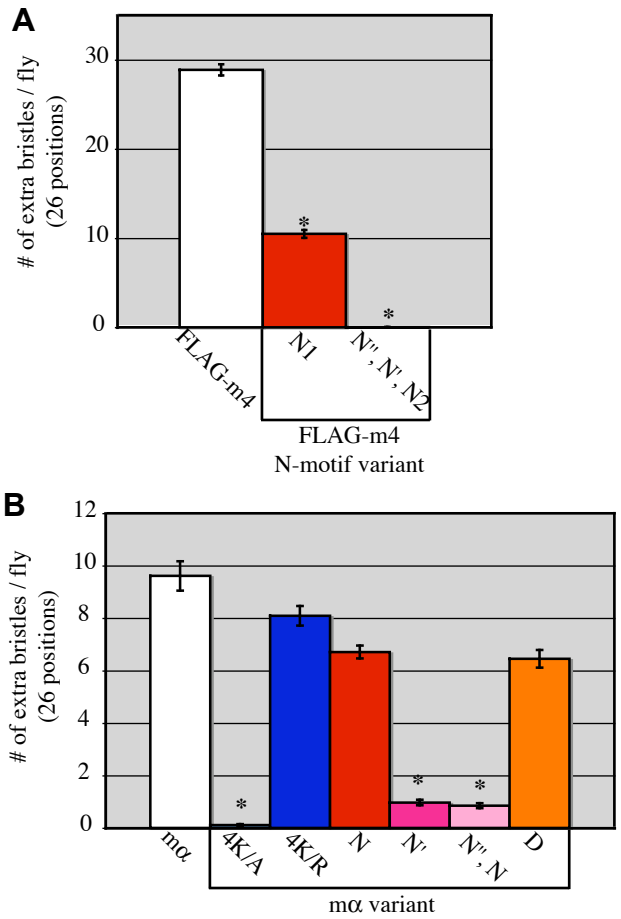

Figure 1.5: The N motifs of E(spl)m4 and E(spl)mα are required for the gain-of-function phenotype. (A) Misexpression of FLAG-m4 using the *sca-GAL4* driver produces an extra-bristle phenotype that is weakened with the FLAG-m4^{N1} variant and completely absent in the FLAG-m4$^{N", N', N2}$ triple mutant variant. (B) Misexpression of mα with *sca-GAL4* also produces an extra-bristle phenotype that is dependent on the presence of the N motifs. The variant mα$^{4K/A}$ is unable to generate a gain-of-function phenotype, as was observed with FLAG-m4$^{4K/A}$ (see Fig. 1E). Error bars indicate standard errors; asterisks denote statistical significance of differences from the wild-type (A, FLAG-m4; B, mα) results ($P<0.04$; Mann-Whitney *U* test).

Figure 1.6: The intracellular domain of Dl contains an N motif that is required for in vitro binding and in vivo responsiveness to Neur. (A, B) Alignments of segments of the intracellular domains of Dl (A) and Ser (B) show strong conservation of an N motif in the arthropods. (C) Cartoon illustrating the mutant N motif variant of Dl^{intra}. Substituted residues are depicted in red. (D) Western blot of a pulldown assay shows that the N motif of Dl^{intra} is required for its interaction with Neur. Also shown are Coomassie-stained blots depicting amounts of bead-bound GST (control) and GST-Neur proteins in each assay. (E, F) 30-40-μm confocal stack images of anti-Dl antibody stains of wing imaginal disc cells expressing Dl (E), Dl^{N} (F), Dl+Neur (E′), or Dl^{N}+Neur (F′) under the control of the *mα-GAL4* driver. Both apical and basal regions of the tissue are included in the image stack. In contrast to wild-type Dl, the intracellular localization of Dl^{N} is not responsive to the presence of Neur.

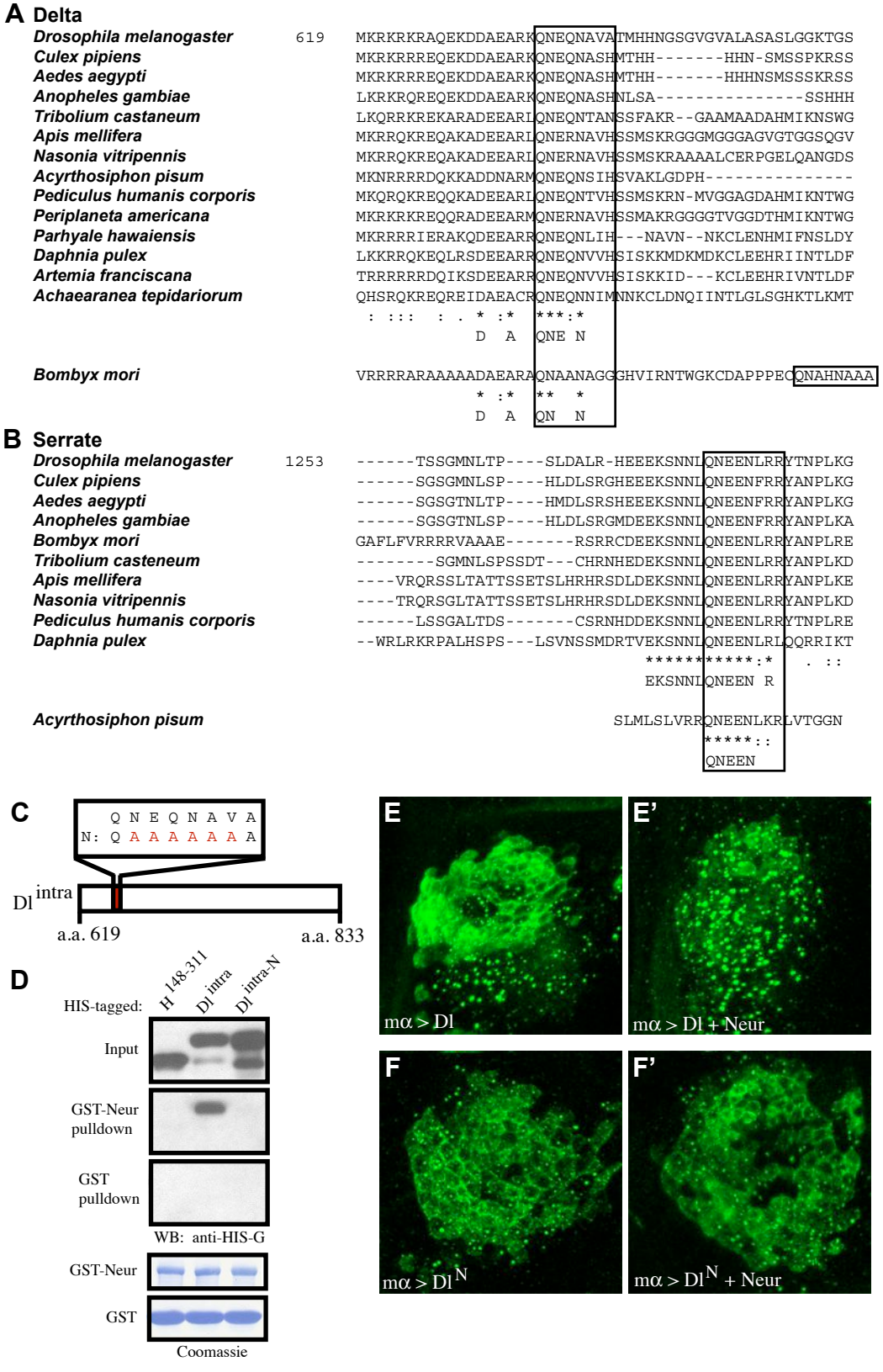
A Delta
Drosophila melanogaster 619 MKRKRKRAQEKDDAEARKQNEQNAVAIMHHNGSGVGVALASASLGGKTGS
Culex pipiens MKRKRRREQEKDDAEARKQNEQNASHMTHH-------HHN-SMSSPKRSS
Aedes aegypti MKRKRRREQEKDDAEARKQNEQNASHMTHH-------HHHNSMSSSKRSS
Anopheles gambiae LKRKRQREQEKDDAEARKQNEQNASHNLSA---------------SSHHH
Tribolium castaneum LKQRRKREKARADEEARLQNEQNTANSSFAKR--GAAMAADAHMIKNSWG
Apis mellifera MKRRQKREQAKADEEARLQNERNAVHSSMSKRGGGMGGGAGVGTGGSQGV
Nasonia vitripennis MKRRQKREQAKADEEARLQNERNAVHSSMSKRAAAALCERPGELQANGDS
Acyrthosiphon pisum MKNRRRRDQKKADDNARMQNEQNSIHSVAKLGDPH---------------
Pediculus humanis corporis MKQRQKREQQKADEEARLQNEQNTVHSSMSKRN-MVGGAGDAHMIKNTWG
Periplaneta americana MKRKRKREQQRADEEARMQNERNAVHSSMAKRGGGGTVGGDTHMIKNTWG
Parhyale hawaiensis MKRRRRIERAKQDEEARRQNEQNLIH---NAVN--NKCLENHMIFNSLDY
Daphnia pulex LKKRRQKEQLRSDEEARRQNEQNVVHSISKKMDKMDKCLEEHRIINTLDF
Artemia franciscana TRRRRRRDQIKSDEEARRQNEQNVVHSISKKID---KCLEEHRIVNTLDF
Achaearanea tepidariorum QHSRQKREQREIDAEACRQNEQNNIMNNKCLDNQIINTLGLSGHKTLKMT
Bombyx mori VRRRRARAAAAADAEARAQNAANAGGGHVIRNTWGKCDAPPPECQNAHNAAA
B Serrate
Drosophila melanogaster 1253 ------TSSGMNLTP----SLDALR-HEEEKSNNLQNEENLRRYTNPLKG
Culex pipiens ------SGSGMNLSP----HLDLSRGHEEEKSNNLQNEENFRRYANPLKG
Aedes aegypti ------SGSGTNLTP----HMDLSRSHEEEKSNNLQNEENFRRYANPLKG
Anopheles gambiae ------SGSGTNLSP----HLDLSRGMDEEKSNNLQNEENFRRYANPLKA
Bombyx mori GAFLFVRRRRVAAAE-------RSRRCDEEKSNNLQNEENLRRYANPLRE
Tribolium casteneum --------SGMNLSPSSDT---CHRNHEDEKSNNLQNEENLRRYANPLKD
Apis mellifera ----VRQRSSLTATTSSETSLHRHRSDLDEKSNNLQNEENLRRYANPLKE
Nasonia vitripennis ----TRQRSGLTATTSSETSLHRHRSDLDEKSNNLQNEENLRRYANPLKD
Pediculus humanis corporis ------LSSGALTDS-------CSRNHDDEKSNNLQNEENLRRYTNPLRE
Daphnia pulex --WRLRKRPALHSPS---LSVNSSMDRTVEKSNNLQNEENLRLQQRRIKT
EKSNNLQNEEN R
Acyrthosiphon pisum SLMLSLVRRQNEENLKRLVTGGN
QNEEN
C
Q N E Q N A V A
N: Q A A A A A A A
Dl intra
a.a. 619
a.a. 833
D
HIS-tagged:
H 148-311
Dl intra
Dl intra-N
Input
GST-Neur pulldown
GST pulldown
WB: anti-HIS-G
GST-Neur
GST
Coomassie
E
mα > Dl
E'
mα > Dl + Neur
F
mα > Dl N
F'
mα > Dl N + Neur

Figure 1.7: The genome of the crustacean *Daphnia pulex* encodes a Brd family protein capable of binding to *Drosophila* Neur. (A) GenePalette illustration of the genomic region containing the *Daphnia Brd* family gene. Blue rectangle indicates the protein-coding region of this intronless gene; white rectangles represent untranslated regions. Transcriptional and post-transcriptional regulatory sequence motifs shared with other arthropod *Brd* family genes (see Materials and methods) are shown. (B) ClustalW alignment of the predicted sequence of the *Daphnia* BFM with *D. mel* E(spl)mα (blue box=B domain, longer in the *Daphnia* sequence to include an extended region of high amphipathicity; red box=N motif; green box=G motif). (C) Helical wheel plot of the *Daphnia* BFM's B domain. (D) Western blot of a pulldown assay, showing the conserved ability of the *Daphnia* BFM to interact specifically with *Drosophila* Neur. Also shown are Coomassie-stained blots depicting amounts of bead-bound GST (control) and GST-Neur proteins in each assay.

A

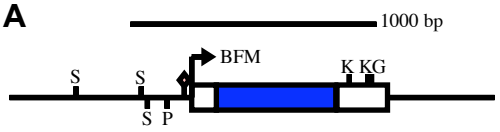

◆: TATA Box
G: GY Box
K: K Box
S: Su(H) binding site
P: Proneural binding site

B

```
D. pulex      MVSQSFN-SKLTQKLRLITKKVSNLVKPLLTKRHNKKTTSQGQKAEPMTP 49
D. mel mα     MCQQVVVVANTNNKMK-TSYSIKQVLKTLFKKQQKQQQKPQGS-LESLES 48
              * .* .  :: .:*::  : .:.:::*.*:.*::::: .:**.  *.: .
              M  Q          K          K L  K          QG   E

D. pulex      VNRSWMHPSQLKSSEYVDCCQHEADENALNEALEAKLRQLIVTEYANRRT 99
D. mel mα     VDN--LRNAQVEEAYYA-----EIDENAANEKL-AQLAH--SQEFEIVEE 88
              *:.  :: :*::.: *.     * **** ** * *:* :    *:   .
              V        Q     Y      E DENA NE L A L      E

D. pulex      TSTAPVSLHIQGHLTITPSTQPEGT-FWTTSSSSSLTADADICWRDCSVV 148
D. mel mα     QEDEE-DVYVP--VRFARTT--AGTFFWTTNLQPVASVEPAMCY---SM- 129
               .    .:::   : :: :*   ** ****. ..  :.:. :*:   *:
                             T   GT FWTT            C    S

D. pulex      SQPQKAERQTPLLY 162
D. mel mα     -QFQ--DRWAQA-- 138
               * *  :* :
               Q Q   R
```

C

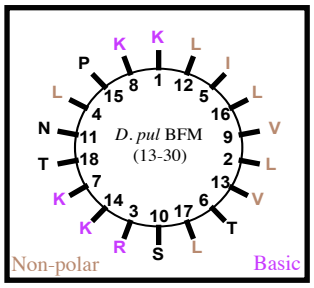

D

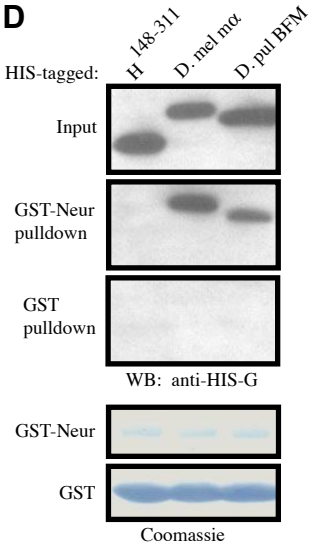

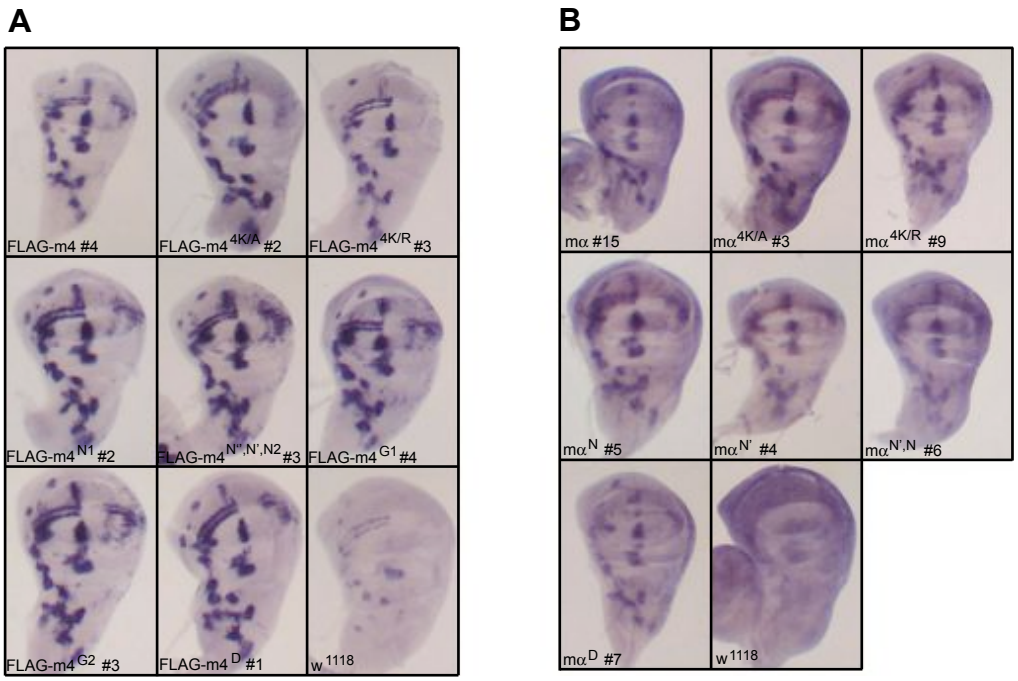

Figure 1.S1: Transcript accumulation from *FLAG-m4* and *E(spl)mα* variant *UAS* transgenes. (A,B) In situ hybridizations using (A) *E(spl)m4* probe or (B) *E(spl)mα* probe, showing levels of transcript accumulation in late third-instar wing discs from representative lines carrying the indicated *UAS* transgenes, expressed under the control of *sca-GAL4*, compared to wild type (*w*^{1118}).

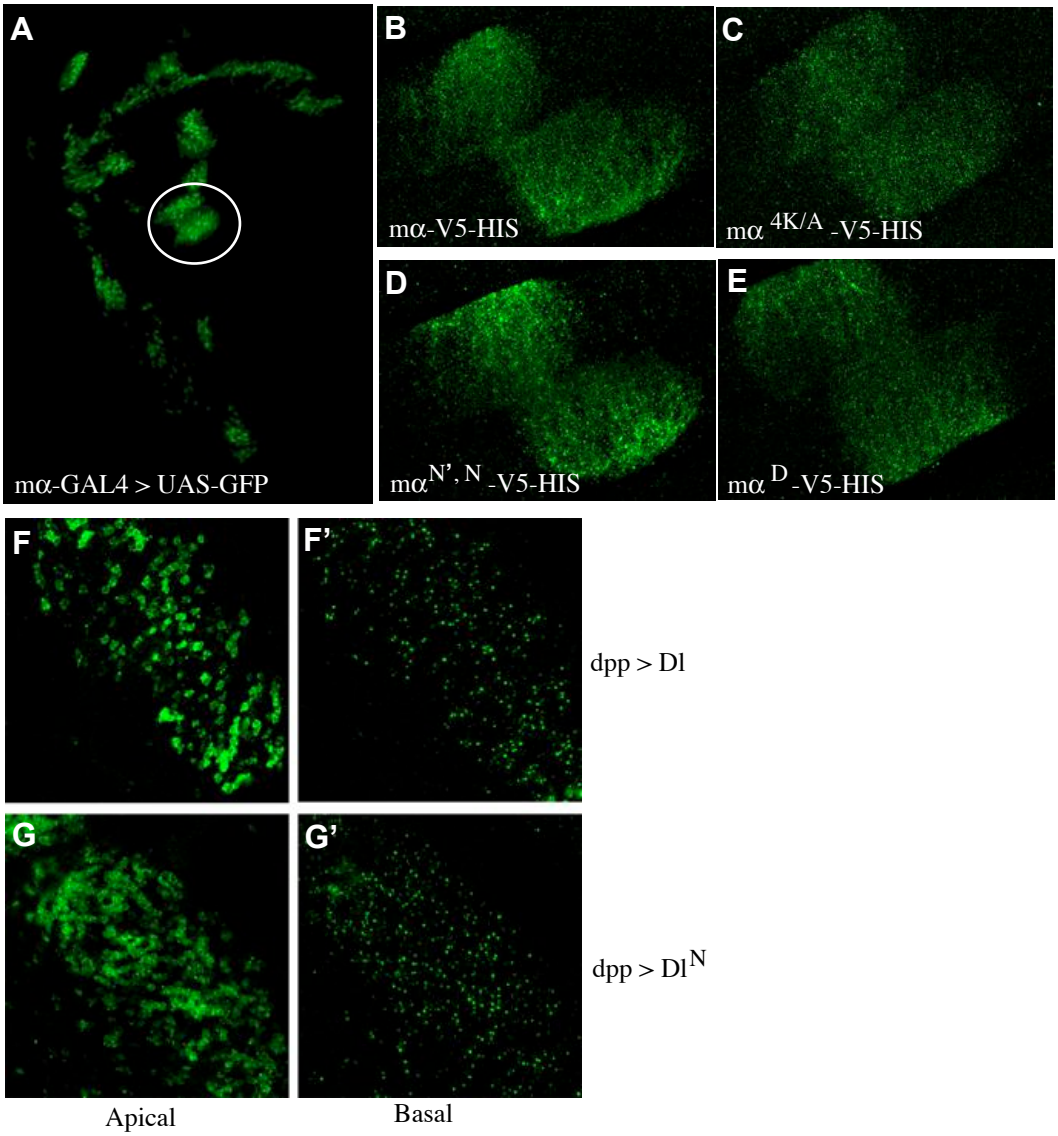

Figure 1.S2: Localization and/or levels of accumulation displayed by variants of E(spl)mα and Dl proteins when misexpressed in imaginal disc tissue. (A) Expression of GFP driven by *mα-GAL4* in the late third-instar wing disc. The region magnified in B-E is circled. (B-E) 15-20-μm confocal stack images of wing disc tissue expressing (*mα-GAL4* driver) the indicated tagged E(spl)mα protein variants stained with anti-V5 antibody. (F,G) Comparison of the accumulation and subcellular localization of Dl and Dl^N. Shown are 1-μm confocal slice images of anti-Dl antibody stains of wing imaginal disc tissue expressing Dl (F, apical level; F', basal level) or Dl^N (G, apical level; G', basal level) under the control of the *dpp-GAL4* driver.

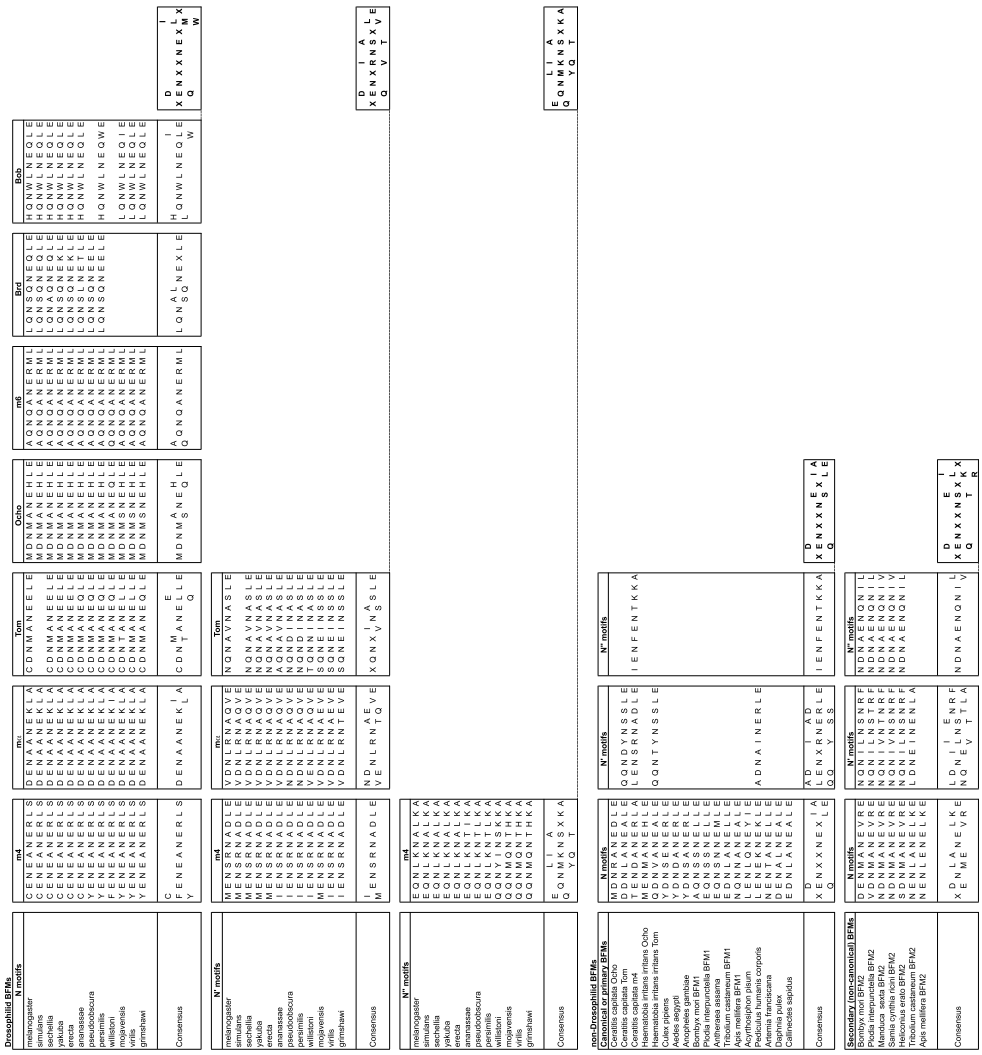

Figure 1.S3: Deriving consensus sequences for NXXN motifs in Brd family proteins. The NXXN motifs of known BFMs in (A) the 12 fully sequenced *Drosophila* species and (B) other arthropods are aligned. Combining the original NXXN motifs recognized in *Drosophila* BFMs (A, upper row) with the NXXN motifs in the canonical or primary BFMs of other species (B, upper row) yields the eight-residue consensus (D/E/Q)NXXNEX(I/L/M). Every species listed for which whole-genome sequence data are available possesses a Brd family protein with an NXXN motif fitting this consensus.

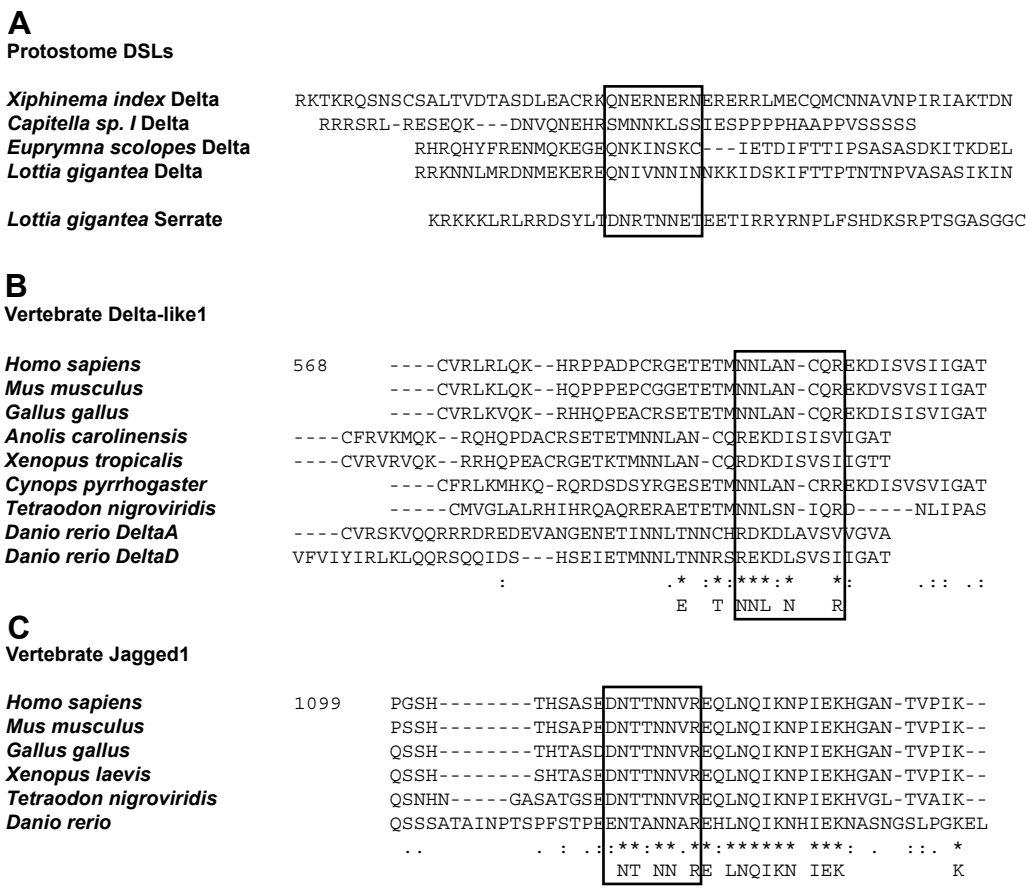

Figure 1.S4: Alignment of putative NXXN motifs in the intracellular domains of Notch ligands. Shown are the portions of the intracellular domains immediately adjacent to the transmembrane domains of (A) Dl and Ser orthologs of various non-arthropod protostomes, (B) Delta-like 1 orthologs of representative vertebrate species, and (C) vertebrate Jagged1 orthologs. Putative NXXN motifs are boxed, and fully conserved residues indicated.

References

Apidianakis, Y., Nagel, A.C., Chalkiadaki, A., Preiss, A., Delidakis, C., 1999. Overexpression of the *m4* and *mα* genes of the *E(spl)-Complex* antagonizes Notch mediated lateral inhibition. Mech. Dev. 86, 39–50.

Bailey, A.M., Posakony, J.W., 1995. Suppressor of Hairless directly activates transcription of *Enhancer of split* Complex genes in response to Notch receptor activity. Genes Dev. 9, 2609–2622.

Bardin, A., Schweisguth, F., 2006. Bearded family members inhibit Neuralized-mediated endocytosis and signaling activity of Delta in *Drosophila*. Dev. Cell 10, 245–255.

Barolo, S., Carver, L.A., Posakony, J.W., 2000. GFP and β-galactosidase transformation vectors for promoter/enhancer analysis in *Drosophila*. BioTechniques 29, 726–732.

Bellaiche, Y., Gho, M., Kaltschmidt, J., Brand, A., Schweisguth, F., 2001. Frizzled regulates localization of cell-fate determinants and mitotic spindle rotation during asymmetric cell division. Nat. Cell Biol. 3, 50–57.

Brand, A.H., Perrimon, N., 1993. Targeted gene expression as a means of altering cell fates and generating dominant phenotypes. Development 118, 401–415.

Castro, B., Barolo, S., Bailey, A.M., Posakony, J.W., 2005. Lateral inhibition in proneural clusters: cis-regulatory logic and default repression by Suppressor of Hairless. Development 132, 3333–3344.

De Renzis, S., Yu, J., Zinzen, R., Wieschaus, E., 2006. Dorsal–ventral pattern of Delta trafficking is established by a Snail-Tom-Neuralized pathway. Dev. Cell 10, 257–264.

Deblandre, G.A., Lai, E.C., Kintner, C., 2001. *Xenopus* neuralized is a ubiquitin ligase that interacts with XDelta1 and regulates Notch signaling. Dev. Cell 1, 795–806.

Furukawa, T., Kobayakawa, Y., Tamura, K., Kimura, K., Kawaichi, M., Tanimura, T., Honjo, T., 1995. Suppressor of Hairless, the *Drosophila* homologue of RBP-Jk, transactivates the neurogenic gene E(spl)m8. Jpn. J. Genet. 70, 505–524.

Giot, L., Bader, J.S., Brouwer, C., Chaudhuri, A., Kuang, B., Li, Y., Hao, Y.L., Ooi, C.E., Godwin, B., Vitols, E., Vijayadamodar, G., Pochart, P., Machineni, H., Welsh, M., Kong, Y., Zerhusen, B., Malcolm, R., Varrone, Z., Collis, A., Minto, M., Burgess, S., Mcdaniel, L., Stimpson, E., Spriggs, F., Williams, J., Neurath, K., Ioime, N., Agee, M., Voss, E., Furtak, K., Renzulli, R., Aanensen, N., Carrolla, S., Bickelhaupt, E., Lazovatsky, Y., Dasilva, A., Zhong, J., Stanyon, C.A., Finley Jr., R.L., White, K.P., Braverman, M., Jarvie, T., Gold, S., Leach, M., Knight, J., Shimkets, R.A., Mckenna, M.P., Chant, J., Rothberg, J.M., 2003. A protein interaction map of *Drosophila melanogaster*. Science 302, 1727–1736.

Glittenberg, M., Pitsouli, C., Garvey, C., Delidakis, C., Bray, S., 2006. Role of conserved intracellular motifs in Serrate signalling, cis-inhibition and endocytosis. EMBO J. 25, 4697–4706.

Hinz, U., Giebel, B., Campos-Ortega, J.A., 1994. The basic-helix–loop–helix domain of *Drosophila* lethal of scute protein is sufficient for proneural function and activates neurogenic genes. Cell 76, 77–87.

Kasanov, J., Pirozzi, G., Uveges, A., Kay, B., 2001. Characterizing Class I WW domains defines key specificity determinants and generates mutant domains with novel specificities. Chem. Biol. 8, 231–241.

Lai, E.C., 1999. Regulation of pattern formation during development of the *Drosophila* peripheral nervous system. PhD Dissertation, Department of Biology, University of California San Diego.

Lai, E.C., 2002. Micro RNAs are complementary to 3′ UTR sequence motifs that mediate negative post-transcriptional regulation. Nat. Genet. 30, 363–364.

Lai, E.C., Posakony, J.W., 1997. The Bearded box, a novel 3′ UTR sequence motif, mediates negative post-transcriptional regulation of *Bearded* and *Enhancer of split* Complex gene expression. Development 124, 4847–4856.

Lai, E.C., Rubin, G.M., 2001. *neuralized* functions cell-autonomously to regulate a subset of Notch-dependent processes during adult *Drosophila* development. Dev. Biol. 231, 217–233.

Lai, E.C., Burks, C., Posakony, J.W., 1998. The K box, a conserved 3′ UTR sequence motif, negatively regulates accumulation of *Enhancer of split* Complex transcripts. Development 125, 4077–4088.

Lai, E.C., Bodner, R., Kavaler, J., Freschi, G., Posakony, J.W., 2000a. Antagonism of Notch signaling activity by members of a novel protein family encoded by the *Bearded* and *Enhancer of split* gene complexes. Development 127, 291–306.

Lai, E.C., Bodner, R., Posakony, J.W., 2000b. The *Enhancer of split* Complex of *Drosophila* includes four Notch-regulated members of the Bearded gene family. Development 127, 3441–3455.

Lai, E.C., Deblandre, G.A., Kintner, C., Rubin, G.M., 2001. *Drosophila* Neuralized is a ubiquitin ligase that promotes the internalization and degradation of Delta. Dev. Cell 1, 783–794.

Lai, E., Tam, B., Rubin, G., 2005. Pervasive regulation of *Drosophila* Notch target genes by GY-box-, Brd-box-, and K-box-class microRNAs. Genes Dev. 19, 1067–1080.

Lecourtois, M., Schweisguth, F., 1995. The neurogenic Suppressor of Hairless DNA binding protein mediates the transcriptional activation of the *Enhancer of split* Complex genes triggered by Notch signaling. Genes Dev. 9, 2598–2608.

Leviten, M.W., Posakony, J.W., 1996. Gain-of-function alleles of *Bearded* interfere with alternative cell fate decisions in *Drosophila* adult sensory organ development. Dev. Biol. 176, 264–283.

Leviten, M.W., Lai, E.C., Posakony, J.W., 1997. The *Drosophila* gene *Bearded* encodes a novel small protein and shares 3′ UTR sequence motifs with multiple *Enhancer of split* Complex genes. Development 124, 4039–4051.

Li, Y., Baker, N.E., 2004. The roles of cis-inactivation by Notch ligands and of *neuralized* during eye and bristle patterning in *Drosophila*. BMC Dev. Biol. 4, 5.

Lynch, M., Force, A., 2000. The probability of duplicate gene preservation by subfunctionalization. Genetics 154, 459–473.

Mercado-Pimentel, M.E., Jordan, N., Aisemberg, G., 2002. Affinity purification of GST fusion proteins for immunohistochemical studies of gene expression. Protein Expr. Purif. 26, 260–265.

Nakao, K., Campos-Ortega, J.A., 1996. Persistent expression of genes of the *Enhancer of split* complex suppresses neural development in *Drosophila*. Neuron 16, 275–286.

Nellesen, D.T., Lai, E.C., Posakony, J.W., 1999. Discrete enhancer elements mediate selective responsiveness of *Enhancer of split* Complex genes to common transcriptional activators. Dev. Biol. 213, 33–53.

Pavlopoulos, E., Pitsouli, C., Klueg, K.M., Muskavitch, M.A., Moschonas, N.K., Delidakis, C., 2001. Neuralized encodes a peripheral membrane protein involved in Delta signaling and endocytosis. Dev. Cell 1, 807–816.

Rebeiz, M., Posakony, J.W., 2004. GenePalette: a universal software tool for genome sequence visualization and analysis. Dev. Biol. 271, 431–438.

Rubin, G.M., Spradling, A.C., 1982. Genetic transformation of *Drosophila* with transposable element vectors. Science 218, 348–353.

Schlatter, R., Maier, D., 2005. The Enhancer of split and Achaete–Scute complexes of Drosophilids derived from simple ur-complexes preserved in mosquito and honeybee. BMC Evol. Biol. 5, 67.

Simionato, E., Ledent, V., Richards, G., Thomas-Chollier, M., Kerner, P., Coornaert, D., Degnan, B., Vervoort, M., 2007. Origin and diversification of the basic helix–loop–helix gene family in metazoans: insights from comparative genomics. BMC Evol. Biol. 7, 33.

Singson, A., Leviten, M.W., Bang, A.G., Hua, X.H., Posakony, J.W., 1994. Direct downstream targets of proneural activators in the imaginal disc include genes involved in lateral inhibitory signaling. Genes Dev. 8, 2058–2071.

Stark, A., Brennecke, J., Russell, R., Cohen, S., 2003. Identification of *Drosophila* microRNA targets. PLoS Biol. 1, E60.

Wang, W., Struhl, G., 2004. *Drosophila* Epsin mediates a select endocytic pathway that DSL ligands must enter to activate Notch. Development 131, 5367–5380.

Zaffran, S., Frasch, M., 2000. *Barbu*: an *E(spl) m4/ma*-related gene that antagonizes Notch signaling and is required for the establishment of ommatidial polarity. Development 127, 1115–1130.

Chapter 1, in full, is a reprint of the material as it appears in Developmental Biology 2009. Fontana, Joseph R.; Posakony, James W., Elsevier Inc., 2009. The dissertation author was the primary investigator and primary author of this paper. It has been reformatted to fit the required specifications for this Dissertation.

Chapter 2

The basic amphipathic α-helix of Bearded proteins is a PI(3)P-binding domain that mediates trafficking of Neuralized to late endosomes

Abstract

Neuralized (Neur) is a conserved E3 ubiquitin ligase that is required to activate the signaling potential of Notch (N) receptor ligands during many developmental events. Multiple members of the *Bearded* (*Brd*) gene family are directly activated by N signaling, and the small proteins they encode have been shown to inhibit the activity of Neur. In vivo, this inhibitory activity of Brd proteins is dependent on the presence of one or more NXXN motifs and a predicted basic amphipathic α-helix termed the B domain. NXXN motifs mediate direct binding to Neur, and the NXXN motifs of Brd proteins and N ligands compete for Neur binding in vitro. However, the role of the B domain has remained uncharacterized. Here we show that the B domain mediates a specific interaction with the phosphatidyl inositol PI(3)P. In vivo, Brd proteins colocalize with Neur in PI(3)P-positive endosomes. Depletion of PI(3)P levels is sufficient to inhibit the colocalization of Neur and Brd proteins in endosomes. We find that the B domain and NXXN motifs of the Brd protein E(spl)mα are both required for this colocalization pattern. Using combinations of markers for multiple endocytic compartments, we show that E(spl)mα and Neur colocalize in endosomes positive for the late endosomal and lysosomal proteins Rab7 and LAMP1. These data indicate that proper endosomal localization of Brd proteins, dependent on the B domain, is essential to their in vivo function as Neur antagonists.

Introduction

The development of multicellular animals relies heavily on the ability of individual cells to detect their extracellular environments and communicate with one another via the activity of various cell-cell signaling pathways. Upon receipt of an exogenous signal, a cell must internally transduce the information so that a proper response, be it transcriptionally, structurally, or biochemically, may be set in motion. In order for development to proceed successfully and consistently, many modes of regulation have evolved to ensure this signal activity is restricted both in time and space. Study of the Notch (N) signaling pathway in *Drosophila* has uncovered many examples of regulation acting in both signal-sending and signal-receiving cells, and an emerging theme in this regulation is the importance of proper transport of various components of the pathway.

The N signaling pathway consists of the transmembrane N receptor that is first processed in the Golgi (by a furin-like convertase) before being transported to the plasma membrane as a heterodimer (Blaumueller et al., 1997; Logeat et al., 1998). Upon activation by its transmembrane ligands, Delta (Dl) or Serrate (Ser) in *Drosophila*, on neighboring cells, the N receptor undergoes two proteolytic cleavages and internalization (Kopan et al., 1996). These events lead to the release of the N intracellular domain (NICD), which is translocated, into the nucleus where it acts as a transcriptional activator in a complex with Suppressor of Hairless [Su(H)] (Fortini and Artavanis-Tsakonas, 1994; Jarriault et al., 1995). In signal-

sending cells, endocytosis of the ligands Dl and Ser is required for an active signal to be sent out (Overstreet et al., 2004; Wang and Struhl, 2004). However, only a subset of these endocytic events, those mediated by the E3 ubiquitin ligases Neuralized (Neur) or Mindbomb (Mib-1), are responsible for enabling a cell to signal successfully to its neighbors (Wang and Struhl, 2005; Pitsouli and Delidakis, 2005; Lai et al., 2005).

Neur has been demonstrated to play important roles in many processes including mesoderm/mesectoderm specification in the embryo (De Renzis et al., 2006) and sensory organ precursor (SOP) specification, via lateral inhibition, during peripheral nervous system (PNS) development both in embryos and larval imaginal discs (Yeh et al., 2000). A C-terminal RING domain contains the E3 ligase activity of the protein, while the NHR1 (Neur Homology Repeat) region has been shown to mediate its interaction with the intracellular domain of Dl (Deblandre et al., 2001; Lai et al., 2001; Yeh et al., 2001; Commisso and Boulianne, 2007). Additionally, a poly-basic sequence motif just N-terminal to the NHR1 region of $Neur^{PA}$ has been found to be important for Neur activity by directing the localization and trafficking of Neur, and Dl with it, from the plasma membrane into Hrs-1 and Rab-11 positive endosomes (Skwarek et al., 2007). While the activity of Neur is required for N ligand activation in the above mentioned instances, during both mesoderm/mesectoderm specification and SOP specification, Neur expression is detected in cells in which its activity is not desired (De Renzis et al., 2006; S.W. Miller and

J.W. Posakony, unpublished). To overcome this potential threat to proper development, another level of N pathway regulation is employed, involving the *Bearded* (*Brd*) family of N-target genes.

The *Brd* family consists of the Enhancer of split-Complex [E(spl)-C] genes *E*(*spl*)*mα*, *E*(*spl*)*m2*, *E*(*spl*)*m4*, and *E*(*spl*)*m6* and the Brd-Complex genes *Bob*, *Brd*, *Tom*, and *Ocho* (Leviten et al., 1997; Lai et al., 2000a; Lai et al., 2000b). The Brd proteins [with the exception of E(spl)m2, which will be excluded from all further discussions] have been shown to inhibit N signaling (Leviten et al., 1997; Apidianakis et al., 1999; Lai et al., 2000a; Lai et al., 2000b; Zaffran and Frasch, 2000). Specifically, the Brd proteins act by inhibiting the ability of Neur to activate, via endocytic events, the N ligands (De Renzis et al., 2006; Bardin and Schweisguth, 2006). We have previously shown that an NXXN motif, found in one or more copies in all of these Brd proteins [again, excluding E(spl)m2] mediates a direct interaction to Neur (Fontana and Posakony, 2009). Subsequently, we identified an NXXN motif in the intracellular domain of Dl that also mediates a direct Neur interaction. Presence of the NXXN motifs in Brd proteins is required to compete with Dl for binding to Neur in vitro (Fontana and Posakony, 2009). Furthermore, the NHR1 region of Neur has been implicated in the Brd protein interaction, just as it had been for the interaction with Dl (Bardin and Schweisguth, 2006; Commisso and Boulianne, 2007). These data support a model in which the NXXN motifs of Brd proteins and N ligands (Ser also contains an NXXN motif in its

intracellular domain) compete for the same binding site in the NHR1 region of Neur to either inhibit or promote the sending of a N signal from a cell. Several questions remain about this process, however. In addition to the NXXN motif(s), all Brd family members (BFMs) also contain an N-terminal motif termed the B domain (for Basic) that is predicted to encode a highly basic amphipathic α-helix (Leviten et al., 1997; Lai et al., 2000a; Lai et al., 2000b; Zaffran and Frasch, 2000). Replacing the basic Lys residues of the B domain with Ala residues prevents E(spl)mα, E(spl)m4, Brd, and Bob from disrupting lateral inhibition when misexpressed (Fontana and Posakony, 2009; Lai, 1999). However, the role of the B domain in this process remains unclear. The events, if any, that occur after Brd proteins interact with Neur are also unknown.

Here we address the cellular mechanism by which Brd proteins inhibit Neur function and, for the first time, characterize the association of these proteins together in endocytic vesicles. In cell culture, we report a cortical localization pattern of E(spl)mα that is dependent on the basic, amphipathic nature of the B domain. The B domain is also found to be required for a direct in vitro interaction with the phosphoinositide PI(3)P. In vivo, we observe a punctate pattern of localization for E(spl)mα and E(spl)m4. In the presence of Neur, these Brd proteins colocalize with both Neur and a marker for PI(3)P-positive endosomes, myc-2xFYVE. The colocalization of E(spl)mα with Neur in vesicles is inhibited upon depletion of cellular PI(3)P levels. This colocalization is also dependent on the

presence of both the B domain and NXXN motifs of E(spl)mα. Finally, we observe that E(spl)mα and Neur are found together in vesicles positive for the late endosomal and lysosomal markers, Rab7 and LAMP1. We propose a model of N signal inhibition by which Brd proteins complex with Neur and PI(3)P on endocytic vesicles and target Neur for degradation in the lysosome. This process is dependent on the Brd protein's ability to bind Neur via its NXXN motif(s) and PI(3)P via its B domain.

Materials and Methods

Fly stocks

Previously described flies used include: *UAS-neur* (Lai and Rubin, 2001); *UAS-mα-V5-6xHIS* variants (Fontana and Posakony, 2009); *w^{1118} E(spl)mα-GAL4* (Castro et al., 2005); *UAS-myc-2xFYVE* and *UAS-GFPmyc-2xFYVE* (González-Gáitin; Wucherpfennig et al., 2003); *UAS-GFP-LAMP1* (Pulipparacharuvil et al., 2005); *UAS-YFP-Rabs* (Zhang et al., 2007; Bloomington Stock Center). *UAS-m4-V5-6xHIS* was generated by cloning the coding sequence of *E(spl)m4* into *UAS-V5-6xHIS* (Fontana and Posakony, 2009).

Generation of antibodies

The generation of GST-Neur and HIS-mα constructs, the induction of both proteins, and the purification of GST-Neur have been described previously (Fontana and Posakony, 2009). HIS-mα was purified under denaturing conditions using a urea buffer (8 M urea; 10 mM Tris-Cl; 100 mM NaH_2PO_4) and following protocol in "The QIAexpressionist" (Qiagen). GST-Neur was sent for antibody production as a polyacrylamide gel band. HIS-mα was electro-eluted from a polyacrylamide gel and dialyzed in 1x phosphate-buffered saline (PBS) before being sent for antibody production. Antigens were sent to Pocono Rabbit Farm and Laboratory for antibody production. Antibodies against GST-Neur were generated in 2 guinea pigs and 2 rabbits, and react positively against both GST and HIS-Neur in a western blot. Antibodies against HIS-mα were generated in

2 guinea pigs and 2 rats, and react successfully with GST-mα (but not GST, GST-m2, GST-m4, GST-m6, GST-Tom, or GST-Ocho) in a western blot.

CME-W2 cell culture

The CME-W2 *Drosophila* imaginal disc cell line was obtained from the *Drosophila* Genomics Resource Center (DGRC). Cells were cultured in Shields and Sang M3 insect medium (Sigma) supplemented with 5% Fetal Bovine Serum, 2% fly extract, 5 μg/mL Insulin, 2.5 mg/mL Bacto-Peptone, 1 mg/mL Yeast Extract (protocols can be found at the DGRC website: https://dgrc.cgb.indiana.edu). E(spl)mα variants were cloned into the pAc5.1/V5-HIS expression vectors (Invitrogen). Transient transfections were performed using Effectene Transfection Reagent (Qiagen).

Purification of HIS-mα variants for PIP strip assays

Generation of HIS-mα in vitro constructs and induction of proteins have been described previously (Fontana and Posakony, 2009). 100 mL bacterial pellets containing induced proteins were resuspended in 6 mL of Cell Lysis Buffer (20 mM Tris-HCl pH 8.0; 200 mM NaCl; 0.5% Nonidet P-40; 0.2 mM PMSF; 1 μg/mL Pepstatin-A) and lysed with 100 μg/mL lysozyme on ice for 30 minutes. Lysates were sonicated briefly to shear DNA and passed through a 22-guage needle to remove any clumps. Imidazole was added to 10 mM and lysates were incubated with 500 μL of TALON metal affinity resin (Clontech) to bind HIS-tagged proteins for 3

hours at 4°C. Beads were washed 2 x 6 mL with Cell Lysis Buffer + 10 mM Imidazole, 2 x 6 mL with Sodium Phosphate Buffer (50 mM sodium phosphate pH 7.0; 500 mM NaCl) + 10 mM Imidazole, and 2 x 500 μL Sodium Phosphate Buffer + 30 mM Imidazole. HIS-tagged proteins were eluted with 4 x 500 μL Sodium Phosphate Buffer + 300 mM Imidazole.

PIP strip assay

PIP microstrip (Echelon Biosciences Inc.) assays were carried out as per manufacturer's suggestion. 1% nonfat-dry milk was used as block. HIS-tagged proteins were used at 0.5 μg/mL – 1.5 μg/mL concentrations. Mouse anti-HisG antibody (Invitrogen) was used at a 1:2,000 dilution. Goat-anti-mouse-HRP (Jackson Laboratories) was used at a 1:10,000 dilution. ECL Plus Western Blotting Detection System (GE Healthcare) was used for detection.

Wortmannin assay

Late third instar larvae of the appropriate genotypes were rinsed in 1x PBS + 0.1% Triton X-100 (PBT) to remove food stuck to the body. In fresh PBT, the larvae were cut in half, fat bodies and internal organs were removed, and the carcasses were flipped inside out with the CNS and associated imaginal discs still attached. The carcasses were divided into 2 groups, incubated for 2 hours in 1 mL of Shields and Sang M3 insect medium (Sigma) with either 10 μL of DMSO (control) or 100 nM wortmannin (10 μL of 10 μM stock solution in DMSO). After incubation, tissue was rinsed with PBT, fixed with 4% paraformaldehyde in PBT (0.3%

Triton X-100), and washed with PBT. Immunohistochemistry was carried out as needed. Vesicle numbers were scored from a 20 μm maximum confocal projection of the dorsal radius cluster.

Immunohistochemistry

All images were taken from transiently transfected CME-W2 cells or the dorsal radius proneural cluster of late 3rd instar wing imaginal disc tissue. Imaginal disc fixation methods have been described previously (Fontana and Posakony, 2009). Primary antibodies used include mouse monoclonal anti-V5 (Invitrogen) diluted 1:500, rat monoclonal anti-c-myc (Santa Cruz Biotechnology) diluted 1:100, mouse anti-c-myc (Developmental Studies Hybridoma Bank) diluted 1:100, guinea pig 1991 anti-neur diluted 1:2,000, and guinea pig 1852 anti-mα diluted 1:2,000. Secondary antibodies from Molecular Probes were diluted at 1:500 and include Alexa Fluor 488 Donkey anti-mouse IgG, Alexa Fluor 488 Donkey anti-rat IgG, Alexa Fluor 555 Goat anti-rat IgG, Alexa Fluor 555 Goat anti-guinea pig IgG, Alexa Fluor 647 Donkey anti-mouse IgG, and Alexa Fluor 647 Goat anti-rat IgG. Rhodamine-phalloidin (Molecular Probes) was diluted 1:25. Hoechst 33342 (Molecular Probes) was diluted at 1:2,000.

Results

The basic amphipathic α-helix is required for cortical localization of E(spl)mα in CME-W2 cells

To gain further insights into the mechanism by which Brd family proteins inhibit the activity of Neur, we sought to characterize the subcellular localization of the canonical Brd family member E(spl)mα. When expressed in the *Drosophila* wing imaginal disc cell line CME-W2 by transient transfection, E(spl)mα is predominantly observed at the periphery of the cell and colocalizes with a rhodamine-phalloidin stain that marks actin fibers at the cell cortex (Figure 2.1B,B'). Both the untagged E(spl)mα protein and a C-terminally V5-6xHIS-tagged version exhibit this same localization pattern (Figure 2.1B; data not shown). A minority of the E(spl)mα protein is found in vesicular structures in CME-W2 cells (Figure 2.1B). This localization pattern is unperturbed when the G or D motifs are mutated or deleted, respectively, or when four lysine residues of the B domain are replaced with arginine residues (4K/R) (Figure 2.1A,E,G-H). Mutating only the C-terminal NXXN motif of E(spl)mα also does not affect the localization of the protein (Figure 2.1F). However, when the strong amphipathic character of the B domain is disrupted by substituting the basic lysine residues with non-polar alanines (4K/A) or polar glutamines (4K/Q), E(spl)mα no longer localizes cortically, and is instead found

distributed throughout the cell (Figure 2.1A,C-D). These data indicate a critical role for the amphipathic B domain in the localization of E(spl)mα.

The basic amphipathic α-helix is required for an in vitro interaction between E(spl)mα and PI(3)P

The plasma membrane association of E(spl)mα could be achieved in several possible ways. To investigate a potential interaction with membrane phospholipids, N-terminally 6xHIS-tagged E(spl)mα (HIS-mα) was purified and assayed on a PIP microstrip (Figure 2.2A). At concentrations of 0.5 μg/mL and 1.5 μg/mL, HIS-mα interacts strongly with the mono-phosphorylated phosphoinositide PI(3)P (Figure 2.2B; data not shown). Much weaker binding is observed with PI(4)P and PI(5)P. While these weaker interactions may be indicative of the protein's true specificity in vivo, they may also represent non-specific binding in the in vitro assay. At 0.5 μg/mL, mutating both NXXN motifs (HIS-mα$^{N', N}$) or the G motif (HIS-mα^{G2}), or deleting the D motif (HIS-mα^{D}), each has no effect on the interaction of E(spl)mα with PI(3)P (Figures 2.1A, 2.2C-E). By contrast, when the amphipathicity of the B domain is disrupted, the interaction with PI(3)P is abolished. This is observed with both HIS-mα$^{4K/A}$ and HIS-mα$^{4K/Q}$, with the double variant HIS-mα$^{4K/A, D}$, and with HIS-mα$^{5np/Q}$, which substitutes the nonpolar residues of the B domain with polar glutamine residues (Figures 2.1A, 2.2F-I). HIS-mα$^{4K/A, D}$ was tested because of our previous observation that HIS-mα$^{4K/A}$ can exhibit an artifactual in vitro

behavior that is relieved in the double mutant (Fontana and Posakony, 2009). HIS-mα$^{4K/A}$ and HIS-mα$^{4K/A, D}$ were also evaluated in this assay at a three-fold higher concentration, 1.5 μg/mL, but still showed no interaction with any phospholipids (Figure 2.2F',G'). To our surprise, substituting the lysine residues of the B domain with another basic amino acid, arginine (4K/R), also abolishes the interaction of E(spl)mα with PI(3)P at the lower 0.5 μg/mL concentration (Figure 2.2J). This variant shows a wild-type localization pattern in transfected cells (Figure 2.1B,E), suggesting that the PIP assay may be more sensitive to protein variation than the cell culture assay. Indeed, at the higher 1.5 μg/mL concentration, HIS-mα$^{4K/R}$ shows binding specificity for PI(3)P, and a weaker interaction with PI(4)P, PI(5)P, and phosphatidic acid (Figure 2.2J'). These results show that E(spl)mα interacts strongly with the phosphoinositide PI(3)P in vitro, and that this interaction is dependent on the basic amphipathic nature of the B domain.

E(spl)mα and E(spl)m4 colocalize with Neur in PI(3)P-positive vesicles in vivo

As PI(3)P is a phospholipid found on various endosomes (Johnson et al., 2006; Lindmo and Stenmark, 2006), the interaction of E(spl)mα with PI(3)P suggests that E(spl)mα should show a vesicular pattern of localization in vivo. To investigate the localization of Brd family proteins in relation to PI(3)P-positive vesicles in an endogenous setting, C-terminally

V5-6xHIS-tagged E(spl)mα (mα-V5) and E(spl)m4 (m4-V5) were expressed in flies using the *UAS-GAL4* system . When expressed in the non-SOP cells of proneural clusters (their wild-type expression domain) using the *E(spl)mα-GAL4* driver, a punctate pattern of localization is observed for both mα-V5 and m4-V5 (Figure 2.3A,C). For mα-V5, these puncta are concentrated near the periphery of the cell and overlap with a rhodamine-phalloidin stain, while m4-V5 puncta are found much more uniformly dispersed throughout the cytoplasm. To test for the colocalization of these Brd protein puncta with PI(3)P, the population of PI(3)P-positive vesicles was marked by the expression of myc-2xFYVE (Wucherpfennig et al., 2003). Interestingly, neither mα-V5 nor m4-V5 puncta localize to PI(3)P-positive vesicles (Figure 2.3A,C).

Neur has been reported to have a vesicular pattern of localization (Lai et al., 2001; Commisso and Boulianne, 2007; unpublished observations). Given the direct interaction between Brd family proteins and Neur, and the primary role of Brd proteins in inhibiting Neur activity, we reasoned that E(spl)mα and E(spl)m4 should colocalize with Neur in vivo. When mα-V5 and Neur are coexpressed, a dramatic change in the localization pattern of mα-V5 is observed. In the presence of Neur, mα-V5 is found more highly concentrated in large cytoplasmic puncta compared to when Neur is not present (Figure 2.3A-B). In 100% of these large puncta (n>100), mα-V5 colocalizes with Neur (Figure 2.3B). In

addition, many of these mα-V5/Neur puncta (>90%) colocalize with myc-2xFYVE (Figure 2.3B). Many smaller mα-V5 puncta are also observed in the presence of Neur, and there are many small Neur puncta. However, we do not find significant colocalization with these populations. Similar results are obtained when m4-V5 and Neur are coexpressed. The two proteins are observed to colocalize in myc-2xFYVE-positive vesicles (Figure 2.3D). These data show that, in vivo, Brd proteins and Neur colocalize in PI(3)P-positive endocytic vesicles.

PI(3)P depletion inhibits the vesicular colocalization of E(spl)mα and Neur

To determine if the vesicular colocalization observed with mα-V5 and Neur is dependent on the presence of PI(3)P, the PI3K inhibitor wortmannin was used. The effect of wortmannin on the number of PI(3)P-positive vesicles was assessed via detection of myc-2xFYVE expressed in non-SOP cells. Third-instar larval wing discs were incubated with 100 nM wortmannin, a low concentration that has been shown to selectively inhibit Class I and III PI(3)Ks (Prior and Clague, 1999). With this treatment we observed a 96% decrease in the number of PI(3)P-positive vesicles in a 20 μm thick section of the dorsal radius cluster as compared to control DMSO-treated discs (18 vesicles per cluster versus 406 for the control) (Figure 2.3E-F). This decrease coincides with an increase in diffuse background detection of the myc-2xFYVE protein, indicating that the levels of the PI(3)P marker have not significantly changed. Moreover, there appears to be no general defect in vesicle formation, as there are

over 300 YFP-Rab5 vesicles present per cluster under both DMSO and wortmannin treatment (Figure 2.3G-H).

When Neur and mα-V5 are coexpressed and the tissue is treated in the same manner, there is a 71% decrease in the number of mα-V5/Neur vesicles as compared to the control (23 vesicles per cluster versus 78 for the control) (Figure 2.3I-J). We conclude from these results that the colocalization of E(spl)mα and Neur in endocytic vesicles requires the production of PI(3)P.

Association of E(spl)mα with Neur and PI(3)P requires both the B domain and NXXN motifs

Our observation that mα-V5 is found in PI(3)P-positive vesicles only when Neur is present suggested that an interaction with Neur through E(spl)mα's NXXN motifs might be sufficient to produce this localization pattern. To address this question, the localization patterns of E(spl)mα variants were characterized in vivo, with and without coexpression of Neur.

When Neur is not coexpressed, the variants $m\alpha^{4K/R}$-V5, $m\alpha^{N',N}$-V5, and $m\alpha^{D}$-V5 produce a wild-type localization pattern, in that they are found in puncta that do not colocalize with myc-2xFYVE but that do highly overlap with rhodamine-phalloidin (Figure 2.4E,G,K). The $m\alpha^{G2}$-V5 variant pattern of localization is reminiscent of m4-V5 localization in that it is observed in cytoplasmic puncta that do not seem to overlap significantly

with rhodamine-phalloidin (Figure 2.4I). Both mα$^{4K/A}$-V5 and mα$^{4K/A, D}$-V5 also show no significant overlap with either rhodamine-phalloidin or myc-2xFYVE, but are more diffusely cytoplasmic than the mα^{G2}-V5 variant (Figure 2.4A,C).

Upon Neur coexpression, mα$^{4K/R}$-V5, mα^{G2}-V5, and mα^{D}-V5 colocalize with both Neur and myc-2xFYVE, similar to wild-type mα-V5 (Figure 2.4F,J,L). The mα$^{N',N}$-V5 variant does not colocalize with either Neur or myc-2xFYVE (Figure 2.4H). Upon Neur coexpression, both mα$^{4K/A}$-V5 and mα$^{4K/A, D}$-V5 are still diffusely cytoplasmic and do not show significant colocalization with either Neur or myc-2xFYVE. However, there are a number of vesicles positive for myc-2x-FYVE and Neur that also contain a small amount of these variant mα proteins. In summary, we find that E(spl)mα requires both its basic amphipathic α-helical B domain and its NXXN motifs to associate strongly with Neur in PI(3)P-positive endosomes. In the absence of a B domain, E(spl)mα may weakly associate with Neur in vesicles, although the former never accumulates to significant levels.

E(spl)mα and Neur colocalize with markers of late endosomes and lysosomes

PI(3)P is found on many endocytic vesicles, including Rab5-positive early endosomes (EE) [following recruitment of PI(3)K], the sorting endosome/multivesicular body (SE/MVB), and Rab7-positive late

endosomes (LE) (Johnson et al., 2006; Lindmo and Stenmark, 2006). The Rab proteins are a family of small GTPases involved in various aspects of intracellular trafficking (Seachrist and Ferguson, 2003; Markgraf et al., 2007). Rab5 is found on both EEs that bud from the plasma membrane as well as the SE/MVB. Rab4 is localized to both the SE/MVB and recycling endosomes (RE) that transport material back to the plasma membrane. Rab7 can be found on SE/MVBs, LEs, and the lysosome. Coexpressing myc-2xFYVE with YFP-tagged Rab proteins allows us to distinguish various endosomal populations within the cell (Table 2.1).

Using these markers of endocytic compartments, the localization of mα-V5 in the presence of Neur was studied. We find that 68% of the mα-V5-positive vesicles are Rab5+/PI(3)P+, while 0% are Rab5+/PI(3)P- (Table 2.2, Figure 2.5A). When testing for colocalization with Rab4, 79% of the mα-V5-positive vesicles are Rab4+/PI(3)P+, while none are Rab4+/PI(3)P- (Figure 2.5B). Finally, in a test for colocalization with Rab7, we find that 59% of the mα-V5-positive vesicles are Rab7+/PI(3)P+ and 6% are Rab7+/PI(3)P- (Figure 2.5C). Since we also found that all endosomal mα-V5 colocalizes with Neur, these results are suggestive of an E(spl)mα/Neur complex being trafficked in PI(3)P+ SE/MVBs and Rab7+ LE/lysosomes.

Limitations of the assay prevented the simultaneous staining of Neur and mα-V5 with the above combination of markers, but we sought to verify their colocalization in this endocytic pathway. To test this, GFP-

LAMP1 (Lysosomal Associated Membrane Protein 1) was used as a marker of the late endosomal and lysosomal compartments (Bucci et al., 2000; Pulipparacharuvil et al., 2005). In this assay, Neur and mα-V5 are observed to colocalize in GFP-LAMP1 vesicles (Figure 2.5D) These data further support a model in which Neur and E(spl)mα are trafficked together into LE/lysosomes.

Discussion

Localization requirements for Brd protein activity

To more fully elucidate the mechanism of inhibition of Neur by BFMs, we have documented multiple aspects of BFM localization. By comparing and contrasting the patterns observed for wild-type E(spl)mα, wild-type E(spl)m4, and variants of E(spl)mα, we were able to determine the localization characteristics that are functionally important for BFM activity. In CME-W2 cells, E(spl)mα shows a tight cortical localization pattern that is dependent on the basic amphipathic nature of the B domain (see Figure 2.1). While these data allowed us to identify a potential role for the B domain in localization, several in vivo observations indicate that the cortical localization itself may not be physiologically relevant. In vivo, E(spl)mα is found in puncta clustered at the cortex of the cell, but not to the same extent as seen in cell culture (see Figure 2.3). Interestingly, E(spl)m4 is also seen in puncta, but they are not observed to localize cortically in vivo. In addition, the Brd protein Tom has been reported to be predominantly cytoplasmic in the embryo (Zaffran and Frasch, 2000). Since these BFMs all retain the ability to disrupt N signaling, it seems that cortical localization is not a requirement for activity.

When coexpressed, Neur colocalizes with both E(spl)mα and E(spl)m4 in PI(3)P+ vesicles. The only manipulations of E(spl)mα found to prevent the strong association with Neur in PI(3)P+ vesicles were those that disrupted the NXXN motifs or the basic amphipathic nature of the B

domain (see Figures 2.3,2.4). These mutations also prevent BFMs from disrupting lateral inhibition when misexpressed (Fontana and Posakony, 2009; Lai, 1999). These data suggest that the common ability of BFMs to colocalize with Neur and PI(3)P is the primary localization characteristic required for their activity.

Sequence patterns in a highly diverged structural domain

The defining characteristic of all BFMs identified to date is the presence of a predicted basic amphipathic α-helix near the N terminus of the protein, referred to as the B domain (Leviten et al., 1997; Lai et al., 2000a; Lai et al., 2000b; Zaffran and Frasch, 2000). The amino acid sequence of individual BFM B domains is strikingly diverged. Despite this seeming lack of constraint, an α-helical "wheel" plot of the domain invariably shows a structure with hydrophobic residues clustered on one side and the basic residues Lys and Arg on the other. It seemed clear that this conserved property of the B domain has some functional significance ; however, none had previously been assigned to it. Here we have presented several lines of evidence that implicate the B domain in mediating a direct protein-phospholipid interaction. E(spl)mα interacts quite specifically with the phosphoinositide PI(3)P in an in vitro PIP binding assay (see Figure 2.2). The systematic mutation of all conserved regions of E(spl)mα reveals that only disruption of the basic amphipathic nature of the B domain eliminates binding to PI(3)P. This can be achieved by mutating the basic Lys residues as well as by mutating the non-polar

residues. The interaction appears to have physiological importance, as both E(spl)mα and E(spl)m4 colocalize with Neur in PI(3)P-positive vesicles in vivo (see Figure 2.3A-D). Depletion of PI(3)P, through the use of the PI(3)K inhibitor wortmannin, prevents E(spl)mα from colocalizing with Neur in endocytic vesicles (see Figure 2.3E-J).

Beyond its basic amphipathic character, can we discern any additional sequence or structural constraints that apply to the B domain and might help explain its specificity for PI(3)P? Answering this question is made more difficult by the fact that the boundaries of the domain are not yet clearly defined by objective criteria. Nevertheless, Table 2.3 shows that a large proportion of known BFMs (mainly of the "canonical" class) include in their B domains a sequence that does conform to a specific motif definition. In this motif, a hydrophobic residue occurs at positions 1, 4, 5, 8, and 9. The basic residues Lys or Arg fill positions 2 and 6. It is possible that this pattern represents a single motif, or the overlap of a repeated motif spanning positions 1-5 and 5-9. In either case, the observed conservation warrants a focus on these residues in future studies of B domain function.

The B domain and NXXN motifs are both required for Brd protein function

As our list of BFMs identified in various species grows , the importance of possessing both a B domain and an NXXN motif becomes more evident. Excluding the Drosophilids, we have identified one or more BFMs in at least 28 different species of insects and crustaceans. Within

almost all BFMs for which we have enough sequence data to analyze, we find both a predicted basic amphipathic α-helix and at least one NXXN motif. The only exceptions are the E(spl)m2-type Brd proteins, which are missing an NXXN motif; these have been identified only in the Dipteran suborder Brachycera.

While the B domain and NXXN motifs have been assigned distinct roles, we find that their functions in vivo are tightly coupled. If either the B domain or NXXN motifs are mutated, the Brd protein is no longer able to inhibit N signaling (Fontana and Posakony, 2009; Lai, 1999). We also do not observe strong association of either of these E(spl)mα variants with Neur or PI(3)P in vivo (Figure 2.4). But if the B domain mediates the interaction with PI(3)P, why do we see the in vivo association of BFMs with PI(3)P only when Neur is also present? One explanation might be that the binding of Neur to the NXXN motifs induces an allosteric conformational change in the BFM. This change could expose critical residues of the B domain, allowing an interaction with PI(3)P to take place. In a similar model, Neur might ubiquitinate BFMs upon binding; this modification could then cause a conformational change that exposes the critical residues of the B domain. Currently, however, there is no evidence indicating that BFMs are ubiquitinated by Neur. An alternative model for a conditional PI(3)P interaction is one of cooperative binding. The “4K/A” and “4K/A, D” variants of E(spl)mα can be found associated with Neur in PI(3)P+ vesicles, but this association is both weak and rare. Neur has

been shown to exhibit promiscuous affinity for multiple phosphoinositide phosphates in several different assays (Skwarek et al., 2007). It is possible that when Neur and a BFM are bound together, their combined affinities for phospholipids stabilize a specific association with PI(3)P.

In the above models, PI(3)P binding by BFMs is preceded by an initial BFM-Neur interaction. However, we find that E(spl)mα is capable of binding strongly to PI(3)P in vitro when no Neur is present (Figure 2.2). Therefore, it may not be appropriate to assume this initial BFM-Neur interaction. Neur has been observed in endosomes in the absence of BFMs (Lai et al., 2001; Commisso and Boulianne, 2007; unpublished observations), so another possible model is one in which the dual association with Neur and PI(3)P is what promotes the endosomal localization of BFMs. This would be similar to how EEA1 associates with endosomes by its dual affinities for activated Rab5, via a C_2H_2 zinc finger motif, and PI(3)P, via a FYVE domain (Simonsen et al., 1998). This model nicely encompasses the requirement for both a B domain [for PI(3)P interaction] and an NXXN motif (for Neur interaction). Without either, the BFM could not associate with the endosome. The model also offers an explanation as to why BFMs do not associate with PI(3)P in vivo when Neur is not present, and why they do not associate strongly with Neur when PI(3)P is depleted. This proposal is likewise compatible with the observation that BFMs mutant in either the B domain or NXXN motifs cannot disrupt lateral inhibition.

Transport to the late endosome/lysosome

Observing the colocalization of BFMs and Neur in PI(3)P+ endosomes led us to examine their trafficking in the endocytic pathway more closely. In the presence of Neur, we failed to observe localization of E(spl)mα in Rab4+/PI(3)P- endosomes. This leads us to conclude that a BFM-Neur complex is not being trafficked through recycling endosomes. By contrast, the presence of E(spl)mα in Rab7+/PI(3)P- endosomes suggested that Neur and E(spl)mα were being trafficked in the late endosomal pathway. Colocalization of Neur and E(spl)mα with LAMP1 gave further support to a model in which BFMs and Neur are trafficked to the LE/lysosome.

Transport of a BFM-Neur complex to the lysosome may be carried out in several ways. The ESCRT (Endosomal-Sorting Complex Required for Transport) complexes are involved in the formation of the internal vesicles of the MVB (Hurley and Emr, 2006; Nickerson et al., 2007; Woodman and Futter, 2008). A mature MVB/LE then fuses with vesicles containing lysosomal enzymes, leading to the degradation of cargo. Components of the ESCRT complex can bind ubiquitinated cargo, targeting them for the internal vesicles of the MVB. If Neur binding leads to the ubiquitination of BFMs, this may signal targeting of a BFM-Neur complex to these internal vesicles. Other ESCRT complex components bind PI(3)P, recruiting the complex to PI(3)P-rich domains of the endosome. The binding of BFMs to PI(3)P may also target a BFM-Neur

complex to these PI(3)P-rich domains, leading to their inclusion in the internal vesicles formed (Tanowitz and von Zastrow, 2002). High-resolution electron microscopy may allow us to determine if BFMs and Neur are indeed found in these internal vesicles, lending support to a model in which the proteins are targeted for lysosomal degradation.

Neur inhibition and transport

Endosomal colocalization of BFMs and Neur suggests several possibilities for the mechanism by which BFMs inhibit the activation of N ligands by Neur. In one model, binding of BFMs to Neur would inhibit the binding of Neur to N ligands, thereby preventing activation of the N ligands. Previous work shows that this competition between BFMs and Dl for binding to Neur does occur in vitro (Fontana and Posakony, 2009). But where would this competitive inhibition take place in vivo? The intracellular location of the functionally important interaction between Neur and Dl is currently unknown. What is apparent is that Dl is endocytosed from the plasma membrane in many Neur-independent events (Wang and Struhl, 2004; Wang and Struhl, 2005). Activated Rab5 on early endosomes interacts with the p150 subunit of Vps34, a class III PI(3)K. This recruitment promotes the synthesis of PI(3)P on early endosomes (Christoforidis et al., 1999). It would be attractive to suggest that BFMs are recruited to Neur-positive endosomes at this point. Our observation that in the presence of Neur, mα-V5 is found on Rab5+/PI(3)P+ endosomes, but not Rab5+/PI(3)P- endosomes, would support this (Table

2.2). If the relevant Dl-Neur interaction takes place at these endosomes, BFMs could be recruited to prevent it. In this model, the transport of BFMs and Neur to LE/lysosomes would not be the cause of Neur inhibition, but rather a consequence of the BFM-Neur interaction.

Alternatively, BFM-Neur trafficking to the lysosome could be an important component of Neur inhibition, by continuously preventing Neur from activating any N ligand molecules. Such a model would be compatible with the functionally important interaction between Dl and Neur occurring either at the plasma membrane or in endosomes. It would also encompass a BFM-Neur interaction occurring either before or after the Dl-Neur interaction. In all scenarios, BFMs would bind Neur on PI(3)P+ endosomes, inducing transport to the LE/lysosome. This would prevent any future activation of N ligands by Neur, regardless of its past activity.

Acknowledgements

We would like to thank Sui Zhang for her help in developing the Neuralized antibodies. Mariano Loza Coll provided expertise in setting up the lab for cell culture. We thank Inês Ribeiro for providing useful fly strains and many helpful discussions. We also thank Marcos González-Gáitin and the Bloomington Stock Center for providing fly stocks. Steven W. Miller and Feng Liu provided very useful critical comments during the preparation of the manuscript. J.R.F. was supported by a National Institutes of Health (NIH) pre-doctoral training grant in Developmental Biology. This work was supported by NIH grant GM075270 to J.W.P.

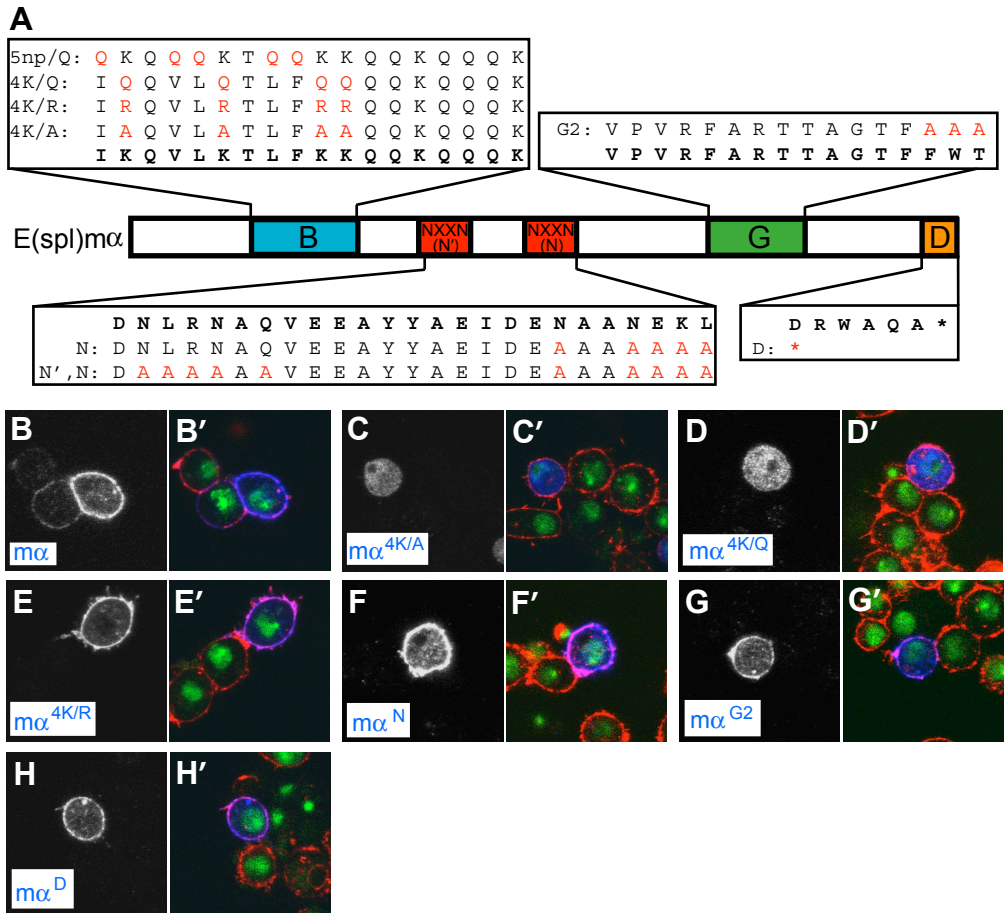

Figure 2.1: The basic amphipathic α-helix of E(spl)mα is required for cortical localization in CME-W2 cells. (A) Illustration of the conserved motifs of E(spl)mα. Amino acid sequences of motifs are boxed with the substitutions made in the protein variants depicted in red. (B-H) 1 μm confocal slice of CME-W2 cells transiently transfected with a plasmid to direct the expression of mα (B), mα$^{4K/A}$ (C), mα$^{4K/Q}$ (D), mα$^{4K/R}$ (E), mα^{N} (F), mα^{G2} (G), or mα^{D} (H). Only disruption of the basic amphipathic α-helix disrupts the wild-type cortical localization pattern. Blue = anti-mα. Red = rhodamine-phalloidin (cortical actin). Green = Hoechst 33342 (DNA).

Figure 2.2: The basic amphipathic α-helix of E(spl)mα mediates binding to PI(3)P. (A) Illustration of the phospholipids spotted on the PIP microstrip. (B-J) PIP strip assay results for HIS-mα and variants. (B-E) At 0.5 μg/mL, HIS-mα (B), HIS-mα$^{N', N}$ (C), HIS-mα^{G2} (D), and HIS-mα^{D} (E) show a strong and specific interaction with PI(3)P. (F,G,H-J) There are no phospholipid interactions seen with 0.5 μg/mL HIS-mα$^{4K/A}$ (F), HIS-mα$^{4K/A, D}$ (G), HIS-mα$^{4K/Q}$ (H), HIS-mα$^{5np/Q}$ (I), or HIS-mα$^{4K/R}$ (J). (F',G',J') At 1.5 μg/mL HIS-mα$^{4K/A}$ (F') and HIS-mα$^{4K/A, D}$ (G') still do not show any phospholipid interaction, while HIS-mα$^{4K/R}$ (J') interacts predominantly with PI(3)P. Asterisks denote position of PI(3)P spot on PIP microstrips.

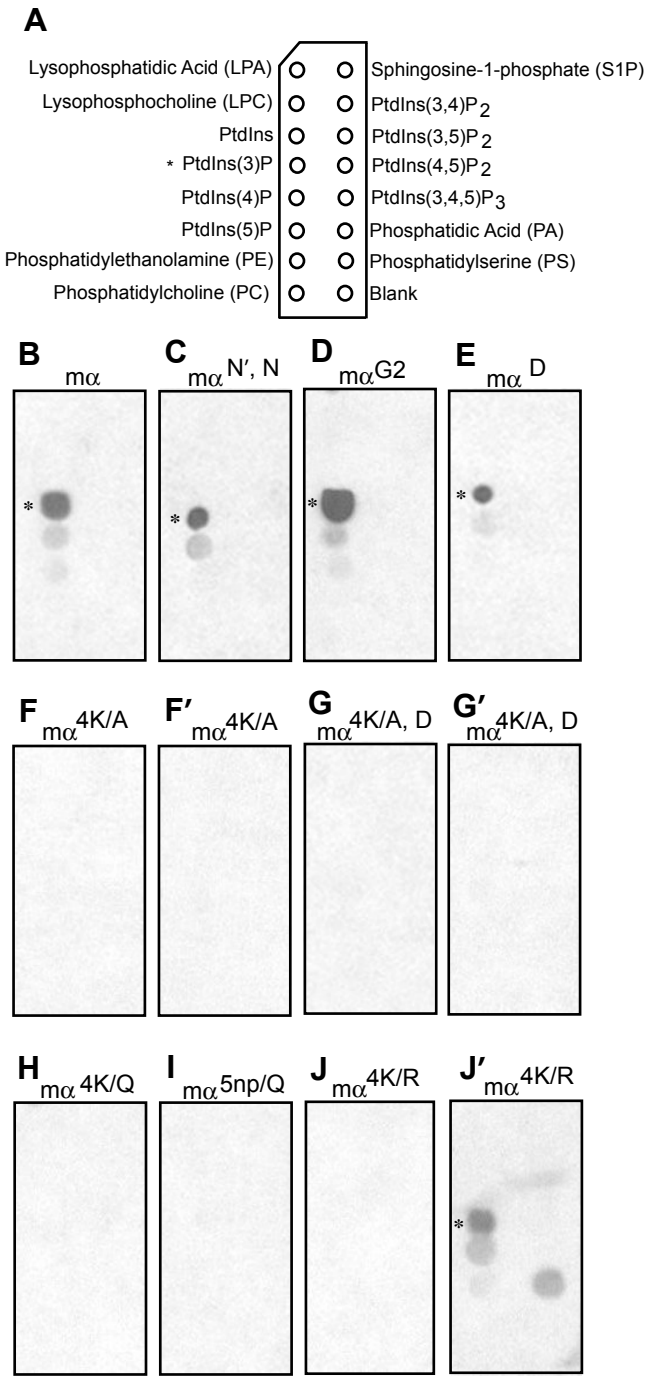
A
Lysophosphatidic Acid (LPA)
Lysophosphocholine (LPC)
PtdIns
* PtdIns(3)P
PtdIns(4)P
PtdIns(5)P
Phosphatidylethanolamine (PE)
Phosphatidylcholine (PC)
Sphingosine-1-phosphate (S1P)
PtdIns(3,4)P2
PtdIns(3,5)P2
PtdIns(4,5)P2
PtdIns(3,4,5)P3
Phosphatidic Acid (PA)
Phosphatidylserine (PS)
Blank
B mα
C mαN′, N
D mαG2
E mα D
F mα4K/A
F′ mα4K/A
G mα4K/A, D
G′ mα4K/A, D
H mα 4K/Q
I mα5np/Q
J mα4K/R
J′ mα4K/R

Figure 2.3: E(spl)mα and E(spl)m4 associate with Neur in PI(3)P+ endosomes in vivo.
(A) *E(spl)mα-GAL4/+; UAS-myc-2xFYVE/+; UAS-mα-V5/+*.
(B) *E(spl)mα-GAL4/+; UAS-myc-2xFYVE/UAS-neur; UAS-mα-V5/+*.
(C) *E(spl)mα-GAL4/+; UAS-myc-2xFYVE/+; UAS-m4-V5/+*.
(D) *E(spl)mα-GAL4/+; UAS-myc-2xFYVE/UAS-neur; UAS-m4-V5/+*.
(A-D) 3 μm confocal stack of the dorsal radius proneural cluster in wing imaginal discs. (A) mα-V5 does not colocalize with myc-2xFYVE (A') but overlaps with rhodamine-phalloidin (A"). (B) When Neur is coexpressed, mα-V5 colocalizes with both myc-2xFYVE (B') and Neur (B"). (C) m4-V5 does not colocalize with myc-2xFYVE (C') or rhodamine-phalloidin (C"). (D) When Neur is coexpressed, m4-V5 colocalizes with both myc-2xFYVE (D') and Neur (D"). For (A) and (C), arrows mark positions of myc-2xFYVE vesicles, blue = anti-V5, red = rhodamine-phalloidin, and green = anti-c-myc. For (B) and (D), arrows indicate positions of colocalization between Brd proteins (Blue = anti-V5), Neur (Red = anti-Neur) and myc-2xFYVE (Green = anti-c-myc). Arrowheads in (B) indicate colocalization of mα-V5 and Neur, but not myc-2xFYVE.
(E-J) 20 μm confocal stack of the dorsal radius proneural cluster. Proteins were expressed using E(spl)mα-GAL4. (E-F) myc-2xFYVE vesicles (Red = anti-c-myc) after treatment with DMSO (E) or wortmannin (F). (G-H) YFP-Rab5 vesicles (Green) after treatment with DMSO (G) or wortmannin (H). (I-J) Neur (Red = anti-Neur) and mα-V5 (Blue = anti-V5) after treatment with DMSO (I) or wortmannin (J). Bars are 10 μm. Scale is the same for A-D, and for E-J.

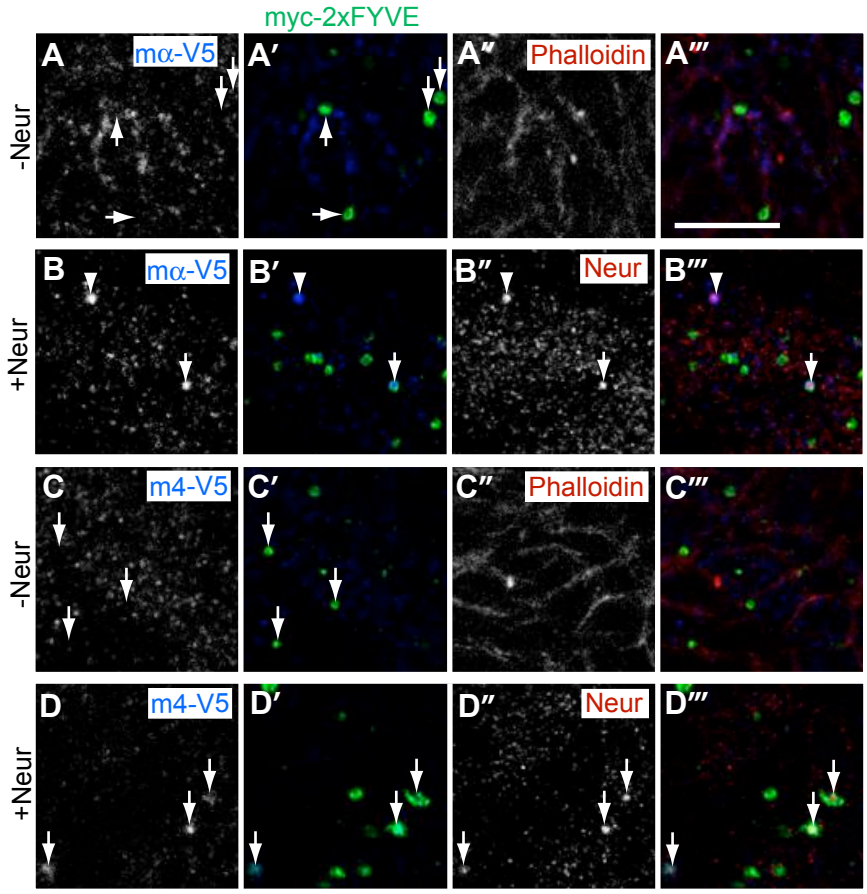
myc-2xFYVE
A
mα-V5
A′
A″
Phalloidin
A‴
-Neur
B
mα-V5
B′
B″
Neur
B‴
+Neur
C
m4-V5
C′
C″
Phalloidin
C‴
-Neur
D
m4-V5
D′
D″
Neur
D‴
+Neur

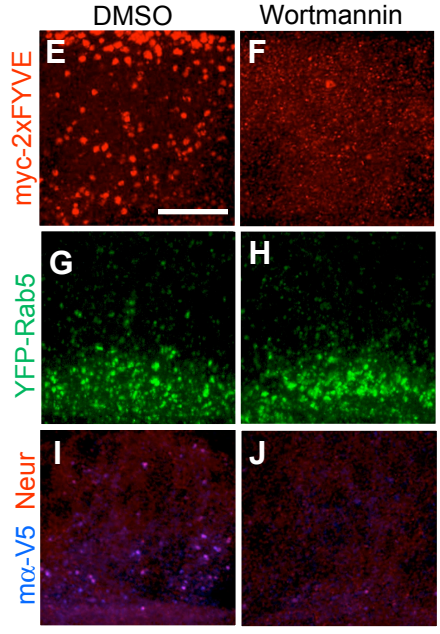
DMSO
Wortmannin
myc-2xFYVE
E
F
YFP-Rab5
G
H
mα-V5 Neur
I
J

Figure 2.4: Localization of E(spl)mα variants with and without coexpression of Neur. (A-L) 3 μm confocal stack of the dorsal radius proneural cluster in wing imaginal discs. Proteins were expressed using *E(spl)mα-GAL4*. (A-B) $m\alpha^{4K/A}$-V5. (C-D) $m\alpha^{4K/A,\ D}$-V5. (E-F) $m\alpha^{4K/R}$-V5. (G-H) $m\alpha^{N',\ N}$-V5. (I-J) $m\alpha^{G2}$-V5. (K-L) $m\alpha^{D}$-V5. Left panels (A,C,E,G,I,K) coexpress mα-V5 variant (Blue = anti-V5) and myc-2xFYVE (Green = anti-c-myc). Red = rhodamine-phalloidin. Cortical localizatoin of E(spl)mα is disrupted by mutating the basic amphipathic nature of the B domain (A,C) and by mutating the G motif (I). Right panels (B,D,F,H,J,L) coexpress mα-V5 variant (Blue = anti-V5), Neur (Red = anti-Neur), and myc-2xFYVE (Green = anti-c-myc). Arrows mark colocalization of the mα-V5 variant, Neur and myc-2xFYVE. Arrowheads mark colocalization of Neur and myc-2xFYVE, but not the mα-V5 variant. Integrity of the basic amphipathic α-helical B domain and the NXXN motifs are required by E(sp)mα for strong colocalization with Neur in PI(3)P+ vesicles. Only weak association with Neur is seen in the “4K/A” and “4K/A, D” variants, an example of which is marked in panel (D) with an arrow. Bar is 10 μm. Scale is the same for all panels.

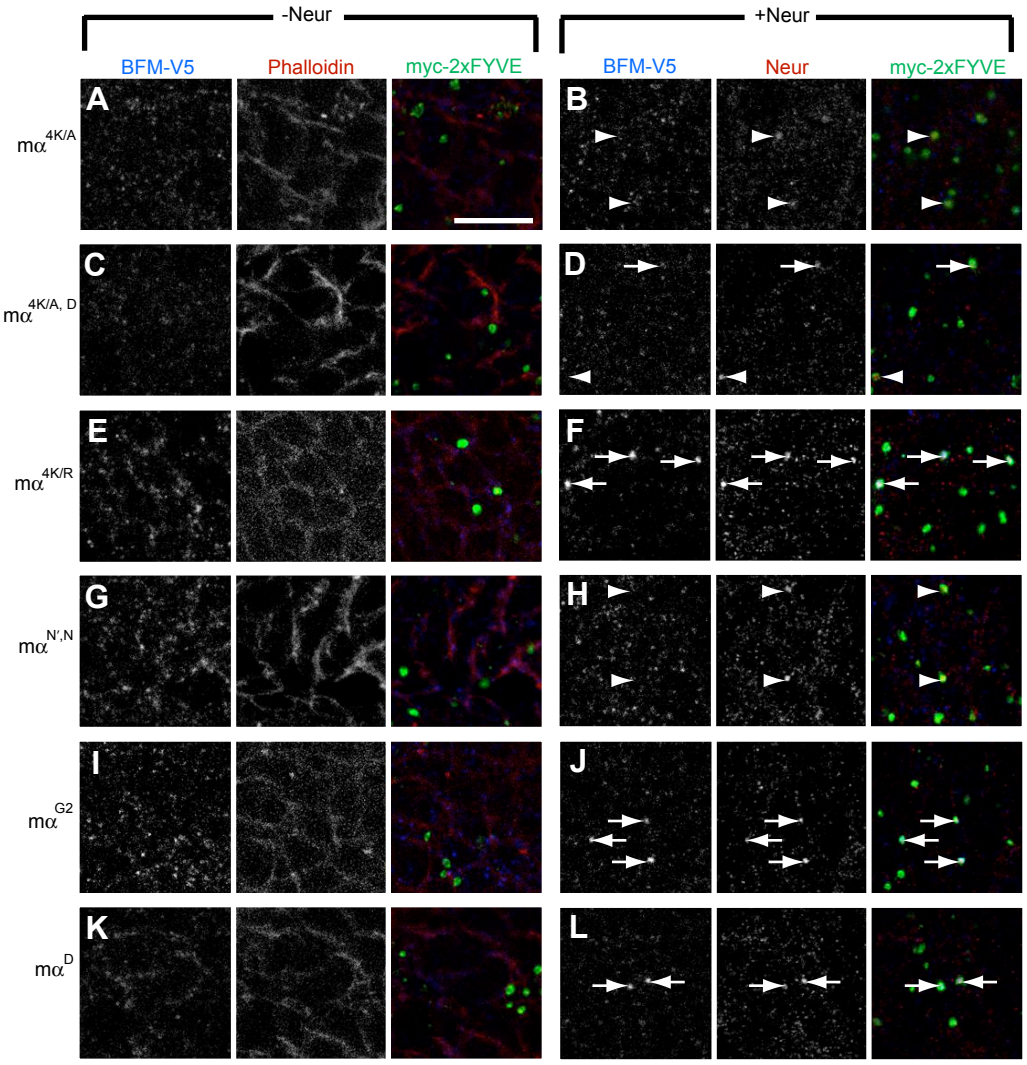
-Neur
+Neur
BFM-V5
Phalloidin
myc-2xFYVE
BFM-V5
Neur
myc-2xFYVE
A
B
mα4K/A
C
D
mα4K/A, D
E
F
mα4K/R
G
H
mαN',N
I
J
mαG2
K
L
mαD

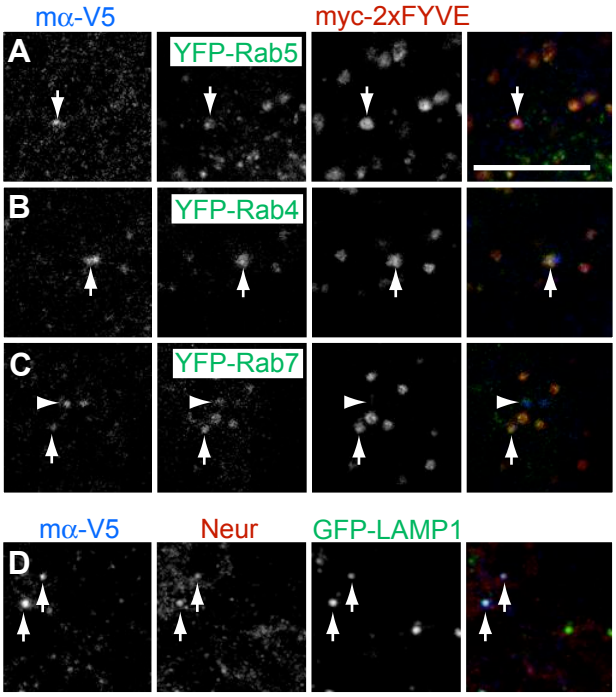

Figure 2.5: E(spl)mα and Neur colocalize with markers of the LE/lysosome. (A-D) 3 μm confocal stack of the dorsal radius proneural cluster in wing imaginal discs. Proteins were expressed using *E(spl)mα-GAL4*. (A-C) Coexpression of mα-V5 (Blue = anti-V5), Neur, and myc-2xFYVE (Red = anti-c-myc) with (A) YFP-Rab5 (Green), (B) YFP-Rab4 (Green), or (C) YFP-Rab7 (Green). Arrows mark colocalization of mα-V5, YFP-Rab, and myc-2xFYVE. Arrowhead in (C) marks colocalization of mα-V5 with YFP-Rab7, but not myc-2xFYVE. (D) Coexpression of mα-V5 (Blue = anti-V5), Neur (Red = anti-Neur), and GFP-LAMP1 (Green). Arrows mark colocalization of all three proteins. Bar is 10 μm. Scale is the same for all panels.

Table 2.1: Colocalization of myc-2xFYVE with YFP-Rab markers.

Vesicle size		YFP-Rab4 +	YFP-Rab5 +	YFP-Rab7 +
>0.82μm	myc-2xFYVE +	**100.0%** (104)	**100.0%** (159)	**86.7%** (143)
	myc-2xFYVE -	**0.0%** (0)	**0.0%** (0)	**13.3%** (22)
<0.82μm	myc-2xFYVE +	**56.4%** (53)	**60.6%** (146)	**59.8%** (61)
	myc-2xFYVE -	**43.6%** (41)	**39.4%** (95)	**40.2%** (41)

Table 2.2: Colocalization of mα-V5 with myc-2xFYVE and YFP-Rab markers.

Rab Marker	mα only	mα + FYVE only	mα + FYVE + Rab	**mα + Rab only**
YFP-Rab5	**6.1%** (5)	**25.6%** (21)	**68.3%** (56)	**0%** (0)
YFP-Rab4	**12.7%** (8)	**7.9%** (5)	**79.4%** (50)	**0%** (0)
YFP-Rab7	**10.8%** (11)	**24.5%** (25)	**58.8%** (60)	**5.9%** (6)

Table 2.3: A 9 amino acid sequence motif is conserved in the B domain of most Brd proteins. Alignment of a conserved 9 amino acid stretch of sequence in the B domain across multiple species of insects and crustaceans. Conserved hydrophobic residues are shown in red. Conserved basic residues are shown in blue.

						1	2	3	4	5	6	7	8	9					
Drosophila Ocho	S	P	S	R	R	L	K	N	L	L	K	P	L	L	G	Q	F	F	N
Drosophila Tom	M	A	M	R	S	L	R	K	L	V	K	P	L	L	R	L	V	K	K
Drosophila m4	K	L	S	Y	S	V	K	K	L	L	Q	K	I	F	K	Q	Q	Q	R
Drosophila mα	K	T	S	Y	S	I	K	Q	V	L	K	T	L	F	K	K	Q	Q	K
Drosophila m2	K	S	T	R	R	M	R	N	V	W	K	P	L	S	R	L	L	K	V
Drosophila m6			M	S	K	V	K	N	L	L	A	K	M	L	Q	R	F	G	K
Ceratitis capitata Ocho	S	P	S	R	R	L	K	N	L	L	K	P	L	L	G	R	V	F	K
Ceratitis capitata Tom	M	A	M	R	S	V	K	K	L	L	R	P	L	M	R	I	I	K	K
Ceratitis capitata m4	K	A	S	Y	S	I	K	R	L	L	K	Q	L	F	K	Q	H	N	K
Ceratitis capitata m2	K	S	K	R	K	L	C	K	M	W	R	P	L	L	R	L	M	A	R
Glossina morsitans Ocho	S	P	A	R	R	L	K	N	L	L	K	P	V	F	K	F	I	F	K
Glossina morsitans m4	K	L	T	Y	S	L	K	K	L	I	K	Q	Y	F	K	Q	R	K	S
Glossina morsitans m2	S	E	K	C	T	L	K	K	I	L	K	P	L	E	R	L	I	S	L
Teleopsis dalmanni Tom	T	A	M	R	S	L	K	K	L	I	K	P	L	L	R	I	I	K	K
Teleopsis dalmanni m4	K	V	S	Y	S	I	K	K	V	L	K	Q	L	F	K	Q	H	K	T
Teleopsis dalmanni mα	K	P	S	Y	S	I	K	K	V	L	K	T	L	F	K	K	Q	Q	K
Haematobia irritans irritans Ocho	S	P	S	R	R	L	K	N	M	L	K	P	V	L	G	R	I	F	K
Haematobia irritans irritans Tom	M	A	M	R	S	L	K	K	L	V	K	P	L	L	R	L	V	R	K
Haematobia irritans irritans BFM1C	T	M	T	Y	S	I	K	R	L	F	K	Q	L	F	K	H	Q	K	C
Lutzomyia longipalpis	S	P	A	H	R	V	K	K	M	L	K	P	L	L	K	F	L	T	Q
Mayetiola destructor	S	P	S	Y	R	I	K	K	I	L	K	P	I	L	R	I	L	R	Q
Culex pipiens	S	P	V	Y	K	L	K	K	I	L	K	P	I	A	A	L	L	K	S
Culex quinquefaciatus	S	P	V	Y	K	L	K	K	I	L	K	P	I	A	A	L	L	K	S
Aedes aegypti	S	P	V	Y	K	L	K	K	I	L	K	P	I	A	A	L	L	K	S
Anopheles gambiae	S	A	V	Y	R	L	K	K	I	L	K	P	L	V	T	L	L	K	S
Anopheles funestus	S	A	V	Y	R	L	K	K	I	L	K	P	L	V	T	L	L	K	S
Bombyx mori BFM1	M	K	N	S	G	I	K	A	L	L	R	P	L	M	K	M	I	K	K
Antheraea assama	M	K	N	S	G	I	K	A	L	L	X	P	L	M	K	I	I	K	K
Tribolium castaneum BFM1	S	A	F	H	Q	L	K	K	L	I	S	A	L	V	K	K	P	K	N
Apis mellifera BFM1	T	T	P	K	R	V	R	G	V	L	R	P	I	L	R	L	L	K	K
Acyrthosiphon pisum	R	K	M	H	K	I	N	K	T	I	K	P	I	L	R	A	L	C	R
Pediculus humanis corporis	E	S	I	S	H	V	V	K	K	I	K	P	V	I	K	S	H	L	K
Gryllus bimaculatus	S	L	V	H	R	I	K	K	M	L	K	P	V	A	R	L	V	S	R
Artemia franciscana	A	V	K	A	L	S	K	K	I	V	K	P	V	L	T	L	V	K	R
Daphnia pulex	L	I	T	K	K	V	S	N	L	V	K	P	L	L	T	K	R	H	N
Callinectes sapidus	F	S	T	H	S	L	K	K	A	I	K	K	L	I	K	K	T	R	P

References

Apidianakis, Y., Nagel, A.C., Chalkiadaki, A., Preiss, A., Delidakis, C., 1999. Overexpression of the *m4* and *mα* genes of the *E(spl)-Complex* antagonizes Notch mediated lateral inhibition. Mech. Dev. 86, 39–50.

Bardin, A., Schweisguth, F., 2006. Bearded family members inhibit Neuralized-mediated endocytosis and signaling activity of Delta in *Drosophila*. Dev. Cell 10, 245-255.

Blaumueller, C.M., Qi, H., Zagouras, P., Artavanis-Tsakonas, S., 1997. Intracellular cleavage of Notch leads to a heterodimeric receptor on the plasma membrane. Cell 90, 281-291.

Bucci, C., Thomsen, P., Nicoziani, P., McCarthy, J., van Deurs, B., 2000. Rab7: A key to lysosome biogenesis. Mol. Biol. Cell 11, 467-480.

Castro, B., Barolo, S., Bailey, A.M., Posakony, J.W., 2005. Lateral inhibition in proneural clusters: cis-regulatory logic and default repression by Suppressor of Hairless. Development 132, 3333–3344.

Christoforidis, S., Miaczynska, M., Ashman, K., Wilm, M., Zhao, L., Yip, S.-C., Waterfield, M.D., Backer, J.M., Zerial, M., 1999. Phosphatidylinositol-3-OH kinases are Rab5 effectors. Nat. Cell Biol. 1, 249-252

Commisso, C., Boulianne, G.L., 2007. The NHR1 domain of Neuralized binds Delta and mediates Delta trafficking and Notch signaling. Mol. Biol. Cell 18, 1-13.

De Renzis, S., Yu, J., Zinzen, R., Wieschaus, E., 2006. Dorsal-ventral pattern of Delta trafficking is established by a Snail-Tom-Neuralized pathway. Dev. Cell 10, 257-264.

Deblandre, G.A., Lai, E.C., Kintner, C., 2001. *Xenopus* neuralized is a ubiquitin ligase that interacts with XDelta1 and regulates Notch signaling. Dev. Cell 1, 795–806.

Fontana, J.R., Posakony, J.W., 2009. Both inhibition and activation of Notch signaling rely on a conserved Neuralized-binding motif in Bearded proteins and the Notch ligand Delta. Dev. Biol. 333, 373-385.

Fortini, M.E., Artavanis-Tsakonas, S., 1994. The Suppressor of Hairless protein participates in Notch receptor signaling. Cell 79, 273-282.

Hurley, J.H., Emr, S.D., 2006. The ESCRT complexes: Structure and mechanism of a membrane-trafficking network. Annu. Rev. Biophys. Biomol. Struct. 35, 277-298.

Jarriault, S., Brou, C., Logeat, F., Schroeter, E.H., Kopan, R., Israel, A., 1995. Signalling downstream of activated mammalian Notch. Nature 377, 355-358.

Johnson, E.E., Overmeyer, J.H., Gunning, W.T., Maltese, W.A., 2006. Gene silencing reveals a specific function of hVps34 phosphotidylinositol 3-kinase in late versus early endosomes. J. Cell Sci. 119, 1219-1232.

Kopan, R., Schroeter, E.H., Weintraub, H., Nye, J.S., 1996. Signal transduction by activated mNotch: Importance of proteolytic processing and its regulation by the extracellular domain. Proc. Natl. Acad. Sci. USA 93, 1683-1688.

Lai, E.C., 1999. Regulation of pattern formation during development of the *Drosophila* peripheral nervous system. PhD Dissertation, Department of Biology, University of California San Diego.

Lai, E.C., Bodner, R., Kavaler, J., Freschi, G., Posakony, J.W., 2000a. Antagonism of Notch signaling activity by members of a novel protein family encoded by the Bearded and Enhancer of split gene complexes. Development 127, 291-306.

Lai, E.C., Bodner, R., Posakony, J.W., 2000b. The Enhancer of split Complex of *Drosophila* includes four Notch-regulated members of the Bearded gene family. Development 127, 3441-3455.

Lai, E.C., Deblandre, G.A., Kintner, C., Rubin, G.M., 2001. *Drosophila* Neuralized is a ubiquitin ligase that promotes the internalization and degradation of Delta. Dev. Cell 1, 783-794.

Lai, E.C., Roegiers, F., Qin, X., Jan, Y.N., Rubin, G.M., 2005. The ubiquitin ligase *Drosophila* Mind bomb promotes Notch signaling by regulating the localization and activity of Serrate and Delta. Development 132, 2319-2332.

Leviten, M.W., Lai, E.C., Posakony, J.W., 1997. The *Drosophila* gene *Bearded* encodes a novel small protein and shares 3′ UTR sequence motifs with multiple *Enhancer of split* Complex genes. Development 124, 4039–4051.

Lindmo, K., Stenmark, H., 2006. Regulation of membrane traffic by phosphoinositide 3-kinases. J. Cell Sci. 119, 605-614.

Logeat, F., Bessia, C., Brou, C., LeBail, O., Jarriault, S., Seidah, N.G., Israël, A., 1998. The Notch1 receptor is cleaved constitutively by a furin-like convertase. Proc. Natl. Acad. Sci. USA 95, 8108-8112.

Markgraf, D.F., Peplowska, K., Ungermann, C., 2007. Rab cascades and tethering factors in the endomembrane system. FEBS Lett. 581, 2125-2130.

Nickerson, D.P., Russell, M.R.G., Odorizzi, G., 2007. A concentric circle model of multivesicular body cargo sorting. EMBO Rep. 8, 644-650.

Overstreet, E., Fitch, E., Fischer, J.A., 2004. Fat facets and Liquid facets promote Delta endocytosis and Delta signaling in the signaling cells. Development 131, 5355-5366.

Pitsouli, C., Delidakis, C., 2005. The interplay between DSL proteins and ubiquitin ligases in Notch signaling. Development 132, 4041-4050.

Prior, I.A., Clague, M.J., 1999. Localization of a Class II phosphatidylinositol 3-kinase, PI3KC2α, to clathrin-coated vesicles. Mol. Cell. Biol. Res. Commun. 1999, 162-166.

Pulipparacharuvil, S., Akbar, M.A., Ray, S., Sevrioukov, E.A., Haberman, A.S., Rohrer, J., Krämer, H., 2005. *Drosophila* Vps16A is required for trafficking to lysosomes and biogenesis of pigment granules. J. Cell Sci. 118, 3663-3673.

Seachrist, J.L., Ferguson, S.S.G., 2003. Regulation of G protein-coupled receptor endocytosis and trafficking by Rab GTPases. Life Sci. 74, 225-235.

Simonsen, A., Lippé, R., Christoforidis, S., Gaullier, J.-M., Brech, A., Callaghan, J., Toh, B.-H., Murphy, C., Zerial, M., Stenmark, H., 1998. EEA1 links PI(3)K function to Rab5 regulation of endosome fusion. Nature 394, 494-498

Skwarek, L., Garroni, M.K., Commisso, C., Boulianne, G.L., 2007. Neuralized contains a phosphoinositide-binding motif required downstream of ubiquitination for Delta endocytosis and Notch signaling. Dev. Cell 13, 783-795.

Tanowitz, M., von Zastrow, M., 2002. Ubiquitination-independent trafficking of G protein-coupled receptors to lysosomes. J. Biol. Chem. 277, 50219-50222.

Wang, W., Struhl, G., 2004. *Drosophila* Epsin mediates a select endocytic pathway that DSL ligands must enter to activate Notch. Development 131, 5367–5380.

Wang, W., Struhl, G., 2005. Distinct roles for Mind bomb, Neuralized and Epsin in mediating DSL endocytosis and signaling in *Drosophila*. Development 132, 2883-2894.

Woodman, P.G., Futter, C.E., 2008. Multivesicular bodies: co-ordinated progression to maturity. Curr. Opin. Cell Biol. 20, 408-414.

Wucherpfenning, T., Wilsch-Bräuninger, M., Gonzáles-Gáitan, M., 2003. Role of *Drosophila* Rab5 during endosomal trafficking at the synapse and evoked neurotransmitter release. J. Cell Biol. 161, 609-624

Yeh, E., Zhou, L., Rudzik, N., Boulianne, G.L., 2000. Neuralized functions cell autonomously to regulate *Drosophila* sense organ development. EMBO J. 19, 4827-4837.

Yeh, E., Dermer, M., Commisso, C., Zhou., L., McGlade, C.J., Boulianne, G.L., 2001. Neuralized functions as an E3 ubiquitin ligase during *Drosophila* development. Curr. Biol. 11, 1675-1679.

Zaffran, S., Frasch, M., 2000. *Barbu*: an *E(spl) m4/m*α-related gene that antagonizes Notch signaling and is required for the establishment of ommatidial polarity. Development 127, 1115-1130.

Zhang, J., Schulze, K.L., Hiesinger, P.R., Suyama, K., Wang, S., Fish, M., Acar, M., Hoskins, R.A., Bellen, H.J., Scott, M.P., 2007. Thirty-one flavors of Drosophila Rab proteins. Genetics 176, 1307-1322.

Chapter 2, in full, is currently being prepared for submission for publication of the material. Fontana, Joseph R.; Posakony, James W. The dissertation author was the primary investigator and author of this material. It has been reformatted to fit the required specifications for this Dissertation.

Chapter 3

Loss-of-function analyses of multiple *Bearded* family members reveals a redundant role during Notch-mediated lateral inhibition

Abstract

During mechanosensory organ development in *Drosophila melanogaster*, the Notch cell-cell signaling pathway mediates the specification of a single sensory organ precursor (SOP) cell from a field of cells known as the proneural cluster (PNC). In the SOP, the Notch ligand Delta (Dl) undergoes ubiquitination-dependent endocytosis mediated by the E3 ligase Neuralized (Neur). This process is required for Dl in the SOP to signal to the surrounding non-SOP cells of the PNC. Receipt of this Notch signal activates a genetic program that inhibits an SOP cell fate in the non-SOP cells. Among the genes directly activated by this Notch signal in non-SOP cells are the *Bearded* genes. Through imprecise excisions of P-element insertions and homologous recombination, we have generated null alleles of the *Brd* genes *Brd*, *Tom*, *E(spl)mα*, and *E(spl)m4*. Our data indicate that *Brd* genes act redundantly during lateral inhibition to ensure the specification of the proper number of SOPs. We find that loss of *Brd* gene function in the PNC results in the specification of extra SOPs. Brd proteins have a role in inhibiting the function of Neur, and we show that the loss of *Brd* genes renders cells of the PNC more susceptible to levels of Neur activity.

Introduction

The Notch (N) signaling pathway is utilized extensively during the development of multicellular animals to direct binary cell fate choices. In the developing peripheral nervous system (PNS) of *Drosophila*, it controls the decision between sensory organ precursor (SOP) fate and epidermal cell fate within the proneural clusters (PNCs) of larval imaginal discs.

Successful N-signaling requires an activated transmembrane ligand, Delta (Dl) or Serrate (Ser) in *Drosophila*, to interact with the transmembrane N receptor on neighboring cells. During SOP specification, Dl is activated through an interaction with the E3 ubiquitin ligase Neuralized (Neur). This interaction leads to the ubiquitination-dependent endocytosis of Dl, a process necessary for generating an active N signal (Lai et al., 2005; Le Borgne et al., 2005; Wang and Struhl, 2005). Activated Dl in the presumptive SOP signals to N receptor on the surrounding cells of the PNC. This leads to the proteolytic processing of the N receptor, allowing its cleaved intracellular domain to be translocated into the nucleus (Pan and Rubin, 1997; Sotillos et al., 1997; Struhl and Adachi, 1998; De Strooper et al., 1999). In the nucleus, the N intracellular domain complexes with the sequence specific transcription factor Suppressor of Hairless [Su(H)] to activate transcription of N-target genes (Bailey and Posakony, 1995; Tamura et al., 1995; Barolo et al., 2002). This activates a genetic program in the non-SOP cells that prevents them from also adopting an SOP fate, a process referred to as “lateral inhibition”

(Muskavitch, 1994; Chitnis, 1995). These “inhibited” cells then go on to adopt an epidermal fate.

Among the direct targets of N signaling in the non-SOP cells of PNCs are the *Bearded* (*Brd*) genes. This gene family is made up of the *Enhancer of split* [*E(spl)*] complex genes *E(spl)mα*, *E(spl)m2*, *E(spl)m4*, and *E(spl)m6* and the *Brd*-complex genes *Brd*, *Bob*, *Tom*, and *Ocho* (Leviten et al., 1997; Lai et al., 2000a; Lai et al., 2000b). It has been observed that misexpression of these genes [with the exception of *E(spl)m2* which will be excluded from all further discussion] throughout the PNC disrupts N signaling, causing a failure of lateral inhibition and the adopting of an SOP fate by many cells of the PNC (Leviten et al., 1997; Apidianakis et al., 1999; Lai et al., 2000a; Lai et al., 2000b; Zaffran and Frasch, 2000). The disruption of N signaling by *Bearded* family members (BFMs) is caused by their ability to inhibit the activity of Neur in signal sending cells (Bardin and Schweisguth, 2006; De Renzis et al., 2006; Fontana and Posakony, 2009). This function of the BFMs is reliant on the presence of an N-terminal predicted basic amphipathic α-helix (B-domain) and one or more NXXN sequence motifs (Lai, 1999; Fontana and Posakony, 2009). The NXXN motifs mediate a direct interaction with Neur, and the B domain mediates an interaction with the phosphoinositide PI(3)P (Fontana and Posakony, 2009; Fontana and Posakony, manuscript in preparation). This motif combination results in the colocalization of BFMs and Neur with endosomes positive for the lysosomal markers Rab7

and LAMP1, hypothesized to lead to the degradation of Neur (Fontana and Posakony, manuscript in preparation).

Much of the work examining the function of Brd proteins has been through misexpression of the proteins. Therefore, we sought to examine their function through loss-of-function analyses. We have generated null alleles of the BFMs *Tom*, *Brd*, *E(spl)m*α, and *E(spl)m4* through the imprecise excisions of P-element insertions and homologous recombination. Single BFM mutants show little or no phenotype, while double BFM mutants produce stronger phenotypes. These data indicate a redundant role for BFMs during development. We show that the loss of multiple BFMs sensitizes non-SOP cells of PNCs to Neur levels, indicating that BFMs function during lateral inhibition to ensure proper specification of the correct number of SOPs.

Materials and Methods

Imprecise Excision of P-element insertions

P-element insertion line (w^{*};; P{w^{+mC}=EP}EP487) (Bloomington Stock Center) was used to create deletions of *Tom*. Insertion line (w^{1118};; P{w^{+mGT}=GT1}BG02319) (Bloomington Stock Center) was used to create deletions of *Brd*. Females of the P element insertion line were crossed to males that provided a source of transposase: (*yw*; *Sco* / *Cy*O; Δ2-3, Sb^{1}, $ry^{+t7.2}$ / TM6B, Tb^{+}) (Bloomington Stock Center). White eyed male progeny of the genotype (Δ2-3, Sb^{1}, $ry^{+t7.2}$ / P-element) (Bloomington Stock Center) were crossed to (w^{1118};; TM2 / TM6C Sb^{1} Tb^{+}) females for 3rd chromosome balancing. White eyed male progeny of the genotype (w^{1118};; excision / TM2) were isolated and propagated individually. Imprecise excisions were screened for via PCR.

Homologous Recombination

Deletions of *E(spl)mα* and *E(spl)m4* were created using the plasmid pW25 and protocol described in Gong and Golic, 2004. Deletion of *E(spl)mα* made use of 3890 bp of upstream sequence and 3271 bp of downstream sequence to delete a fragment spanning nucleotides -820 through +1609 with respect to the transcriptional start site (TSS), eliminating the enhancer and entire transcriptional unit of *E(spl)mα*. Removal of the w^{+} transgene was subsequently performed using the cre-lox system. Deletion of *E(spl)m4* made use of 4248 bp of upstream sequence and 5197 bp of downstream sequence to delete a fragment

spanning nucleotides -372 through +121, eliminating the enhancer and 5' region of the *E(spl)m4* transcriptional unit.

Additional fly strains used

w^{1118} *E(spl)mα-GAL4* (Castro et al., 2005). *UAS-neur* (Lai and Rubin, 2001). *y*^{1} *w*^{67c23} P{*y*$^{+mDint2}$*; Cre-y*}1b;; *D** / TM3, *Sb*^{1} (Bloomington Stock Center).

Immunohistochemistry

Late 3rd instar larvae were dissected in phosphate buffer saline (PBS) + 0.1% Triton X-100, fixed for 25 min with 4% paraformaldehyde in PBS + 0.3% Triton X-100 + 0.1% deoxycholate, and washed 5 x 10 min with PBS + 0.1% Triton X-100. SOPs in *w*^{1118} and (*w*^{1118};; *mα*^{del} *m4*$^{del, w+}$) were assayed using mouse monoclonal anti-Hindsight (1G9; Developmental Studies Hybridoma Bank) diluted to 1:100 and Alexa Fluor 488 donkey anti-mouse IgG (Molecular Probes) diluted to 1:500.

FLAG-m4 *rescue construct*

To create the *FLAG-m4* rescue construct, a genomic DNA fragment containing *E(spl)m4* was amplified from *Drosophila* strain *w*^{1118}. The boundaries of this fragment were 684 bp of sequence upstream of the start Met, and 704 bp of sequence downstream of the stop codon. This region included the upstream binding sites for Su(H) and the proneural proteins as well as the entire 3' UTR. A 1x FLAG-tag epitope (Asp-Tyr-Lys-Asp-Asp-Asp-Asp-Lys) was inserted after the start Met of *E(spl)m4* using standard PCR techniques. This fragment was inserted into a

p*Stinger* vector whose eGFP sequence had been removed (Barolo et al., 2000). *Drosophila* were transformed using a standard P transposable element injection protocol (Rubin and Spradling, 1982).

Bristle count assays

For bristle counts on the notum of adult Drosophila, 26 macrochaete bristle positions were scored (humerals, notopleurals, presuturals, supra-alars, post-alars, dorsocentrals, scutellars). For vibrissae counts on the head of the fly, the dorsal-most positions were scored (2 on each side in wild-type), with left and right side counted separately.

Results

Generation of a Tom *null allele*

Imprecise excisions of the P-element insertion EP487 were generated to obtain deletions at the *Tom* locus on the third chromosome. This P-element is inserted approximately 100 bp upstream of the transcriptional start site (TSS) of *Tom*. After crossing to a fly line containing a source of transposase, we isolated 400 3rd-chromosome balanced, male flies in the F2 generation in which an excision event had occurred (Figure 3.1A). These males were individually mated to 3rd-chromosome balanced females and then batched into groups of 10 for DNA purification and PCR screening. When PCR screening indicated that a batch contained a fly harboring an imprecise excision at the locus, the progeny of flies from that batch were screened individually. This resulted in the isolation of 4 lines containing an imprecise excision at the *Tom* locus: #4g, #19b, #32c, and #40d. Sequencing of the genomic region surrounding the deletions revealed that lines #4g and #40d were identical, thus we discarded line #40d. *Tom^{4g}* is a deletion of 1151 bp (-101 through +1050 from the TSS of *Tom*) and *Tom^{19b}* is a deletion of 1436 bp (-101 through +1335) (Figure 3.1B). Both of these alleles remove the entire transcriptional unit of *Tom*. *Tom^{32c}* is a deletion of 762 bp (-101 through +661) and eliminates the 5' UTR and entire CDS of *Tom*. All three of these *Tom* alleles are homozygous viable and do not produce a bristle phenotype on the notum of the adult fly.

Generation of a Brd *null allele*

Deletion alleles of *Brd* were generated via the imprecise excision of the P-element BG02319. This element resides approximately 180 bp upstream of *Brd*. We generated and screened excisions of this P-element in the same manner as for EP487, described above. From 930 excision events we isolated 3 imprecise excision lines: #23e, #58e, and #82e. Characterization of the deletions revealed that lines #23e and #58e were identical, thus line #58e was discarded. Brd^{23e} is a deletion of 1210 bp (-175 through +1035 from the TSS of *Brd*) and Brd^{82e} deletes 1566 bp (-804 through +762) (Figure 3.1C). Both of these alleles completely remove the transcriptional unit of *Brd*. Similar to the *Tom* alleles generated, these alleles of *Brd* are homozygous viable and show no bristle phenotype on the notum of the adult fly.

Generation of an E(spl)mα *null allele*

Due to the lack of a convenient P-element, and in order to more tightly control deletion boundaries, we decided to make use of the homologous recombination technique to generate a null allele of *E(spl)m*α (Gong and Golic, 2004). We generated reagents that would result in a 2429 bp deletion of *E(spl)m*α, spanning nucleotides -820 through +1609 from the TSS (Figure 3.2A). Following a series of crosses and appropriate heat-shock regime, we isolated 37 w^+ flies (which represent potential homologous recombinants) from 335 vials. 17 of the 37 w^+ lines correctly harbored the w^+ transgene on the third chromosome as indicated via

mapping with balancer chromosomes. Of these 17, 9 were correctly verified, via PCR of both the upstream and downstream regions, as homologous recombinants (Figure 3.2B). The remaining lines either verified for only the upstream region (N = 2) or downstream region (N = 1), or contained a tandem repeat of the downstream region (N = 5). 3 of the 9 correct lines were kept and isogenized to w^{1118}: (w^{1118};; $m\alpha^{del\text{-}O,\ w+}$), ($w^{1118}$;; $m\alpha^{del\text{-}U,\ w+}$), and ($w^{1118}$;; $m\alpha^{del\text{-}Y,\ w+}$) (Figure 3.2B). These lines are homozygous viable and in situ hybridization against the *E(spl)mα* transcript confirms that they are null for *E(spl)mα* (Figure 3.4A,B).

Generation of an E(spl)m4 *null allele*

Deletion of the *E(spl)m4* locus using homologous recombination was done in an ($m\alpha^{del\text{-}O}$ / +) background in order to simultaneously generate an *E(spl)m4* null allele and an *E(spl)mα E(spl)m4* double null. The $m\alpha^{del\text{-}O}$ line was generated by removal of the w^{+} transgene from (w^{1118};; $m\alpha^{del\text{-}O,\ w+}$) using the cre-lox system (Figure 3.2C). The targeting scheme for *E(spl)m4* resulted in a 493 bp deletion spanning nucleotides -372 through +121 from the TSS (Figure 3.3A). We isolated 44 w^{+} flies from 350 vials, 23 of which mapped to the third chromosome and could be PCR verified for both the upstream region and downstream regions (Figure 3.3B). 11 out of the 23 were single mutants of the *E(spl)m4* locus, 4 of which were kept: (w^{1118};; $m4^{del\text{-}B,\ w+}$), (w^{1118};; $m4^{del\text{-}H,\ w+}$), (w^{1118};; $m4^{del\text{-}Q,\ w+}$), and (w^{1118};; $m4^{del\text{-}Ah,\ w+}$). The remaining 12 of the 23 lines contained

a deletion in both *E(spl)mα* and *E(spl)m4*, and 5 lines were kept: (w^{1118};; $mα^{del\text{-}O}$ $m4^{del\text{-}A,\ w+}$), (w^{1118};; $mα^{del\text{-}O}$ $m4^{del\text{-}N,\ w+}$), (w^{1118};; $mα^{del\text{-}O}$ $m4^{del\text{-}X,\ w+}$), (w^{1118};; $mα^{del\text{-}O}$ $m4^{del\text{-}Aa,\ w+}$), and (w^{1118};; $mα^{del\text{-}O}$ $m4^{del\text{-}Af,\ w+}$). All of these lines are homozygous viable and in situ hybridizations against *E(spl)mα* and *E(spl)m4* transcripts verify the alleles are transcript null alleles (Figure 3.4C-G)

Loss-of-function analysis of E(spl)mα *and* E(spl)m4

In larval imaginal discs, *E(spl)mα* and *E(spl)m4* are coexpressed in many of the proneural clusters from which the mechanosensory organs of the adult fly are specified (Leviten et al, 1997; Lai et al., 2000a; Lai et al., 2000b). To investigate the function of *E(spl)mα* and *E(spl)m4* during lateral inhibition and mechanosensory organ development, we characterized bristle phenotypes for the single and double mutants we had generated. The vibrissae are a group of bristles located on the anterior portion of the head extending ventrally on either side of the proboscis. In wild-type *D. mel.*, the most dorsal group of vibrissae consists of 2 bristles on either side (Figure 3.5A). In *E(spl)mα* and *E(spl)m4* single mutants, the average number of vibrissae is increased to 3.0 ± 0.031 (N = 150) and 2.9 ± 0.03 (N = 200) bristles per side, respectively (Figure 3.5A,B). This extra bristle phenotype is further enhanced in the double mutant, with 3.4 ± 0.036 (N = 250) extra vibrissae per fly (Figure 3.5A,B). When we score the number of macrochaete bristles on the notum of the adult fly, we observe a similar weak extra bristle phenotype. We find an average of 1.0

± 0.11 (N = 75) extra bristle in an *E(spl)mα* null and 0.43 ± 0.07 (N = 100) extra bristles per fly in an *E(spl)m4* null (Figure 3.5C). This phenotype is enhanced in the double mutant, with 2.0 ± 0.14 (N = 125) extra bristles per fly (Figure 3.5C).

The appearance of extra bristles may be due to a failure of lateral inhibition, in which extra SOPs arise in a given PNC, or due to a cell fate conversion in the SOP lineage, resulting in extra external cells (shaft and socket) at the expense of the internal cells (neuron and sheath). We examined the developmental basis for this extra-bristle phenotype by staining wing imaginal discs from late third-instar larvae with anti-Hindsight antibody to mark SOPs. At the positions of various macrochaete bristle SOPs in wild-type tissue, we observe additional Hindsight-positive cells in the double mutant (Figure 3.5D,E). These results indicate that commitment of supernumerary PNC cells to the SOP fate underlies the extra-bristle phenotype. These data demonstrate a requirement for BFMs during lateral inhibition in PNCs during adult PNS development.

BFM deletions sensitize cells to Neur activity

BFMs have been shown to inhibit the activity of Neur during development (Bardin and Schweisguth, 2006; De Renzis et al., 2006). To determine if the loss of BFMs renders cells of the PNC more susceptible to Neur activity, we examined the effect of Neur misexpression in BFM mutant backgrounds. Misexpressing Neur in the non-SOP cells of the PNC with *E(spl)mα-GAL4* produces a very weak bristle phenotype on the

notum of the fly, with 1.1 ± 0.2 extra bristle per fly (Figure 3.5F). In an *E(spl)mα* null, the misexpression of Neur results in a slightly greater effect of 2.5 ± 0.2 extra bristles per fly. When Neur is misexpressed in a *E(spl)mα E(spl)m4* double mutant, the observed phenotype is greatly enhanced with 14 ± 1.3 extra bristles per fly. This extra bristle phenotype is suppressed by the addition of an *E(spl)m4* rescue construct (*FLAG-m4*), where 1.7 ± 0.22 extra bristles per fly are observed (Figure 3.5F). This confirms that the strong extra bristle phenotype observed by misexpressing Neur is due to the loss of the BFMs in the double mutant. These data support a model in which BFMs with a similar expression pattern are functioning redundantly to inhibit the activity of Neur.

Discussion

The *Drosophila* genome contains 2 complexes in which multiple members of the *Brd* family of N-target genes can be found, the Brd-C and E(spl)-C. Common transcriptional inputs lead to the coexpression of many family members in embryo and imaginal disc tissue (Leviten et al, 1997; Lai, 1999; Lai et al., 2000a; Lai et al., 2000b). This coexpression, along with a common structural architecture in the protein products, suggests that the BFMs may act redundantly with one another in the cells in which they are expressed. Through imprecise excisions of P-element insertions, we have generated null alleles for the Brd-C genes *Tom* and *Brd* (Figure 3.1). Flies homozygous for either *Tom* or *Brd* null alleles are viable and show no apparent defects, indicating these genes are not individually essential for development. Using homologous recombination, null alleles for the E(spl)-C genes *E(spl)mα* and *E(spl)m4* were created (Figures 3.2-3.5). Flies homozygous for either of these alleles are also viable, however we observe a weak extra-bristle phenotype on the notum of the adult fly. This phenotype is slightly enhanced in the double *E(spl)mα E(spl)m4* mutant, suggesting that these genes may act redundantly during mechanosensory organ development. Using an antibody stain against the SOP marker Hindsight, we find that the nature of this extra bristle phenotype is due to the specification of an extra SOP in the PNC. The phenotype we see in the double mutant is still relatively weak, suggesting that the activity of the other BFMs expressed in these PNCs, *Brd* and

Ocho, may be supplying additional function for proper lateral inhibition to occur. However, it has been observed that there is no strong bristle defect in clones mutant for all of the BFMs (Chanet et al., 2009). This would suggest that there are additional mechanisms in place to ensure proper lateral inhibition occurs consistently. This same report however, does show a redundant role of the BFMs in embryonic development. They find that flies mutant for all BFMs of the Brd-C show reduced embryonic viability. Adding deletions of the E(spl)-C BFMs, *mα*, *m4* and *m6*, leads to complete embryonic lethality. This lethality can be partially rescued by the reintroduction of several family members (Chanet et al., 2009).

One mechanism through which an additional SOP may be specified in a PNC is by this additional cell acquiring a N-signal sending capacity. This capability seems to correspond to this cell also becoming resistant to an incoming signal, preventing it from being inhibited (Jacobsen et al., 1998; Sakamoto et al., 2002). Increasing the level of Neur activity within a PNC cell may provide this signal sending capacity. Indeed, we find misexpressing Neur in presumptive non-SOPs of the PNC leads to a weak extra bristle phenotype. In an endogenous setting, it has been observed that nascent *neur* transcript is produced in multiple cells of the PNC (Miller, S.W., and Posakony, J.W., manuscript in preparation). This would necessitate Brd protein activity to ensure Neur activity is inhibited in these cells. The weak extra bristle phenotype we observe in the double *E(spl)mα E(spl)m4* mutant suggests that these cells may be more

sensitive to Neur levels. To test this, we misexpressed Neur in non-SOP cells. When Neur is misexpressed in an *E(spl)mα E(spl)m4* double mutant background, we observe a large increase in the number extra bristles produced compared to when Neur is misexpressed in a wild-type background (Figure 3.5F). The extra bristle phenotype is suppressed when an *E(spl)m4* rescue construct is supplied, indicating that BFMs are inhibiting Neur activity in this setting. These data support the model of redundant BFM function and implicate BFMs in the process of lateral inhibition, even if their role is not absolutely required. The reagents produced here will provide useful tools in carrying out further studies of both Brd protein and Neur function.

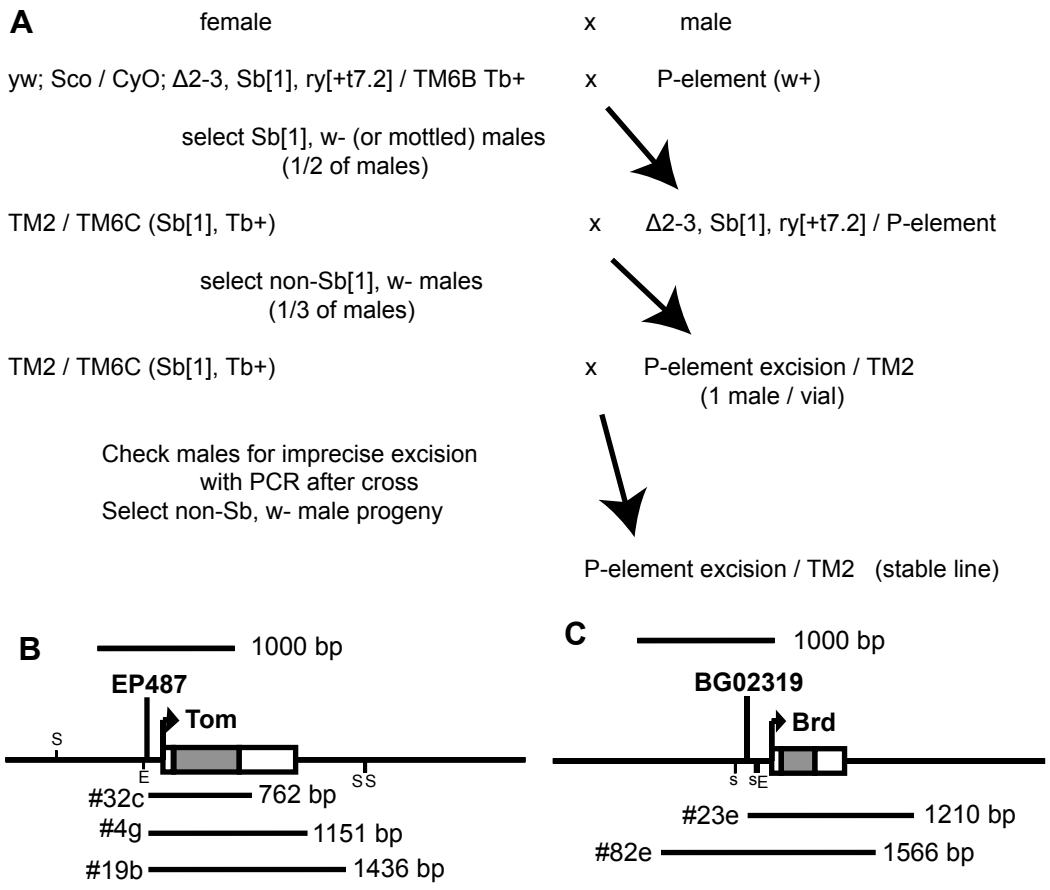

Figure 3.1: Generation of *Tom* and *Brd* null alleles through the imprecise excision of P-element insertions. (A) Crossing scheme used to generate imprecise excisions of P-element insertions. (B-C) GenePalette (Rebeiz and Posakony, 2004) illustrations of the *Tom* (B) and *Brd* (C) loci with P-element insertion sites shown. Deleted regions from imprecise excision lines are depicted under the illustrations and sizes of the deletions are indicated. S = Su(H) binding site (YGTGDGAA); s = weak Su(H) binding site (YRTGDGAD); E = Proneural binding site (RCAGSTG).

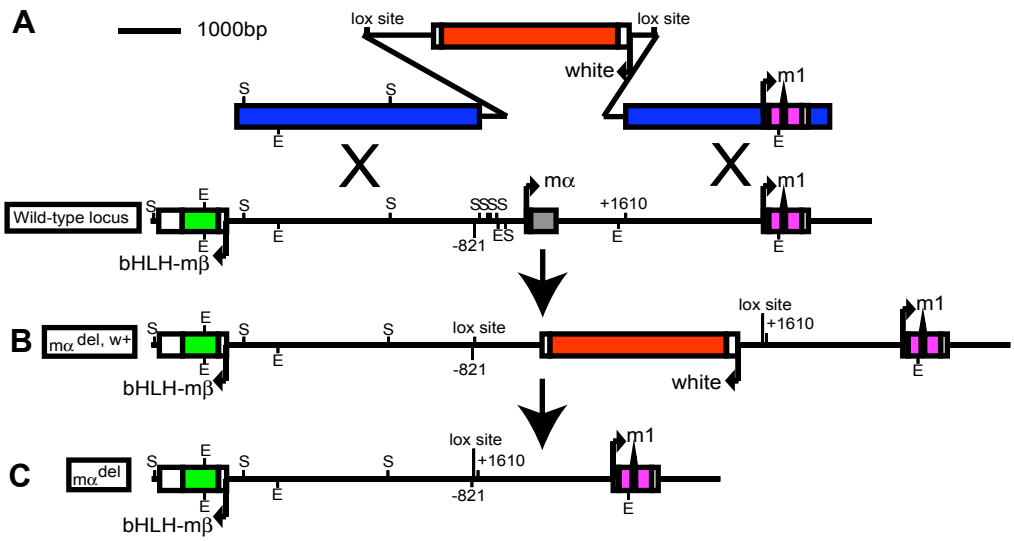

Figure 3.2: Schematic of *E(spl)mα* null allele created via homologous recombination. (A) Wild-type *E(spl)mα* locus with homologous recombination construct design shown above it. (B) Illustration of the *E(spl)mα* null locus after successful homologous recombination has removed the *E(spl)mα* gene. (C) Illustration of the *E(spl)mα* null locus after the cre-lox system was used to remove the *w+* transgene from homologous recombinants. Illustrations were generated using GenePalette (Rebeiz and Posakony, 2004). S = Su(H) binding site (YGTGDGAA); E = Proneural binding site (RCAGSTG).

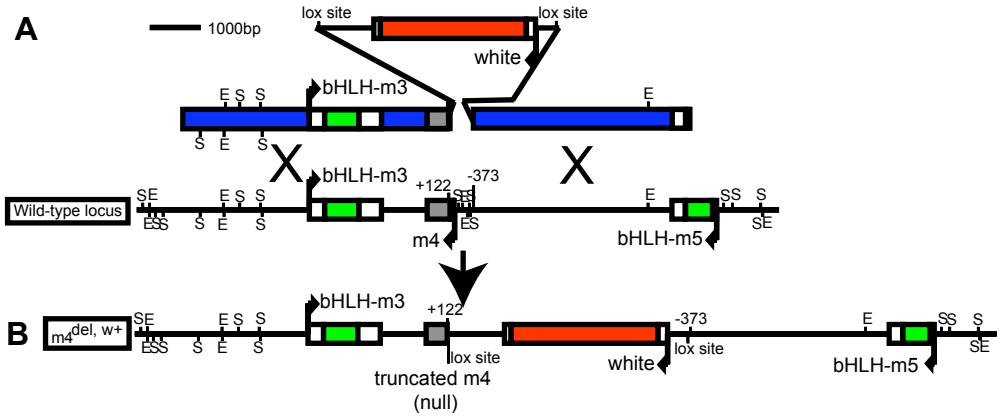

Figure 3.3: Schematic of *E(spl)m4* null allele created via homologous recombination. (A) Wild-type *E(spl)m4* locus with homologous recombination construct design shown above it. (B) Illustration of the *E(spl)m4* null locus after successful homologous recombination has removed the 5' region of the *E(spl)m4* gene. Illustrations were generated using GenePalette (Rebeiz and Posakony, 2004). S = Su(H) binding site (YGTGDGAA); E = Proneural binding site (RCAGSTG).

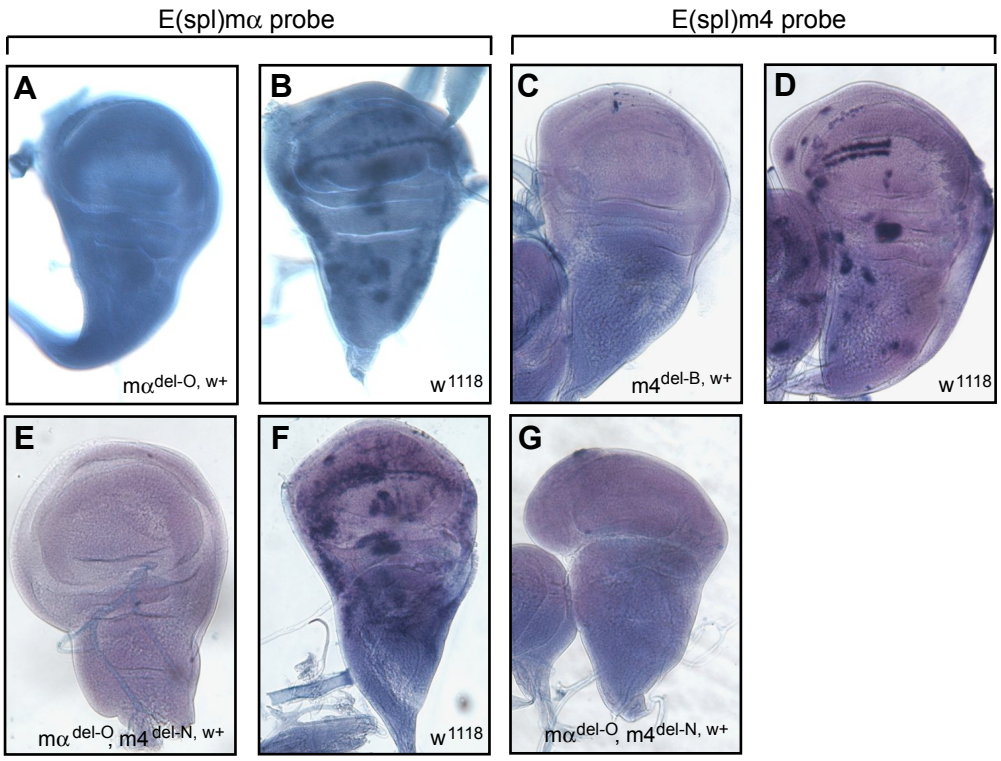

Figure 3.4: In situ hybridizations on larval wing imaginal discs confirm the lack of transcript production from *E(spl)mα* and *E(spl)m4* null alleles. (A-B, E-F) In situ hybridizations using a probe against *E(spl)mα* transcript on *mα del-O, w+* (A), *mα del-O, del-N, w+* (E), and *w1118* (B and F) confirm the deletion of *E(spl)mα*. (C-D, G) In situ hybridizations using a probe against *E(spl)m4* transcript on *m4 del-B, w+* (C), *mα del-O, del-N, w+* (G), and *w1118* (D), confirm the deletion of *E(spl)m4*.

Figure 3.5: Deletions of *E(spl)mα* and *E(spl)m4* result in an extra bristle phenotype and sensitize cells of the PNC to Neur levels. (A-C) Deletions of *E(spl)mα* or *E(spl)m4* result in extra vibrissae (A-B) and notum macrochaetes (C). The phenotype is significantly increased in the double mutant. (D-E) Anti-hindsight antibody stain of larval wing imaginal discs to mark SOP positions. In wild-type tissue (D), a single SOP is specified at each future bristle position (arrow marks the pSA position). In the *E(spl)mα E(spl)m4* double mutant (E), an extra SOP is specified at the pSA position (arrows) indicating the nature of the extra bristle phenotype is due to the specification of extra SOPs in the PNC. (F) Loss of *Brd* function in the PNC sensitizes non-SOP cells to *neur* levels. Misexpressing *neur* in the non-SOP cells of the PNC produces a weak extra bristle phenotype (Lane 1). This phenotype is slightly enhanced in an *E(spl)mα* deletion background (Lane 2) and greatly increased in the *E(spl)mα E(spl)m4* double mutant (Lane 3). This strong extra bristle phenotype produced by misexpressing *neur* in a double mutant background can be rescued by the addition of 1 copy of an *E(spl)m4* rescue construct (FLAGm4; Lane 4). pSA = posterior supra-alar; aPA = anterior post-alar; pPA = posterior post-alar.

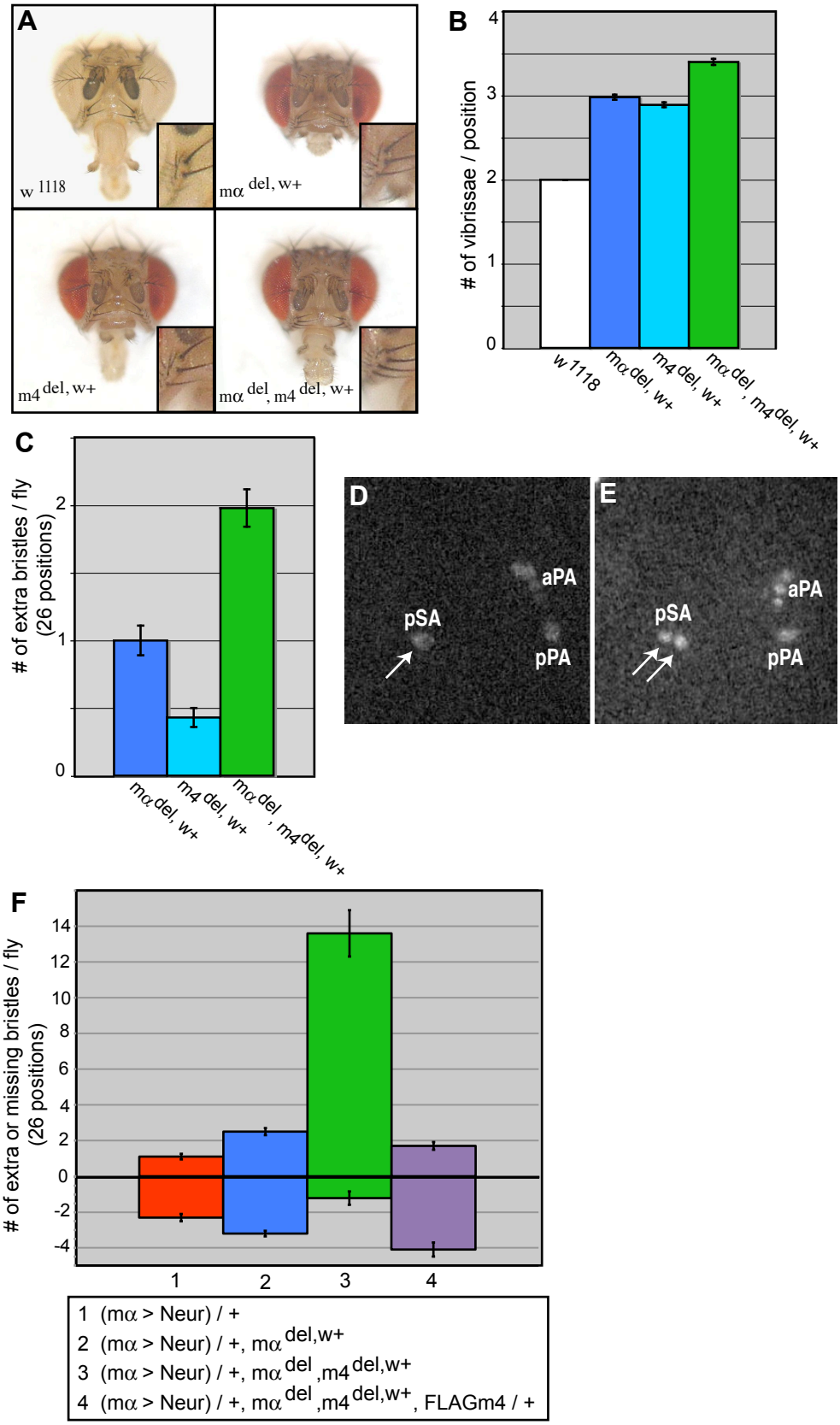
A
w 1118
mα del, w+
m4 del, w+
mα del, m4 del, w+
B
# of vibrissae / position
0
1
2
3
4
w 1118
mα del, w+
m4 del, w+
mα del, m4 del, w+
C
# of extra bristles / fly (26 positions)
0
1
2
mα del, w+
m4 del, w+
mα del, m4 del, w+
D
aPA
pSA
pPA
E
aPA
pSA
pPA
F
# of extra or missing bristles / fly (26 positions)
14
12
10
8
6
4
2
0
-2
-4
1
2
3
4
1 (mα > Neur) / +
2 (mα > Neur) / +, mα del,w+
3 (mα > Neur) / +, mα del ,m4 del,w+
4 (mα > Neur) / +, mα del ,m4 del,w+, FLAGm4 / +

References

Apidianakis, Y., Nagel, A.C., Chalkiadaki, A., Preiss, A., Delidakis, C., 1999. Overexpression of the *m4* and *mα* genes of the *E(spl)-Complex* antagonizes Notch mediated lateral inhibition. Mech. Dev. 86, 39–50.

Bailey, A.M., Posakony, J.W., 1995. Suppressor of Hairless directly activates transcription of Enhancer of split Complex genes in response to Notch receptor activity. Genes Dev. 9, 2609-2622.

Bardin, A., Schweisguth, F., 2006. Bearded family members inhibit Neuralized-mediated endocytosis and signaling activity of Delta in *Drosophila*. Dev. Cell 10, 245-255.

Barolo, S., Carver, L.A., Posakony, J.W., 2000. GFP and β-galactosidase transformation vectors for promoter/enhancer analysis in *Drosophila*. BioTechniques 29, 726–732.

Barolo, S., Stone, T., Bang, A.G., Posakony, J.W., 2002. Default repression and Notch signaling: Hairless acts as an adaptor to recruit the corepressors Groucho and dCtBP to Suppressor of Hairless. Genes Dev. 16, 1964-1976.

Castro, B., Barolo, S., Bailey, A.M., Posakony, J.W., 2005. Lateral inhibition in proneural clusters: cis-regulatory logic and default repression by Suppressor of Hairless. Development 132, 3333-3344.

Chanet, S., Vodovar, N., Mayau, V., Schweisguth, F., 2009. Genome engineering-based analysis of *Bearded* family genes reveals both functional redundancy and a nonessential function in lateral inhibition in Drosophila. Genetics 182, 1101-1108.

Chitnis, A.B., 1995. The role of Notch in lateral inhibition and cell fate specification. Mol. Cell. Neurosci. 6, 311-321.

De Renzis, S., Yu, J., Zinzen, R., Wieschaus, E., 2006. Dorsal-ventral pattern of Delta trafficking is established by a Snail-Tom-Neuralized pathway. Dev. Cell 10, 257-264.

De Strooper, B., Annaert, W., Cupers, P., Craessaerts, K., Mumm, J.S., Schroeter, E.H., Schrijvers, V., Wolfe, M.S., Ray, W.J., Goate, A., Kopan, R., 1999. A presenilin-1-dependent gamma-secretase-like protease mediates release of Notch intracellular domain. Nature 398, 518-522.

Fontana, J.R., Posakony, J.W., 2009. Both inhibition and activation of Notch signaling rely on a conserved Neuralized-binding motif in Bearded proteins and the Notch ligand Delta. Dev. Biol. 333, 373-385.

Gong, W.J., Golic, K.G., 2004. Genomic deletions of the *Drosophila melanogaster Hsp70* genes. Genetics 168, 1467-1476.

Jacobsen, T.L., Brennan, K., Martinez-Arias, A., Muskavitch, M.A.T., 1998. *Cis*-interactions between Delta and Notch modulate neurogenic signalling in *Drosophila*. Development 125, 4531-4540.

Lai, E.C., 1999. Regulation of pattern formation during development of the *Drosophila* peripheral nervous system. PhD Dissertation, Department of Biology, University of California San Diego.

Lai, E.C., Rubin, G.M., 2001. *neuralized* functions cell-autonomously to regulate a subset of Notch-dependent processes during adult *Drosophila* development. Dev. Biol. 231, 217–233.

Lai, E.C., Bodner, R., Kavaler, J., Freschi, G., Posakony, J.W., 2000a. Antagonism of Notch signaling activity by members of a novel protein family encoded by the Bearded and Enhancer of split gene complexes. Development 127, 291-306.

Lai, E.C., Bodner, R., Posakony, J.W., 2000b. The Enhancer of split Complex of *Drosophila* includes four Notch-regulated members of the Bearded gene family. Development 127, 3441-3455.

Lai, E.C., Roegiers, F., Qin, X., Jan, Y.N., Rubin, G.M., 2005. The ubiquitin ligase *Drosophila* Mind bomb promotes Notch signaling by regulating the localization and activity of Serrate and Delta. Development 132, 2319-2332.

Le Borgne, R., Remaud, S., Hamel, S., Schweisguth, F., 2005. Two distinct E3 ubiquitin ligases have complementary functions in the regulation of Delta and Serrate signaling in *Drosophila*. PLoS Biol. 3, e96.

Leviten, M.W., Lai, E.C., Posakony, J.W., 1997. The *Drosophila* gene *Bearded* encodes a novel small protein and shares 3′ UTR sequence motifs with multiple *Enhancer of split* Complex genes. Development 124, 4039–4051.

Muskavitch, M.A.T., 1994. Delta-Notch signaling and *Drosophila* cell fate choice. Dev. Biol. 166, 415-430.

Pan, D., Rubin, G.M., 1997. Kuzbanian controls proteolytic processing of Notch and mediates lateral inhibition during Drosophila and vertebrate neurogenesis. Cell 90, 271-280.

Rebeiz, M., Posakony, J.W., 2004. GenePalette: a universal software tool for genome sequence visualization and analysis. Dev. Biol. 271, 431–438.

Rubin, G.M., Spradling, A.C., 1982. Genetic transformation of *Drosophila* with transposable element vectors. Science 218, 348–353.

Sakamoto, K., Ohara, O., Takagi, M., Takeda, S., Katsube, K., 2002. Intracellular cell-autonomous association of Notch and its ligands: a novel mechanism a Notch signal modification. Dev. Biol. 241, 313-326.

Sotillos, S., Roch, F., Campuzano, S., 1997. The metalloprotease-disintegrin Kuzbanian participates in Notch activation during growth and patterning of *Drosophila* imaginal discs. Development 124, 4769-4779.

Struhl, G., Adachi, A., 1998. Nuclear access and action of Notch in vivo. Cell 93, 649-660.

Tamura, K., Taniguchi, Y., Minoguchi, S., Sakai, T., Tun, T., Furukawa, T., Honjo, T., 1995. Physical interaction between a novel domain of the receptor Notch and the transcription factor RBP-Jκ/Su(H). Curr. Biol. 5, 1416-1423.

Wang, W., Struhl, G., 2005. Distinct roles for Mind bomb, Neuralized and Epsin in mediating DSL endocytosis and signaling in *Drosophila*. Development 132, 2883-2894.

Zaffran, S., Frasch, M., 2000. *Barbu*: an *E(spl) m4/mα*-related gene that antagonizes Notch signaling and is required for the establishment of ommatidial polarity. Development 127, 1115-1130.

Appendix 1

Mapping of the *Buzzcut* mutation

Summary

The original *Buzzcut* (*Bzct*) mutant fly was found in a vial after a cross involving *UAS-neur* #7.5 (cytological location 31F). *Bzct* is a dominant mutation resulting in macrochaete bristles that are shorter and thinner than those seen in wild-type flies (Figure A1.1). Multiple rounds of backcrossing to a stock of w^{1118} wild-type flies segregated the phenotype away from the w^{+} transgene associated with the *UAS-neur* insertion. Mapping of the *Bzct* allele using balancer chromosomes localized the mutation to the 2nd chromosome. It is homozygous lethal, and a stable line is balanced over the *Cy*O chromosome.

Tables A1.1 and A1.2 represent a series of crosses carried out to determine the recombination rate between *Bzct* and several transgene insertions I have generated over the years. Recombination rates between the loci map *Bzct* to chromosome 2L, somewhere between cytological bands 34 and 37.

Tables A1.3 and A1.4 are the results of complementation tests using deficiency lines from the Bloomington Stock center (Kindly provided by Dr. Michelle Juarez in the laboratory of Bill McGinnis). Results of the complementation tests indicate that *Bzct* may lie in the region between cytological bands 36A12 and 36B1, covered by Df(2L)Exel7067.

Tables A1.5 and A1.6 are results of testing the complementation of deficiency lines against one another. Bloomington stock # 7522 does not

behave as would be expected and therefore should not be used in any mapping experiments of the *Bzct* locus.

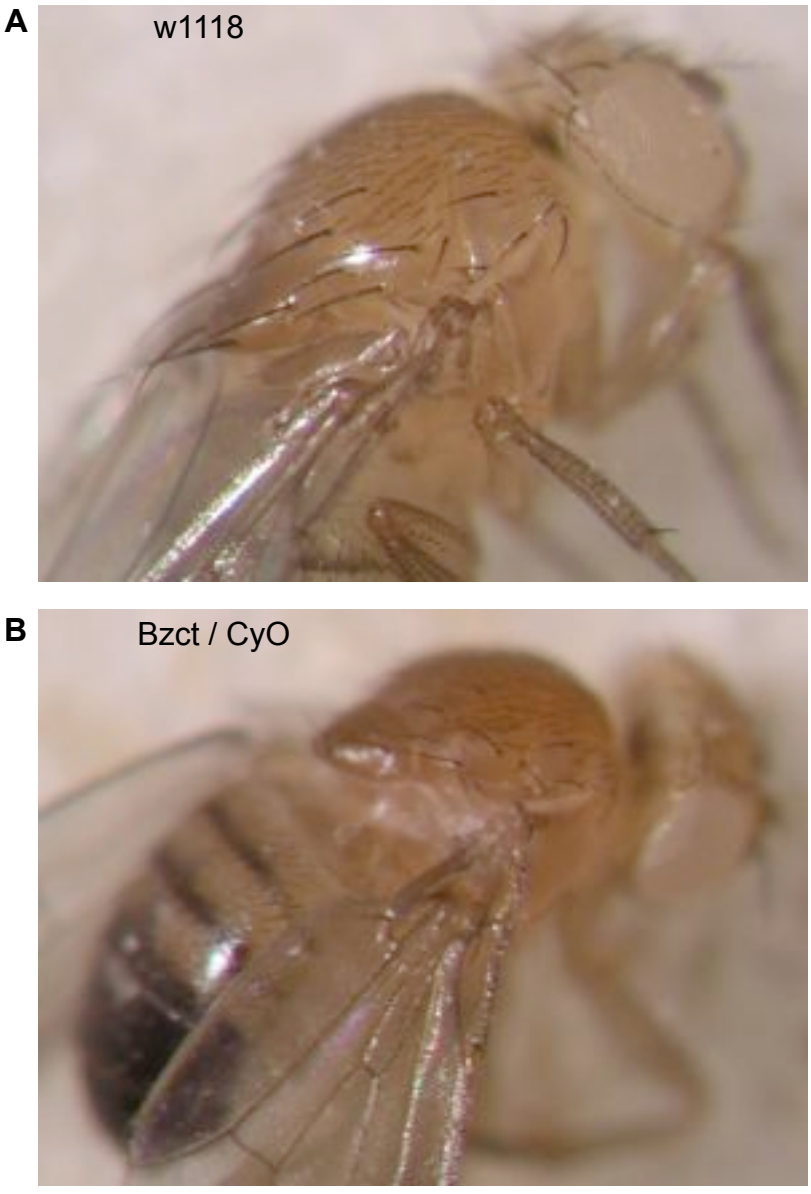

Figure A1.1: Bristle phenotype of the *Bzct* mutant. (A) Wild-type w1118 fly. (B) *Bzct* / *Cy*O fly. The macrochaete bristles of the Bzct mutant fly are shorter and thinner than those of the wild-type fly.

Table A1.1: Recombination between *Bzct* and P-element insertion lines- Part I

Resulting genotypes from : Bzct/P{w+} females X +/+ males

Insertion location & Line I.D.	No recombination between loci		Recombination between loci		Recombination Rate
	Bzct/+	+/P{w+}	Bzct, P{w+}/+	+/+	
23B UAS-m4domN #1	62	90	38	46	35.6%
27F UAS-Tom^{N2} #2	45	57	16	14	22.7%
35D UAS-ma$^{4K/A}$ #2	16	21	0	0	0.0%
37B UAS-TomB #3	108	142	4	9	4.94%
39C UAS-FLAGm4$^{4K/A}$ #3	112	139	8	6	5.28%

Table A1.2: Recombination between *Bzct* and P-element insertion lines- Part II

Resulting genotypes from : Bzct/P{w+} females X +/+ males

Insertion location & Line I.D.	No recombination between loci		Recombination between loci		Recombination Rate
	Bzct/+	+/P{w+}	Bzct, P{w+}/+	+/+	
27F UAS-Tom^{N2} #2	39	47	17	19	29.51%
30B UAS-ma$^{N'}$ #4	72	72	12	19	17.71%
34B UAS-FLAGm4$^{N''N'N2}$	81	97	1	3	2.20%
35D1 UAS-FLAGm4^{G2} #1	72	124	0	0	0.00%
35D4 UAS-ma$^{4K/A}$ #2	78	118	0	0	0.00%
35D1 UAS-ma$^{4K/R}$ #6	143	181	2	2	1.22%
35D1 UAS-ma^{D} #4	69	108	0	0	0.00%
35D1 UAS-ma^{D} #5	68	65	1	0	0.75%
39C UAS-FLAGm4$^{4K/A}$ #3	113	146	11	4	5.47%
44D UAS-ma^{N} #5	64	58	5	6	8.27%
35D1 combined	352	478	3	2	0.60%

Table A1.3: Complementation test of *Bzct* locus-Part I

Crosses at 25°C to Bzct / Cyo

Bloomington Stock #	Exelixis Stock #	Lesion	Complements?	Bzct/CyO	Deletion/ CyO	Bzct/ Deletion
7830	8034	35C5; 35D2	Yes	24	12	16
7831	7063	35D2; 35D4	Yes	41	40	10
7521	6038	35D6; 35E2	Yes	4	9	13
7833	7066	36A1; 36A12	Yes	5	7	5
7522	6039	36A10; 36B3	Yes	6	20	5
7834	**7067**	**36A12; 36B1**	**NO Pupal Lethal**	**40**	**32**	**0**
7835	8036	36B1; 36C9	Yes	10	7	11
7838	7068	36C7; 36C10	Yes	29	27	7
7837	7069	36C10; 36D3	Yes	25	26	14
7836	9044	36C10; 36D1	Yes	10	10	19
7839	7070	36E2; 36E6	Yes	11	15	25
7840	8038	36E5; 36F5	Yes	22	1	12
7841	9033	36F2; 36F2	Yes	14	19	19
7523	6041	36F6; 37A2	Yes	11	9	5

Table A1.4: Complementation test of *Bzct* locus-Part II

Crosses at Room Temp (~22°C) to Bzct / Cyo

Bloomington Stock #	Exelixis Stock #	Lesion	Bzct/ Deletion lethal?	Bzct/CyO	Deletion/ CyO	Bzct/ Deletion
7833	7066	36A1; 36A12	No	14	13	18
7522	6039	36A10; 36B3	No	8	5	9
7834	**7067**	**36A12; 36B1**	**Partial**	**19**	**30**	**7**
7835	8036	36B1; 36C9	No	7	7	5
7838	7068	36C7; 36C10	No	2	9	6
2583		35F6; 36D	**Sterile**	19	22	15

Table A1.5: Testing of deficiency stock # 7834

Crosses at Room Temp (~22°C) to Bloomington Stock #7834 (36A12; 36B1)

Bloomington Stock #	Exelixis Stock #	Lesion	Expect to Comple-ment?	Comple-ment?	Deletion or 7834/ CyO	7834/ Deletion
7833	7066	36A1; 36A12	Yes	Yes	23	9
7522	6039	36A10; 36B3	**No**	**Yes**	22	9
7835	8036	36B1; 36C9	No	No	46	0
7838	7068	36C7; 36C10	Yes	Yes	17	7

Table A1.6: Testing of deficiency stock # 7522

Crosses at Room Temp (~22°C) to Bloomington Stock #7522 (36A10; 36B3)

Bloomington Stock #	Exelixis Stock #	Lesion	Expect to Comple-ment?	Comple-ments?	Deletion or 7522/ CyO	7522/ Deletion
7833	7066	36A1; 36A12	**No**	**Yes**	23	14
7835	8036	36B1; 36C9	**No**	**Yes**	14	13